Supporting Information for

Design and Synthesis of Amphiphilic and Luminescent Tris-Cyclometalated Iridium(III) Complexes Containing Cationic Peptides as Inducers and Detectors of Cell Death via a Calcium-Dependent Pathway

Yosuke Hisamatsu,[a] *Ai Shibuya,*[a] *Nozomi Suzuki,*[a] *Toshihiro Suzuki,*[b] *Ryo Abe,*[b] *and Shin Aoki,**[,a,c]

[a] Faculty of Pharmaceutical Sciences, Tokyo University of Science,

2641 Yamazaki, Noda, Chiba 278-8510, Japan

[b] Research Institute for Biomedical Sciences, Tokyo University of Science,

2641 Yamazaki, Noda, Chiba 278-8510, Japan

[c] Division of Medical Science-Engineering Corporation, Research Institute of Science and Technology,

Tokyo University of Science, 2641 Yamazaki, Noda, Chiba 278-8510, Japan

*Corresponding authors: E-mail, shinaoki@rs.noda.tus.ac.jp

Contents

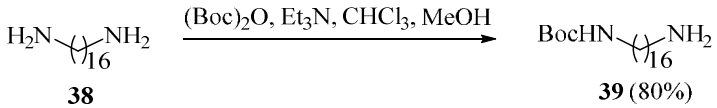

38 **39** (80%)

Chart S1. Synthesis of **39**

Mono-Boc-protected diamine **39**: Boc_2O (36 mg, 0.16 mmol) was dissolved in $CHCl_3$ (25 mL) and added dropwise to 1,16-diaminohexadecane **38**[S1] (0.12 g, 0.48 mmol) in $CHCl_3$ (40 mL) and MeOH (4 mL) at 0 °C for 3 hr. The reaction mixture was allowed to stir overnight at room temperature. The reaction insoluble compounds were filtered off and the filtrate was concentrated under reduced pressure. The residue was purified by NH silica gel column chromatography (hexanes/$CHCl_3$ = 3/1) to give **39** (46 mg, 80%) as a white solid. M.p. 76 °C. IR (ATR): ν = 3370, 2918, 2851, 1686, 1519, 1471, 1247, 1170, 871, 719 cm^{-1}. ^1H NMR (300 MHz, $CDCl_3$/TMS): δ = 4.51 (s, 4H), 3.10 (q, J = 6.6 Hz, 2H), 2.68 (t, J = 6.9 Hz, 2H), 1.39 (s, 4H), 1.25 (s, 33H). FAB-MS (*m/z*) Calcd for $C_{21}H_{45}N_2O_2$ $[M+H]^+$:

357.3481. Found: 357.3481. Anal. Calcd for $C_{21}H_{44}N_2O_2$•1/2MeOH: C, 69.30; H, 12.44; N, 7.52%. Found: C, 69.61; H, 12.71; N, 7.30%.

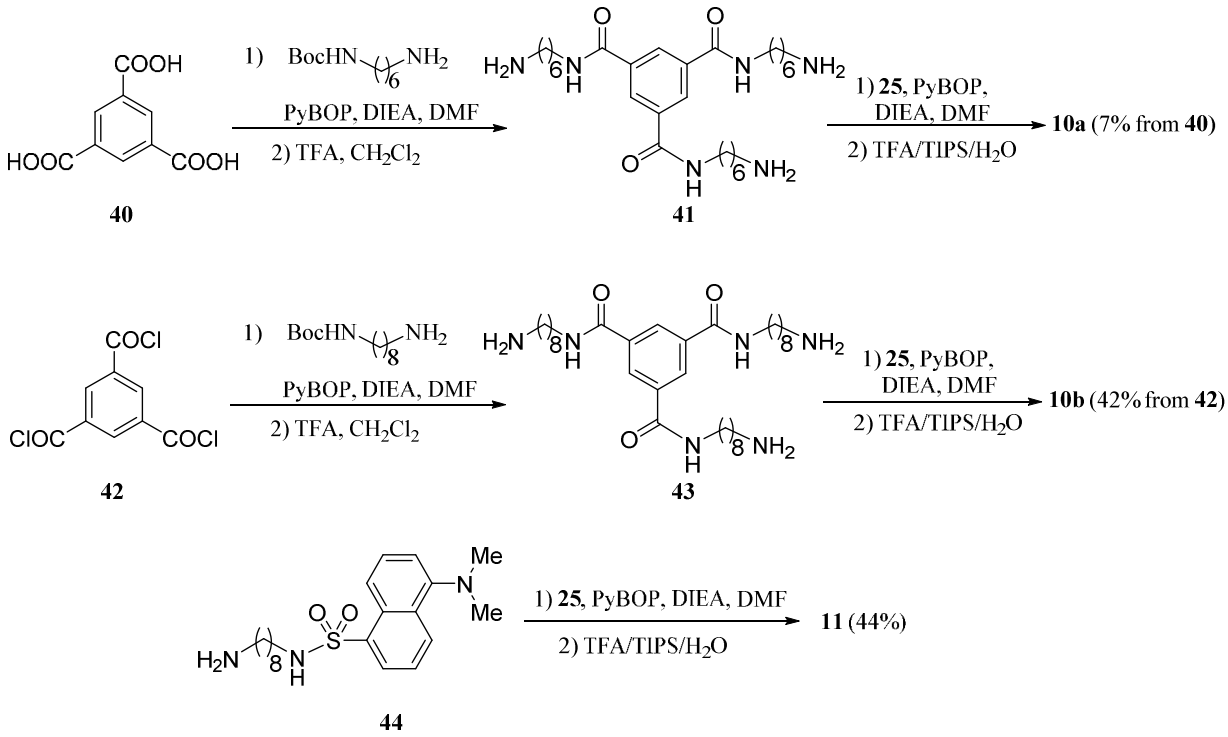

Chart S2. Synthesis of **10a**, **10b**, and **11**

Compound 10a: DIEA (0.49 g, 3.8 mmol), PyBop (1.5 g, 2.9 mmol) and mono-Boc-protected hexamethylenediamine (0.62 g, 2.9 mmol) dissolved in dist. DMF (1 mL) were added to a solution of **40** (0.10 g, 0.48 mmol) in dist. DMF (1 mL). The reaction mixture was stirred at room temperature for 12.5 hr. Then it was concentrated under reduced pressure. Remaining residue was purified by silica gel column chromatography ($CHCl_3$/MeOH = 100/1 to 0/1) and NH silica gel column chromatography (Hexanes/AcOEt = 1/1 to 0/1) to afford the protected compound. TFA (5 mL) was added to the protected compound in CH_2Cl_2 (5 mL). The reaction mixture was stirred at room temperature for 14.5 hr. After evaporation, cold Et_2O was added to the solution. The insoluble compound was centrifuged and washed with Et_2O. The resulting residue was purified by preparative HPLC (H_2O (0.1%TFA)/CH_3CN (0.1%TFA) = 90/10 to 55/45, t_r = 21 min) to give TFA salt of **41** (61 mg) as a colorless amorphous. IR (ATR): ν = 3333, 3079, 2940, 2865, 2525, 1671, 1638, 1544, 1549, 1432, 1297, 1191, 1181, 1111, 838, 801, 722 cm^{-1}. ^1H NMR (400 MHz, D_2O/TSP): δ = 8.24 (s, 3H), 3.45 (t, *J*

= 6.9 Hz, 6H), 3.01 (t, J = 7.5 Hz, 6H), 1.76-1.62 (m, 12H), 1.50-1.40 (m, 12H) ppm. ^{13}C NMR (100 MHz, D_2O/1,4-dioxane): δ = 168.5, 134.9, 128.5, 40.0, 39.4, 28.2, 26.6, 25.6, 25.3 ppm. FAB-MS (*m/z*) Calcd for $C_{27}H_{49}N_6O_3$ $[M+H]^+$: 505.3866. Found: 505.3867.

DIEA (25 mg, 0.19 mmol), PyBOP (0.11 g, 0.21 mmol) and **25** (27 mg, 39 μmol) were added to a solution of **41** (8.2 mg, 9.7 μmol) in dist. DMF (1 mL). The reaction mixture was stirred at room temperature for 18 hr. After evaporation, cold Et_2O was added to the solution. The insoluble compound was centrifuged and washed with Et_2O. TFA cocktail (TFA/H_2O/TIPS = 95/2.5/2.5, 10 mL) was added to the protected compound. The reaction mixture was stirred at room temperature for 6 hr. After evaporation, cold Et_2O was added to the solution. Pale brown solid was centrifuged and washed with Et_2O. The resulting residue was purified by preparative HPLC (H_2O (0.1%TFA)/CH_3CN (0.1%TFA) = 90/10 to 60/40, t_r = 16 min, 6.0mL/min) to give **10a** (11 mg, 7% as 9TFA salt from **40**) as a white powder. ^{1}H NMR (400 MHz, D_2O/TSP): δ = 8.24 (s, 3H), 4.39 (t, J = 7.2 Hz, 3H), 4.06 (t, J = 6.4 Hz, 3H), 4.01 (s, 6H), 3.92-3.91 (m, 6H), 3.43 (t, J = 7.0 Hz, 6H), 3.26-3.19 (m, 6H), 3.04-2.99 (m, 12H), 1.97-1.62 (m, 30H), 1.58-1.34 (m, 30H) ppm. ESI-MS (*m/z*) Calcd for: $C_{75}H_{139}N_{24}O_{15}$ $[M+H]^+$: 1616.0846. Found: 1616.0847.

Compound 10b: Et_3N (58 mg, 0.57 mmol) and **42** (15.5 mg, 0.058 mmol) were added to a solution of mono-Boc-protected octanediamine (58.8 mg, 0.24 mmol) in dist. DMF (1 mL). The reaction mixture was stirred at room temperature for 24 hr. Then it was concentrated under reduced pressure. Remaining residue was purified by silica gel column chromatography (hexanes/$CHCl_3$ = 2/1 to 0/1 to $CHCl_3$/MeOH = 100/1) to afford the protected compound (45 mg). TFA (1 mL) was added to the protected compound (20 mg, 23 μmol) in CH_2Cl_2 (1 mL). The reaction mixture was stirred at room temperature for 5 hr. After evaporation, cold Et_2O was added to the solution. The insoluble compound was centrifuged and washed with Et_2O to give TFA salt of **43** (15 mg) as a colorless amorphous. ^{1}H NMR (300 MHz, CD_3OD/TMS): δ = 8.68 (s, 1H), 8.38 (s, 3H), 3.48-3.33 (m, 6H), 2.91 (t, J = 7.5 Hz, 6H), 1.65 (s, 12H), 1.40 (s, 24H) ppm. FAB-MS (*m/z*) Calcd for: $C_{33}H_{61}N_6O_3$ $[M+H]^+$: 589.4805. Found: 589.4808.

DIEA (59 mg, 0.46 mmol), PyBOP (0.24 g, 0.46 mmol) and **25** (71 mg, 0.10 mmol) were added to a solution of **43** (18 mg, 23 μmol) in dist. DMF (1 mL). The reaction mixture was stirred at room temperature for 17 hr. After evaporation, remaining residue was purified by silica gel column chromatography (Hexanes/AcOEt = 1/2 to $CHCl_3$/MeOH = 100/1 to 0/100) and silica gel column chromatography ($CHCl_3$/MeOH = 50/1 to 10/1) to afford the protected compound. TFA cocktail (TFA/H_2O/TIPS = 95/2.5/2.5, 4 mL) was added to the protected compound. The reaction mixture was stirred at room temperature for 6 hr. After evaporation, cold Et_2O was added to the solution. White solid was centrifuged and washed with Et_2O. The resulting residue was purified by preparative HPLC (H_2O (0.1%TFA)/CH_3CN (0.1%TFA) = 85/15 to 65/35, t_r = 15 min, 6.0mL/min) to give **10b** (40 mg, 42% as 9TFA salt from **42**) as a colorless amorphous. ^{1}H NMR (400 MHz, D_2O/TSP): δ = 8.24 (s, 3H), 4.36 (t, J = 7.2 Hz, 3H), 4.05 (t, J = 7.2 Hz, 3H), 3.99-3.98 (m, 6H), 3.88 (brs, 6H), 3.37 (t, J = 6.8 Hz, 6H), 3.19-3.13 (m, 6H), 3.02-2.97 (m, 12H), 1.93-1.75 (m, 12H), 1.75-1.57 (m, 18H), 1.48-1.43 (m, 18H), 1.32-1.27 (m, 24H) ppm. ESI-MS (*m/z*) Calcd for $C_{81}H_{151}N_{24}O_{15}$ $[M+H]^+$: 1700.1787. Found: 1700.1785.

Compound 11: DIEA (15 mg, 0.12 mmol), PyBOP (62 mg, 0.12 mmol) and **25** (31 mg, 45 μmol) were added to a solution of **44**[S2] (11 mg, 30 μmol) in dist. DMF (1 mL). The reaction mixture was stirred at room temperature for 13 hr, then it was concentrated under reduced pressure. Remaining residue was purified by silica gel column chromatography ($CHCl_3$/MeOH, 20/1 to 10/1) to afford protected compound. TFA cocktail (TFA/H_2O/TIPS = 95/2.5/2.5, 5 mL) was added to the protected compound and the reaction mixture was stirred at room temperature for 5 hr. After evaporation, cold Et_2O was added to the solution. Pale-yellow powder was centrifuged and washed with Et_2O. The resulting residue was purified by preparative HPLC (H_2O (0.1%TFA)/CH_3CN (0.1%TFA) = 85/15 to 65/35, t_r = 16 min, 6.0mL/min) to give **11** (16 mg, 44% as 3TFA salt from **44**) as slightly brown gum. ^{1}H NMR (400 MHz, D_2O/TSP): δ = 8.82 (d, J = 8.8 Hz, 1H), 8.46 (d, J = 8.8 Hz, 1H), 8.40 (d, J = 7.6 Hz, 1H), 8.12 (d, J = 7.6 Hz, 1H), 7.93 (t, J = 8.2 Hz, 2H), 4.38 (t, J = 7.0 Hz, 1H), 4.05 (t, J = 6.4 Hz, 1H), 4.00 (s, 2H), 3.90 (s, 2H), 3.54 (s, 6H), 3.17-3.10 (m, 2H), 3.10-2.94 (m, 6H), 1.93-1.69 (m, 8H), 1.50-1.35

(m, 6H), 1.24-1.20 (m, 2H), 1.10-1.05 (m, 2H), 0.97-0.91 (m, 6H) ppm. ESI-MS (*m/z*) Calcd for $C_{36}H_{62}N_9O_6S$ $[M+H]^+$: 748.4538. Found: 748.4537.

Protected peptides
25: BocHN-Lys(Boc)-Lys(Boc)-Gly-Gly-CO_2H
26: BocHN-D-Lys(Boc)-D-Lys(Boc)-Gly-Gly-CO_2H
27: BocHN-Lys(Boc)-Lys(Boc)-Gly-CO_2H
28: BocHN-Gly-Lys(Boc)-Lys(Boc)-Gly-CO_2H
29: BocHN-Lys(Boc)-Gly-Lys(Boc)-Gly-CO_2H
30: BocHN-Lys(Boc)-Gly-Gly-CO_2H
31: BocHN-Lys(Boc)-Lys(Boc)-Lys(Boc)-Gly-Gly-CO_2H
32: BocHN-Lys(Boc)-Asp(O^{t}Bu)-Lys(Boc)-Lys(Boc)-Gly-Gly-CO_2H
33: BocHN-Lys(Boc)-Lys(Boc)-Asp(O^{t}Bu)-Lys(Boc)-Gly-Gly-CO_2H
34: BocHN-Lys(Boc)-Lys(Boc)-Lys(Boc)-Asp(O^{t}Bu)-Gly-Gly-CO_2H
37: H_2N-Lys-Lys-Gly-Gly-CO_2H

Chart S3. Synthesis of peptides **25-34**, and **37**

Protected Peptide synthesis.

BocHN-Lys(Boc)-Lys(Boc)-Gly-Gly-CO_2H (protected KKGG peptide) **25**:

Fmoc-Gly-2-Cl-Trt-Resin (0.50 g, 0.26 mmol) was deprotected by treatment with 20% piperidine/DMF. Each Fmoc-Xaa-OH (1.1 mmol) was coupled at r.t. for 1 hr to the Fmoc-deprotected resin in the presence of DIC (0.14 g, 1.1 mmol), HOBt (0.14 g, 1.1 mmol), DIEA (0.14 g, 1.1 mmol) in dry DMF (2.5 mL). After repetition of the deprotection and coupling steps, N-terminal Boc-Lys(Boc)-OH was condensed under same coupling conditions. The Boc-protected peptide was cleaved from the resin in a mixture of 1,1,1,3,3,3-hexafluoro-2-propanol (HFIP)/CH_2Cl_2 (60/40). After 6 hr shaking, the resin was filtered and washed several times with CH_2Cl_2. Evaporation of the solvent gave the only C-terminal free peptide, which was purified by silica gel column chromatography ($CHCl_3$/MeOH = 30/1 to 10/1) to give **25** (0.11 g, 64%) as a colorless amorphous. IR (ATR): ν = 3313, 2978, 2935, 1650, 1514, 1454, 1393, 1366, 1248, 1162, 1019, 862, 752 cm^{-1}. ESI-MS (*m/z*) Calcd for $C_{31}H_{56}N_6O_{11}Na$ $[M+Na]^+$: 711.3899. Found: 711.3913.

Other protected peptides **26-34** were synthesized and purified similarly.

BocHN-D-Lys(Boc)-D-Lys(Boc)-Gly-Gly-CO_2H (protected D-K-D-KGG peptide) **26**: a colorless amorphous (95% from resin). IR (ATR): ν = 3313, 3072, 2978, 2934, 1659, 1651, 1514, 1453, 1392, 1366, 1248, 1164, 1018, 864, 756 cm^{-1}. ESI-MS (*m/z*) Calcd for $C_{31}H_{57}N_6O_{11}$ $[M+H]^+$: 689.4080. Found: 689.4085.

BocHN-Lys(Boc)-Lys(Boc)-Gly-CO_2H (protected KKG peptide) **27**: a colorless amorphous (70% from resin). IR (ATR): ν = 3318, 2978, 2935, 2870, 1656, 1514, 1453, 1392, 1366, 1249, 1164, 1044, 1016, 862, 754 cm^{-1}. FAB-MS (*m/z*) Calcd for $C_{29}H_{53}N_5O_{10}$ $[M-H]^-$: 630.3714. Found: 630.3713.

BocHN-Gly-Lys(Boc)-Lys(Boc)-Gly-CO_2H (protected GKKG peptide) **28**: a colorless powder (92% from resin). IR (ATR): ν = 3278, 3085, 2978, 2935, 1688, 1635, 1521, 1454, 1393, 1367, 1249, 1164, 1049, 864, 753 cm^{-1}. FAB-MS (*m/z*) Calcd for $C_{31}H_{55}N_6O_{11}$ $[M–H]^-$: 687.3932. Found: 687.3930.

BocHN-Lys(Boc)-Gly-Lys(Boc)-Gly-CO_2H (protected KGKG peptide) **29**: a colorless amorphous (85% from resin). IR (ATR): ν = 3304, 3072, 2978, 2934, 1660, 1652, 1516, 1454, 1393, 1366, 1248, 1163, 1017, 864, 751 cm^{-1}. FAB-MS (*m/z*) Calcd for $C_{31}H_{57}N_6O_{11}$ $[M+H]^+$: 689.4082. Found: 689.4084.

BocHN-Lys(Boc)-Gly-Gly-CO_2H (protected KGG peptide) **30**: a colorless amorphous (96% from resin). IR (ATR): ν = 3318, 3075, 2979, 2935, 1659, 1516, 1453, 1393, 1367, 1248, 1162, 1020, 861, 752 cm^{-1}. FAB-MS (*m/z*) Calcd for $C_{20}H_{35}N_4O_8$ $[M-H]^-$: 459.2455. Found: 459.2454.

BocHN-Lys(Boc)-Lys(Boc)-Lys(Boc)-Gly-Gly-CO_2H (protected KKKGG peptide) **31**: a colorless amorphous (93% from resin). IR (ATR): ν = 3291, 3077, 2979, 2934, 1682, 1635, 1516, 1452, 1393, 1367, 1249, 1165, 1016, 863 cm^{-1}. ESI-MS (*m/z*) Calcd for $C_{42}H_{76}N_8O_{14}Na$ $[M+Na]^+$: 939.5373. Found: 939.5368.

BocHN-Lys(Boc)-Asp(O^{t}Bu)-Lys(Boc)-Lys(Boc)-Gly-Gly-CO_2H (protected KDKKGG peptide) **32**: A yellow amorphous (quant. from resin). IR (ATR): ν = 3282, 3074, 2981, 2934, 2891, 1690, 1628, 1516, 1454, 1392, 1366, 1249, 1160, 865, 753 cm^{-1}. FAB-MS (*m/z*) Calcd for $C_{50}H_{89}N_9O_{17}Na$ $[M+Na]^+$: 1110.6274. Found: 1110.6279.

BocHN-Lys(Boc)-Lys(Boc)-Asp(O^{t}Bu)-Lys(Boc)-Gly-Gly-CO_2H (protected KKDKGG peptide) **33**: A white amorphous (99% from resin). IR (ATR): ν = 3285, 3075, 2978, 2936, 1684, 1632, 1515, 1454,

1393, 1366, 1249, 1162, 1016, 864, 778 cm^{-1}. FAB-MS (*m/z*) Calcd for $C_{50}H_{89}N_9O_{17}Na$ $[M+Na]^+$: 1110.6274. Found: 1110.6272.

BocHN-Lys(Boc)-Lys(Boc)-Lys(Boc)-Asp(O^{t}Bu)-Gly-Gly-CO_2H (protected KKKDGG peptide) **34**: A colorless amorphous (quant. from resin) . IR (ATR): ν = 3284, 3075, 2978, 2934, 1686, 1629, 1517, 1454, 1393, 1366, 1248, 1160, 1017, 865, 752 cm^{-1}. FAB-MS (*m/z*) Calcd for $C_{50}H_{89}N_9O_{17}Na$ $[M+Na]^+$: 1110.6274. Found: 1110.6275.

H_2N-Lys-Lys-Gly-Gly-CO_2H (deproteected KKGG peptide **37**): TFA cocktail (TFA/H_2O/TIPS = 95/2.5/2.5, 5 mL) was added to **25** (12 mg, 18 μmol) and the reaction mixture was stirred at room temperature for 6 hr. After evaporation, cold Et_2O was added to the solution. White powder was centrifuged and washed with Et_2O. The resulting residue was purified by preparative HPLC (H_2O (0.1%TFA), t_r = 15 min, 6.0mL/min) to give **37** (6.0 mg, 47% as 3TFA salt from **25**) as a colorless amorphous. ESI-MS (*m/z*) Calcd for $C_{16}H_{33}N_6O_5$ $[M+H]^+$: 389.2510. Found: 389.2507.

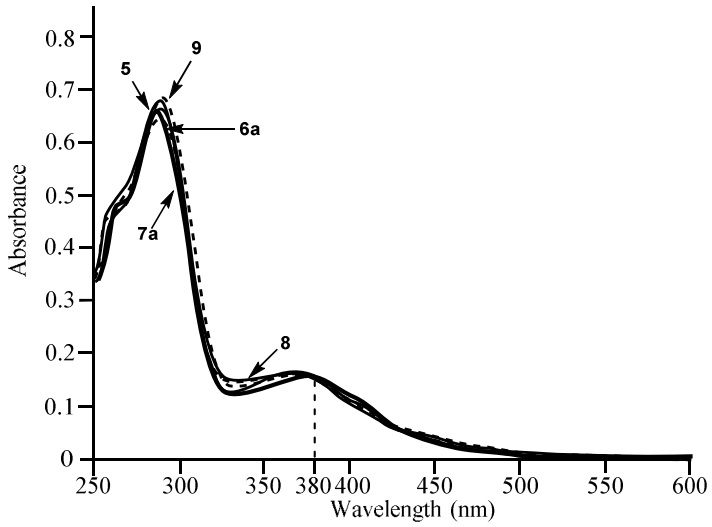

Figure S1. (a) Absorption spectra of **5** (solid curve), **6a** (dashed curve), **7a** (bold curve), **8** (solid curve) and **9** (bold dashed curve) in DMSO at 25 °C. [Ir complex] = 10 μM

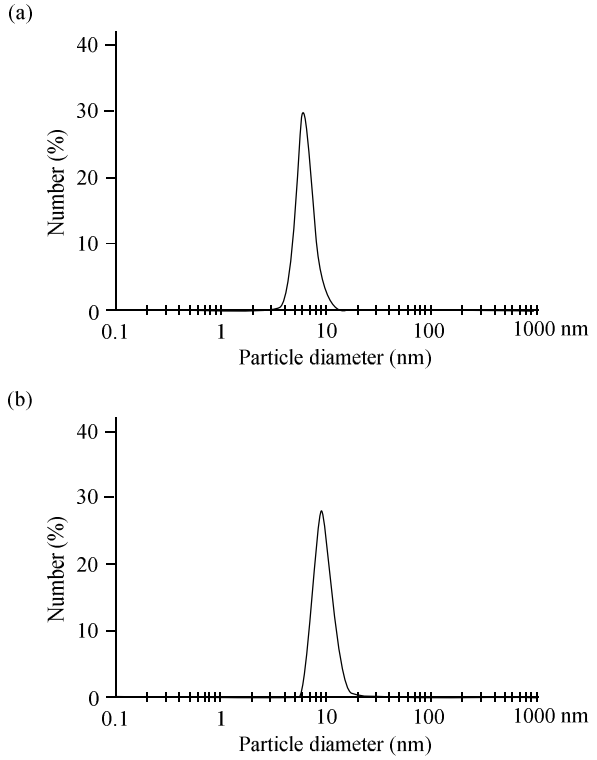

Figure S2. Particle diameter distribution of (a) **8** and (b) **9** in 10 mM PBS (pH 7.4) at 37 ^{o}C (measured on Zetasizer Nano ZS, Malvern Instruments). [Ir complex] = 50 μM

Table S1. Luminesce quantum yields, lifetimes, radiative (k_r) and nonradiative (k_{nr}) rate constants for Ir complexes in degassed 100 mM HEPES (pH7.4) at 25 ^{o}C.

Compound	Φ	τ	k_r (10^5 s^{-1})	k_{nr} (10^5 s^{-1})
5	0.57	1.7 μs	3.4	2.5
6a	0.55	1.7 μs	3.2	2.6
7a	0.54	1.3μs	4.2	3.5
8	0.19	1.2μs	1.6	6.8
9	0.03	0.46 μs	0.7	21

The values of the radiative and nonradiative rate constants, k_r and k_{nr}, are calculated by eqs. 1 and 2 on the assumption that Φ_{isc} is 1.0 due to the strong spin-orbital interaction caused by heavy atom effects of iridium.[3] Phosphorescence yield: Φ_p, Intersystem-crossing yield: Φ_{isc}, Phosphorescence lifetime: τ

$$\Phi_p = \Phi_{isc}\{k_r/(k_{r+} k_{nr})\} \quad (1)$$

$$\tau = (k_{r+} k_{nr})^{-1} \quad (2)$$

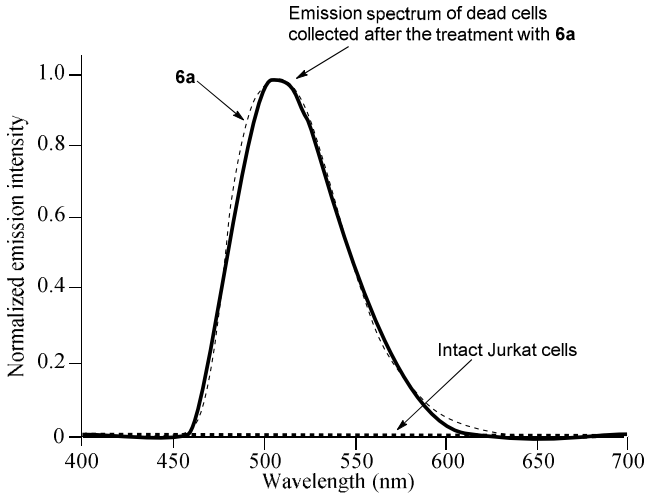

Figure S3. Normalized emission spectra of **6a**-treated Jurkat cells (bold curve), intact Jurkat cells (bold dashed curve) in comparison with emission from **6a** (dashed curve). Jurkat cells (1 x 10^5 cells/mL) were incubated in 10% FCS RPMI medium with **6a** (50 μM) at 37 ^oC for 1 hr. After incubation, the cells were carefully washed three times with ice-cold PBS with 0.1% NaN_3 and 0.5% FCS, and then diluted to (*ca.* 7 x 10^4 cells/mL) in PBS. Emission spectra of cellular suspension were recorded on spectrofluorometer (excitation at 366 nm in PBS at 25 ^oC).

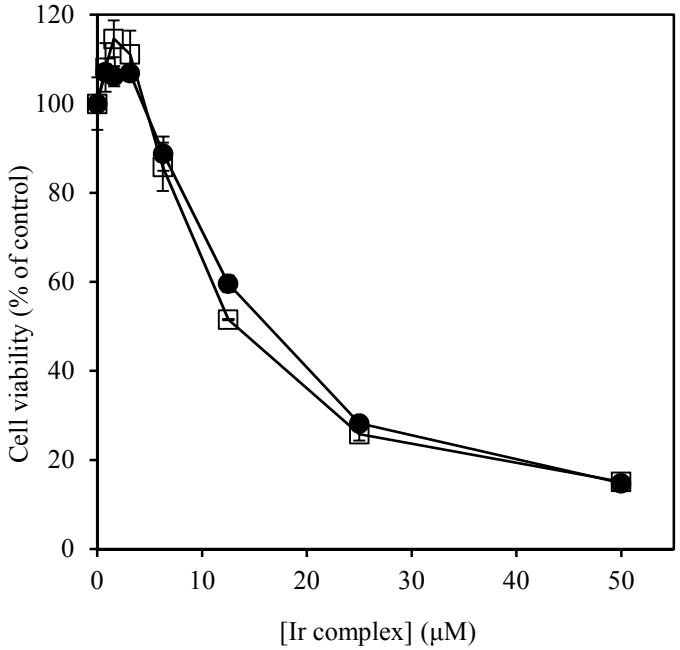

Figure S4. The results of MTT assay of Jurkat cells with Ir complexes **6a** in 5% FCS RPMI1640 (open squares) and in 10% FCS RPMI1640 medium (filled circles) after incubation at 37 ^oC for 16 hr.

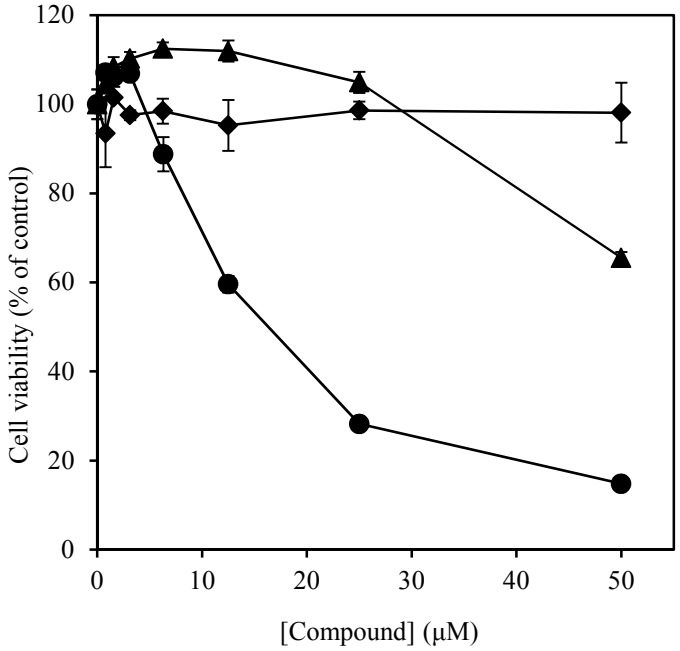

Figure S5. The results of MTT assay with Ir complexes **6a** (filled circles) and benzene-1,3,5-tricarboxamide derivatives **10a** (filled diamonds) and **10b** (filled triangles) against Jurkat cells after incubation at 37 ^{o}C for 16 hr.

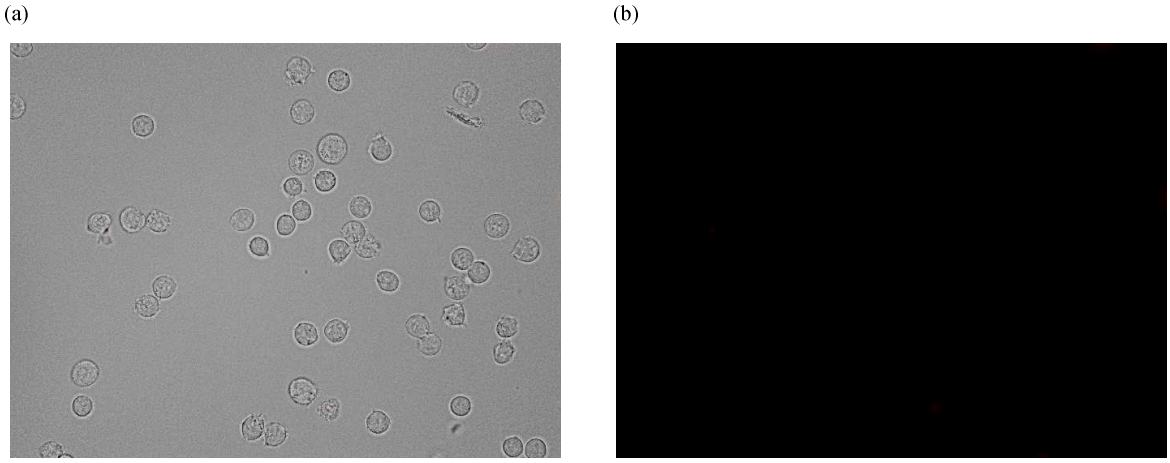

Figure S6. Jurkat cells (1x10^{5} cells/mL) were incubated with **11** (150 μM) at 37 ^{o}C for 16 hr, then stained by PI (30 μM), and observed on Biorevo, BZ-9000 (Keyence) with TRITC filter (Ex.540/25 nm, Em.605/55 nm). (a) Bright field image, (b) emission image of PI.

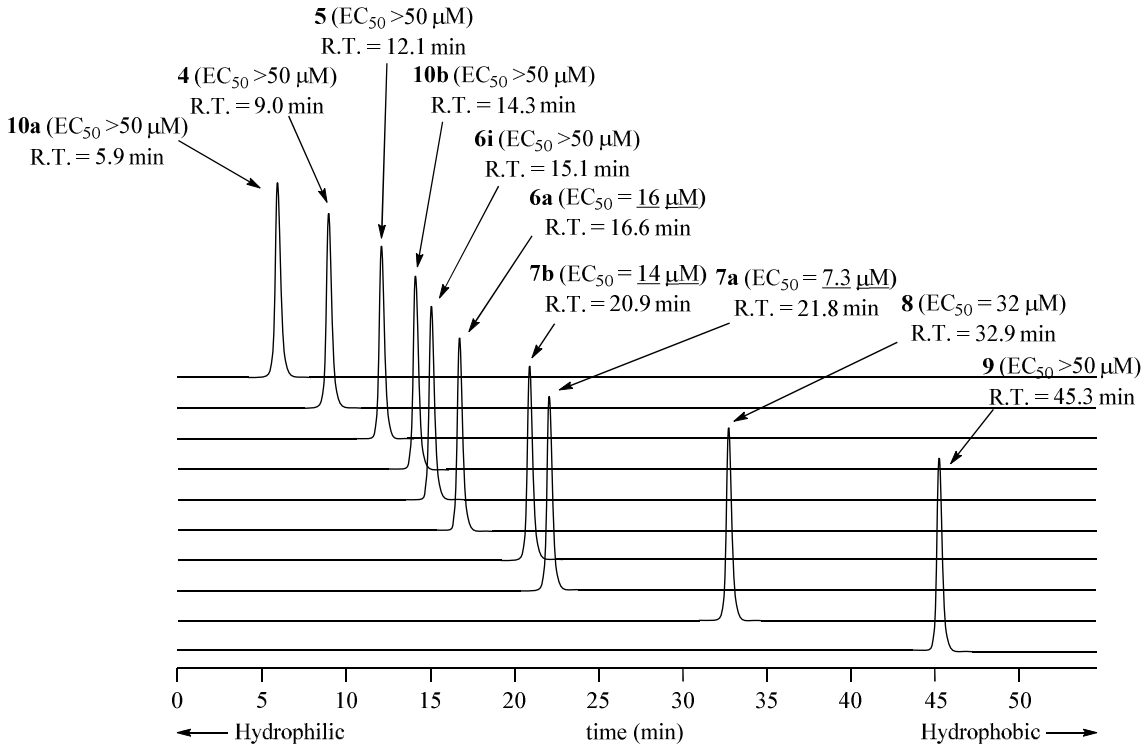

Figure S7. The retention times (R.T.) of **4**, **5**, **6a**, **6i**, **7a**, **7b**, **8**, **9**, **10a**, and **10b** are determined by reverse phase HPLC (SenshuPak PEGASIL ODS, H_2O (0.1% TFA)/CH_3CN (0.1% TFA) = 90/10 to 45/55 (45 min), flow rate: 1.0 mL/min).

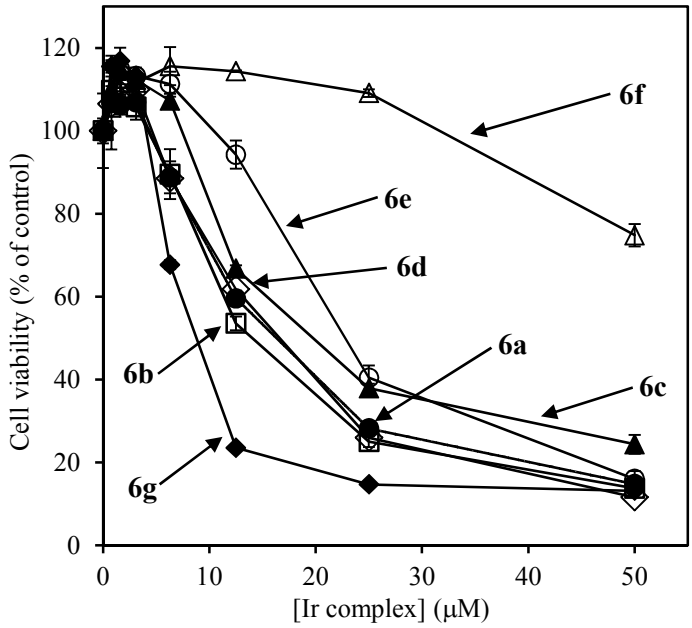

Figure S8. The results of MTT assay of Jurkat cells with Ir complexes **6a** (filled circles), **6b** (open squares), **6c** (filled triangles), **6d** (open diamonds), **6e** (open circles), **6f** (open triangles), **6g** (filled diamonds) after incubation for 16 hr at 37 ^oC.

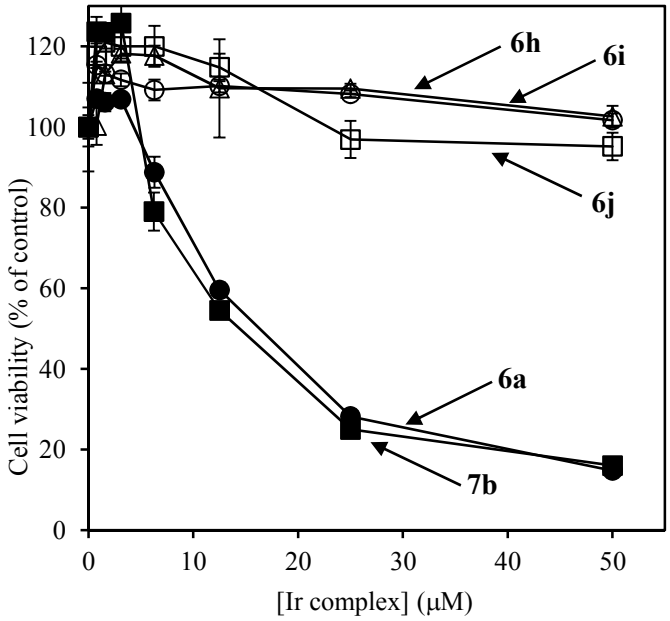

Figure S9. The results of MTT assay of Jurkat cells with Ir complexes **6a** (filled circles), **6h** (open triangles)**, 6i** (open circles)**, 6j** (open squares)**,** and **7b** (filled squares) after incubation at 37 ^{o}C for 16 hr.

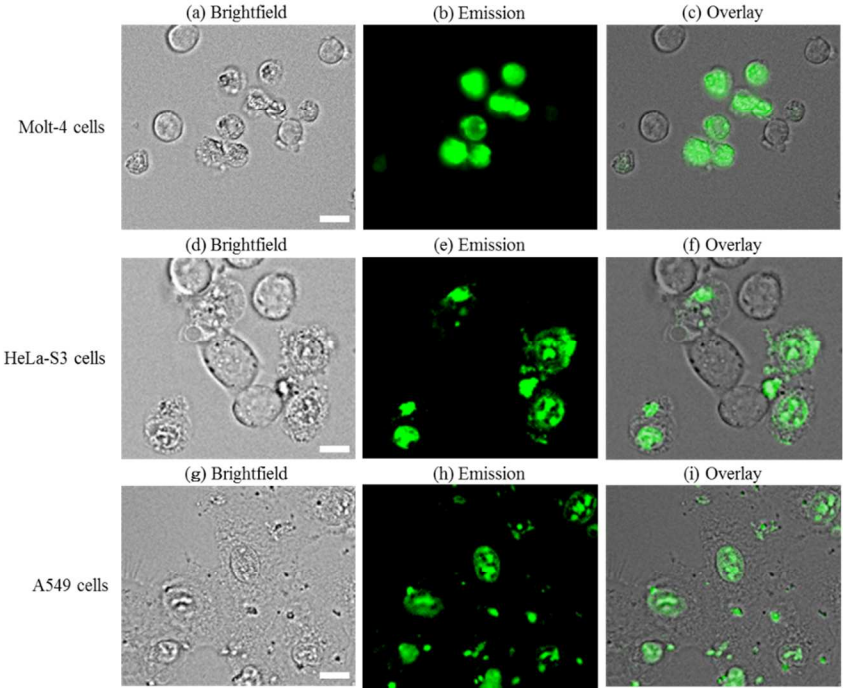

Figure S10. Luminescence microscopy images (Biorevo, BZ-9000, Keyence) of (a)-(c) Molt-4 cells, (d)-(f) HeLa-S3 cells and (g)-(i) A549 cells treated with Ir complexes **6a** (50 μM) for 1 hr at 37 ^{o}C. Excitation at 377 nm. Scale bar (white) = 10 μm.

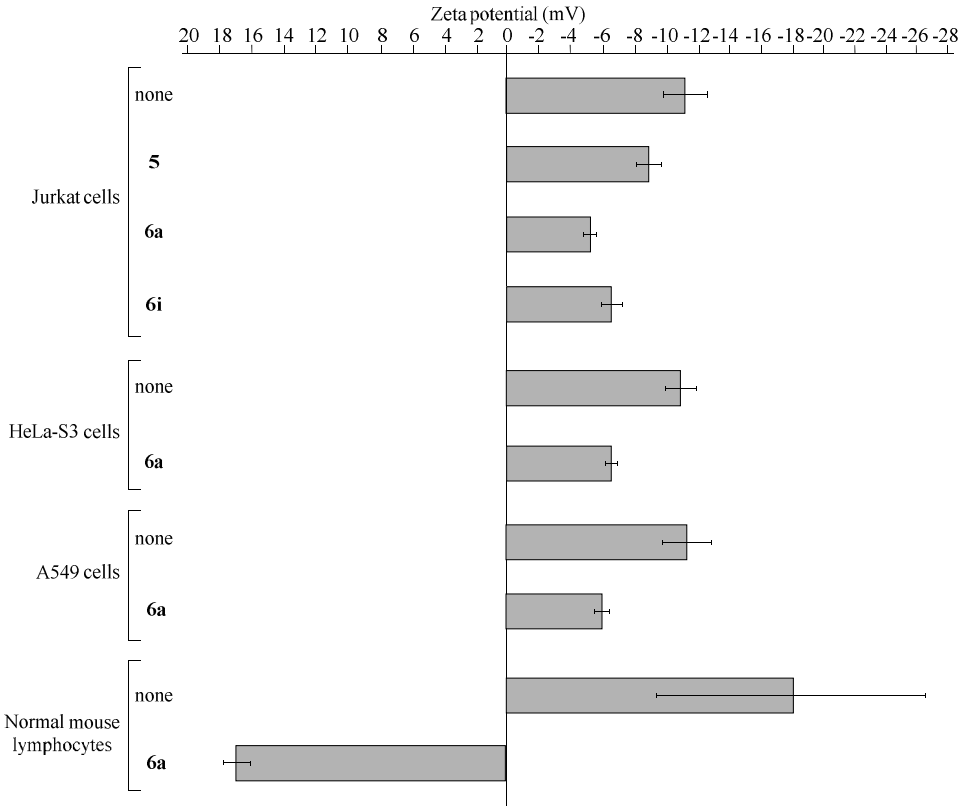

Figure S11. Zeta potential of Jurkat cells, HeLa-S3, A549 cells, and normal mouse lymphocytes in the presence of Ir complexes **5**, **6a**, **6i**. Jurkat cells, HeLa-S3, and A549 cells (3 x 10^5 cells/mL) with or without Ir complexes in PBS (10 mM, pH 7.4) were equilibrated at 37 ^{o}C for 10 min and the potential was then measured. ([Ir complex] = 25 μM)

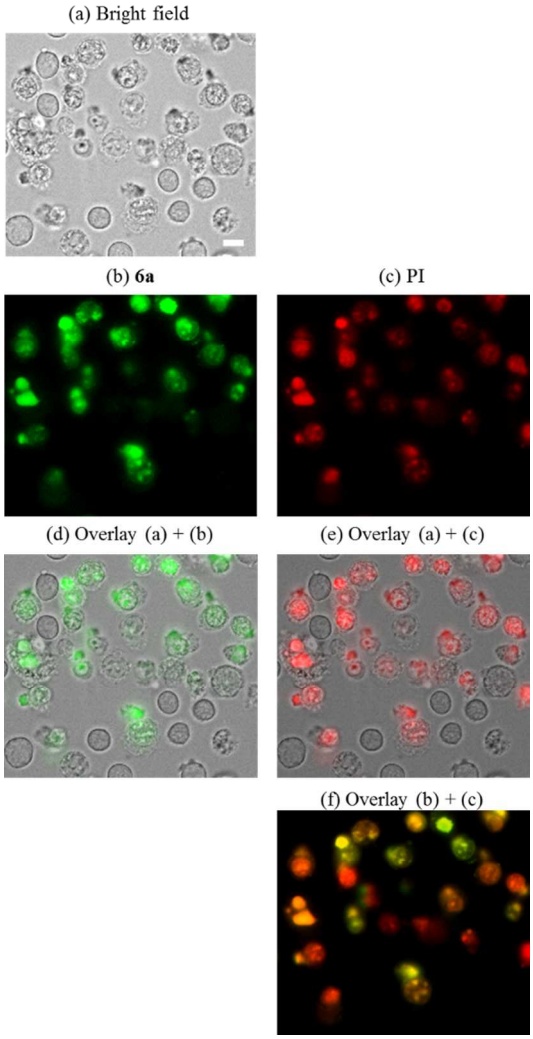

Figure S12. Luminescence microscopy images (Biorevo, BZ-9000, Keyence) of Jurkat cells stained with PI after treatment with **6a** (75 μM) for 1 hr at 37 °C. (a) Bright field image, (b) emission image of **6a**, (c) emission image of PI (d) overlay image of (a) and (b), (e) overlay image of (a) and (c), (f) overlay image of (b) and (c). Excitation at 377 nm for **6a**, excitation at 540 nm for PI. Scale bar (white) = 10 μm.

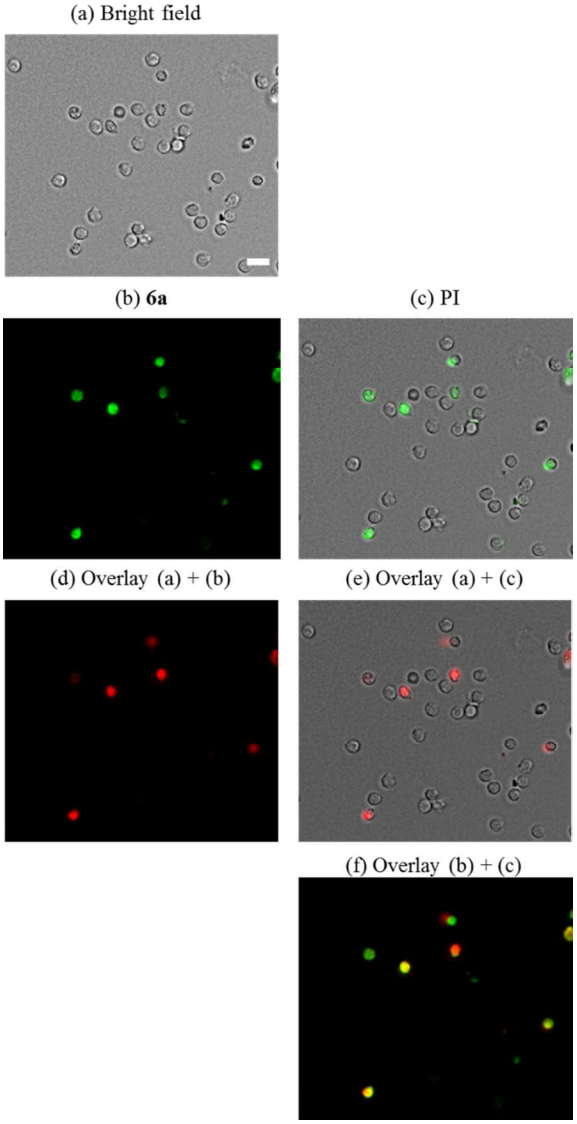

Figure S13. Luminescence microscopy images (Biorevo, BZ-9000, Keyence) of normal mouse lymphocytes stained with PI after treatment with **6a** (50 μM) for 1 hr at 37 ^{o}C. (a) Bright field image, (b) emission image of **6a**, (c) emission image of PI (d) overlay image of (a) and (b), (e) overlay image of (a) and (c), (f) overlay image of (b) and (c). Excitation at 377 nm for **6a**, and excitation at 540 nm for PI. Scale bar = 10 μm.

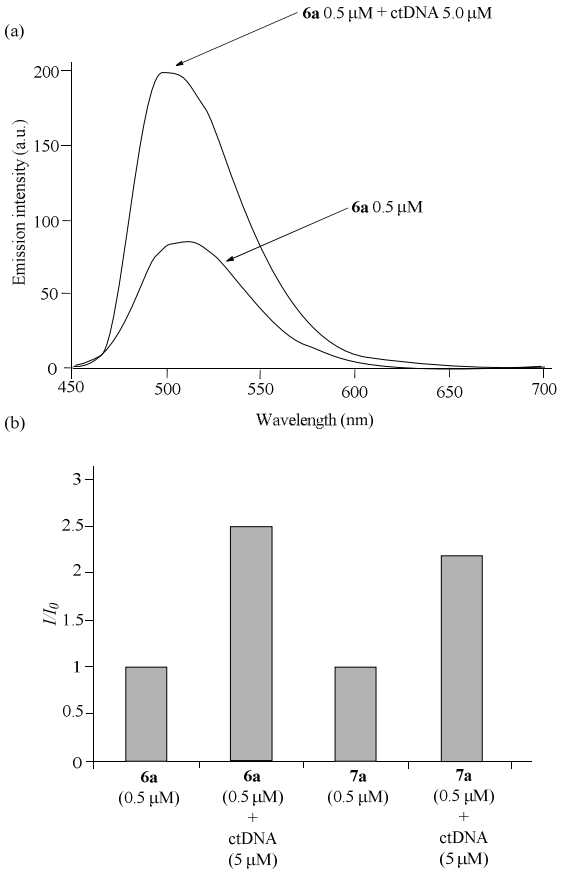

Figure S14. (a) Change in emission spectra of the Ir complex **6a** (0.5 μM) upon the addition of ctDNA (5 μM in phosphate) in 10 mM HEPES (pH 7.4) with $I = 0.1$ ($NaNO_3$) at 25 ^{o}C. Excitation at 366 nm. A.u. is in arbitrary units. (b) Bar represent relative intensity of **6a** and **7a** in the presence of ctDNA. I_0: emission intensity of Ir complex in the absence of ctDNA, I: emission intensity in the presence of ctDNA.

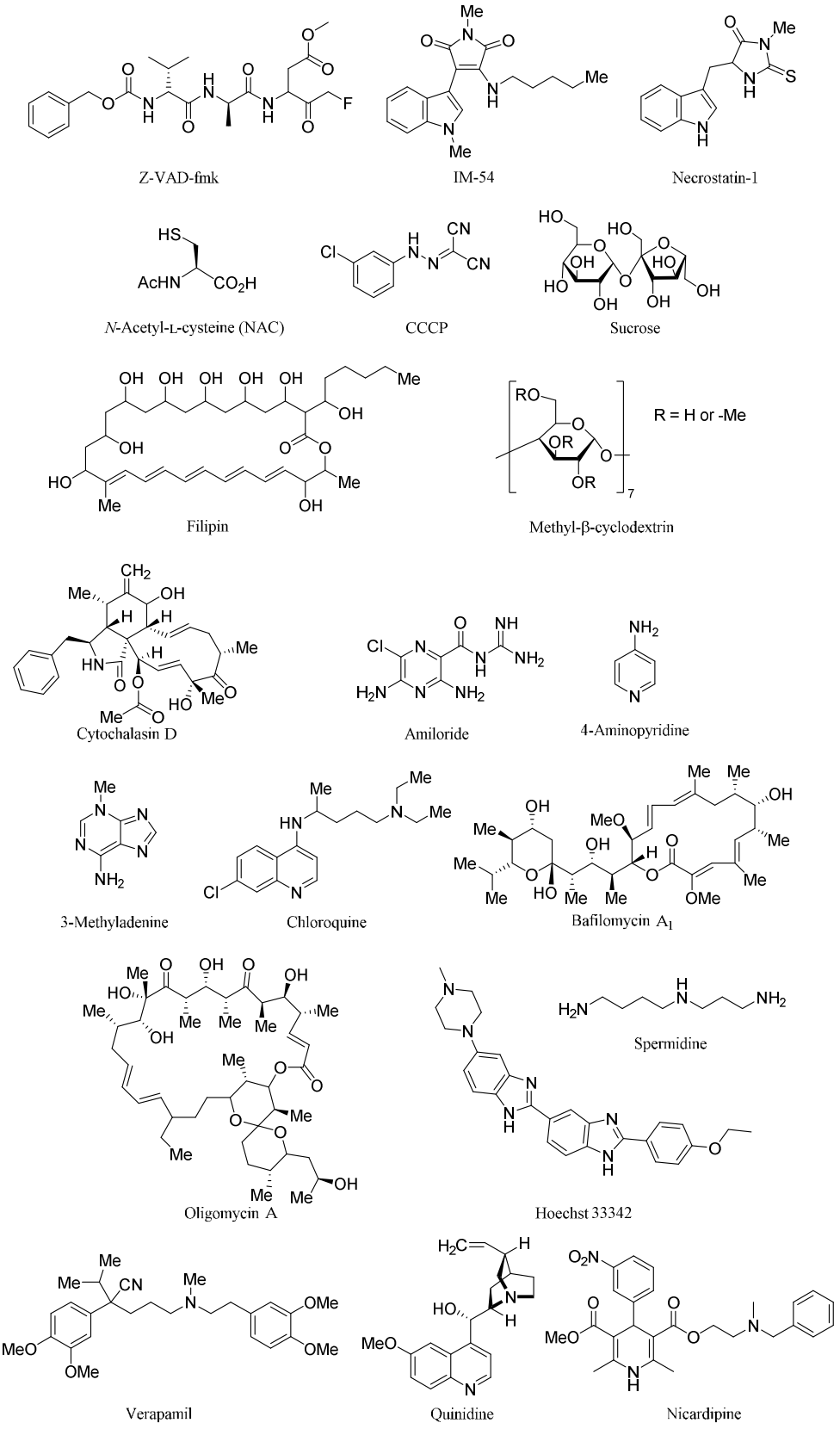

Figure S15. Structures of inhibitors

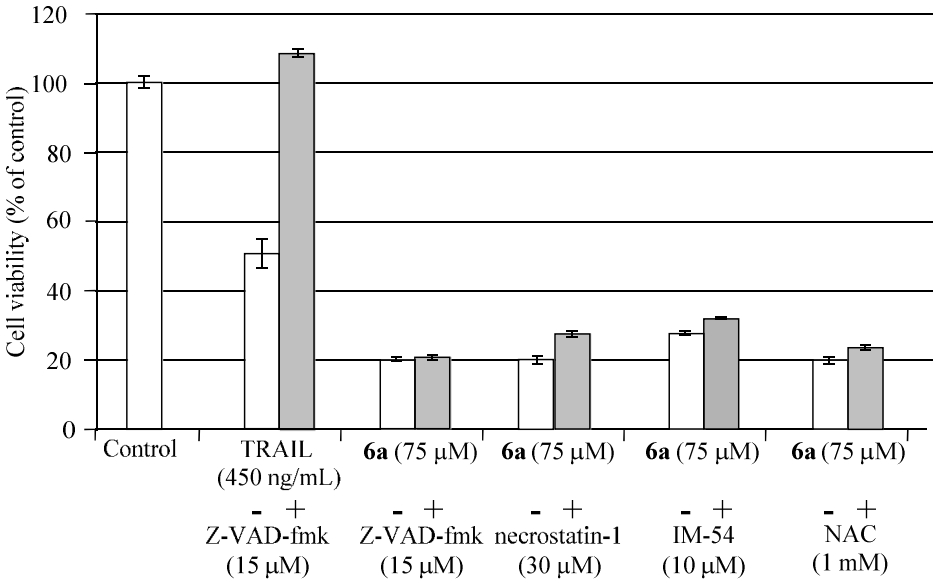

Figure S16. Effect of Z-VAD-fmk (15 μM), necrostatin-1 (30 μM), IM-54 (10 μM), and *N*-acetyl-L-cysteine (NAC) (1 mM) on the cell death of Jurkat cell induced by TRAIL (450 ng/mL) or **6a** (75 μM). Jurkat cells were pre-treated with inhibitors, then TRAIL or Ir complex **6a** was added and incubated at 37 ^{o}C for 16 hr. The cell viability was evaluated by MTT assay. White bar: cell viability in the absence inhibitors; gray bar: cell viability in the presence of inhibitors.

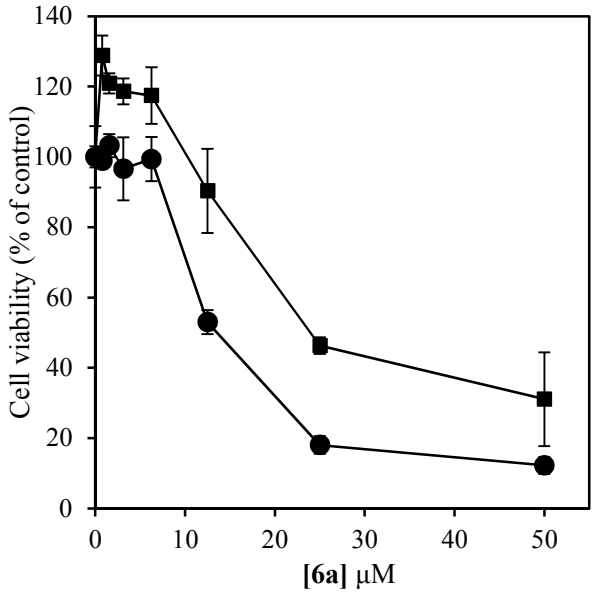

Figure S17. MTT assay of wild type Molt-4 (filled circles) and Bcl-2 overexpressing Molt-4 cells (filled squares) at the different concentration of **6a** (incubation at 37 ^{o}C for 16 hr).

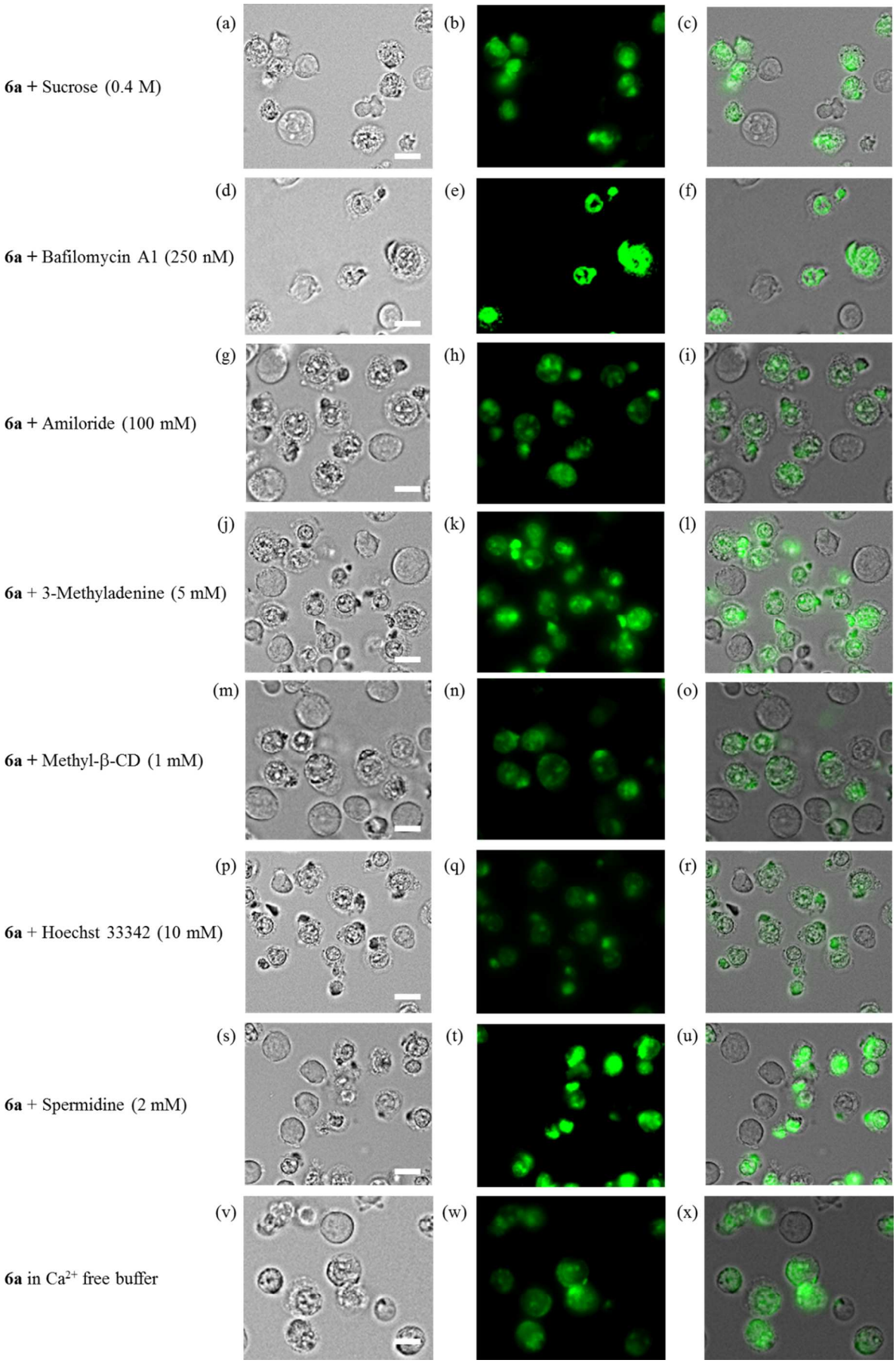
(a)
(b)
(c)
6a + Sucrose (0.4 M)
(d)
(e)
(f)
6a + Bafilomycin A1 (250 nM)
(g)
(h)
(i)
6a + Amiloride (100 mM)
(j)
(k)
(l)
6a + 3-Methyladenine (5 mM)
(m)
(n)
(o)
6a + Methyl-β-CD (1 mM)
(p)
(q)
(r)
6a + Hoechst 33342 (10 mM)
(s)
(t)
(u)
6a + Spermidine (2 mM)
(v)
(w)
(x)
6a in Ca2+ free buffer

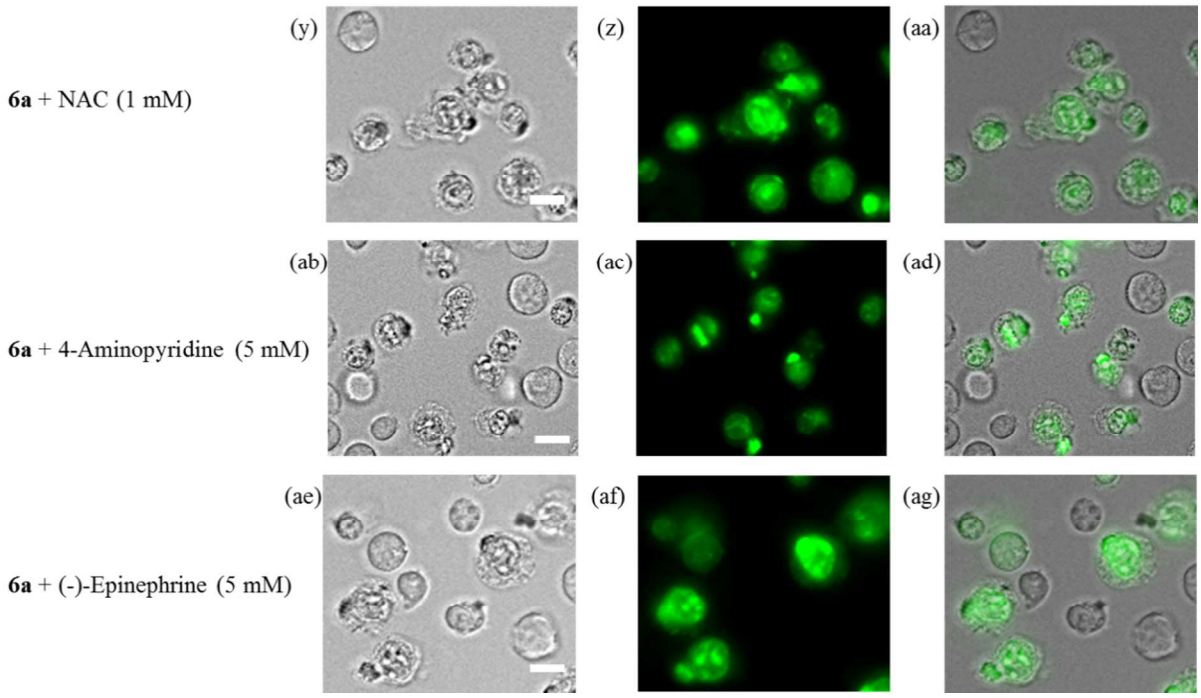

Figure S18. Typical luminescence microscopy images (Biorevo, BZ-9000, Keyence) of Jurkat cells treated with Ir complexes **6a** (50 μM) in the presence of sucrose (a-c), bafilomycin A1 (d-f), amiloride (g-i), 3-methyladenine (j-l), methyl-β-cyclodextrin (methyl-β–CD) (m-o), hoechst 33342 (p-r), spermidine (s-u), Ca^{2+} free buffer (v-x), NAC (y-aa), 4-aminopyridine (ab-ad) and (-)-epinephrine (ae-ag) at 37 ^{o}C for 1 hr. Scale bar (white) = 10 μm.

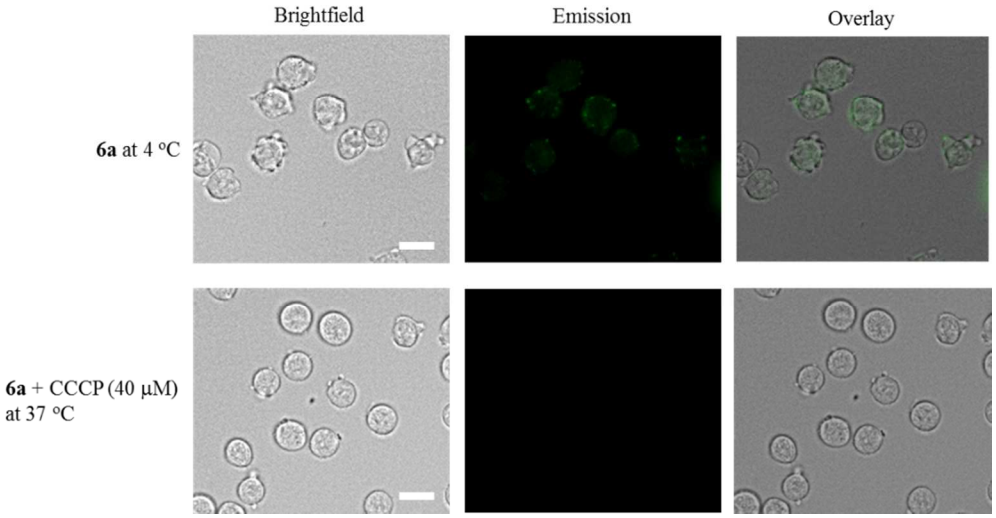

Figure S19. Typical luminescence microscopy images (Biorevo, BZ-9000, Keyence) of Molt-4 cells treated with Ir complexes **6a** (50 μM) in the presence of CCCP (40 μM) at 37 ^{o}C for 1 hr. Scale bar (white) = 10 μm.

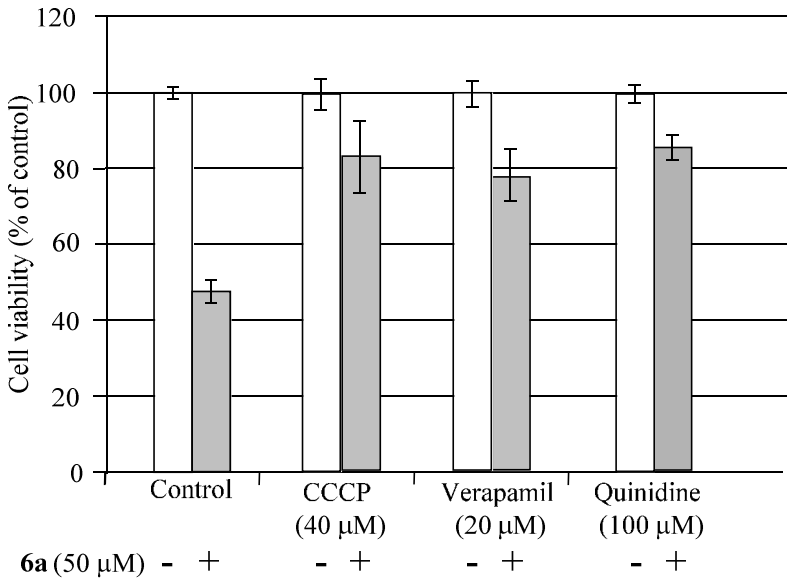

Figure S20. Effect of CCCP (40 μM), verapamil (20 μM), and quinidine (100 μM) on the cell death of Jurkat cells induced by **6a** (50 μM). Jurkat cells were pre-treated with inhibitors for 1 hr at 37 °C, then **6a** was added and incubated for 1 hr at 37 °C. After washing by PBS, the cell viability was evaluated by the number of cells, which is not stained by PI. White bar: cell viability in the absence of inhibitors; gray bar: cell viability in the presence of inhibitors.

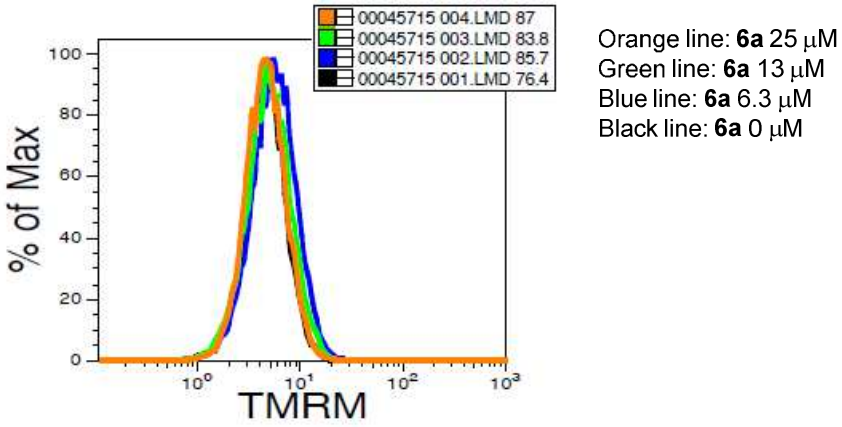

Figure S21. The membrane potential of Jurkat cells stained by TMRM (50 nM) was measured by flow cytometry after treatment of Ir complex **6a**.

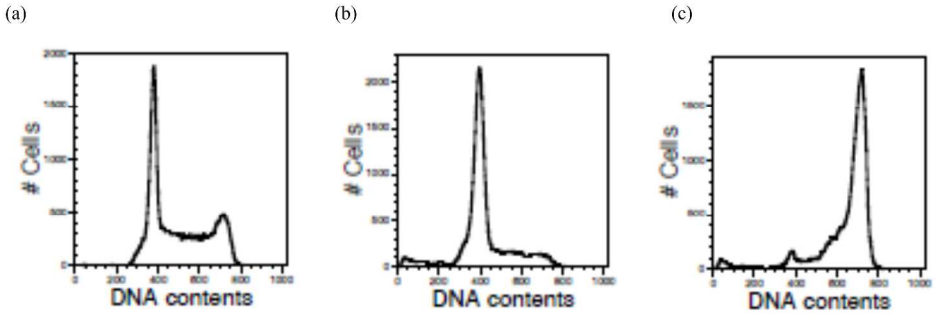

Figure S22. Cell cycle synchronization of Jurkat cells by (a) no treatment, (b) 1 mM thymidine, and 0.15 μg/mL nocodazole. DNA stained by PI were analyzed by a flow cytometer.

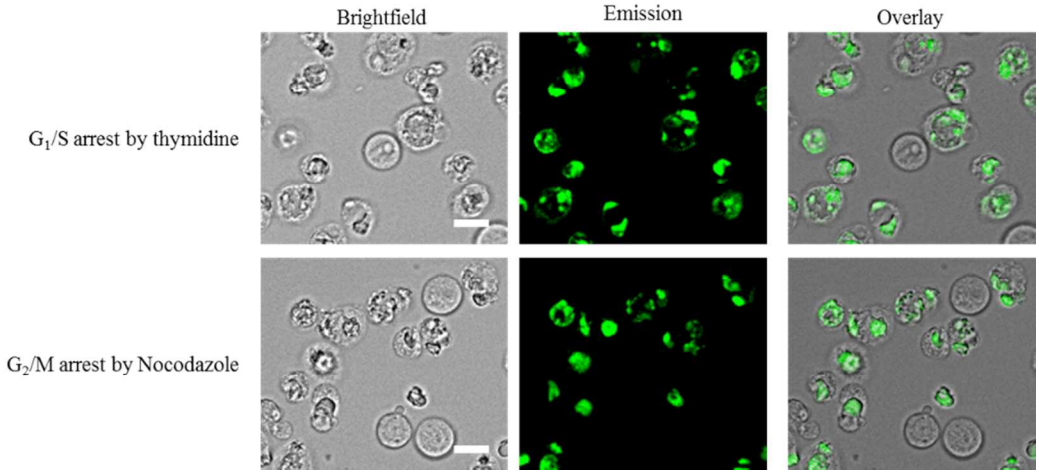

Figure S23. Typical luminescence microscopy images (Biorevo, BZ-9000, Keyence) of synchronized Jurkat cells (G_1/S or G_2/M) treated with Ir complexes **6a** (50 μM) at 37 ^{o}C for 1 hr. Scale bar (white) = 10 μm.

References:

[S1] Muranaka, K.; Sano, A.; Ichikawa, S.; Matsuda, A. *Bioorg. Med. Chem.* **2008**, *16*, 5862-5870.

[S2] Smith, A. B., III; Rucker, P. V.; Brouard, I.; Freeze, B. S.; Xia, S.; Horwitz, S. B. *Org. Lett.* **2005**, *7*, 5199-5202.

[S3] Tsuboyama, A.; Iwawaki, H.; Furugori, M.; Mukaide, T.; Kamatani, J.; Igawa, S.; Moriyama, T.; Miura, S.; Takiguchi, T.; Okada, S.; Hoshino, M.; Ueno, K. *J. Am. Chem. Soc*. **2003**, *125*, 12971–12979.

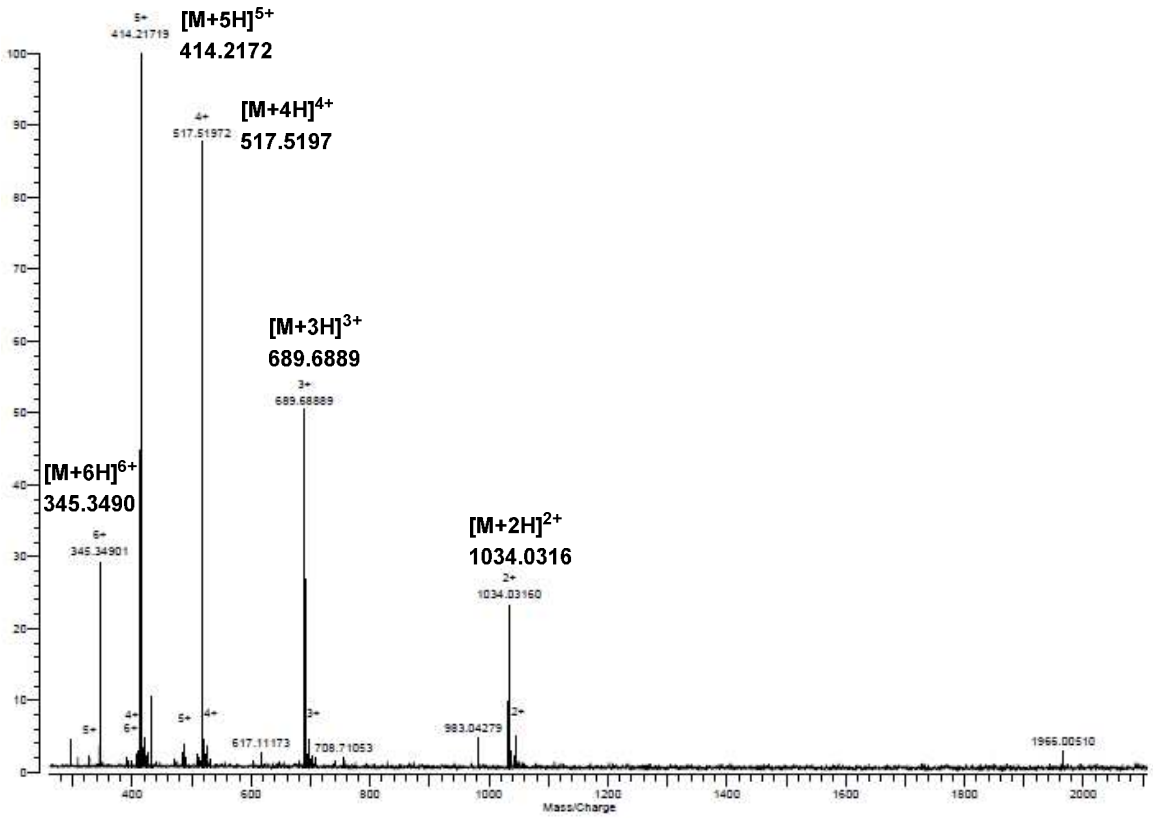

Figure S24. ESI-mass spectrum of **4**

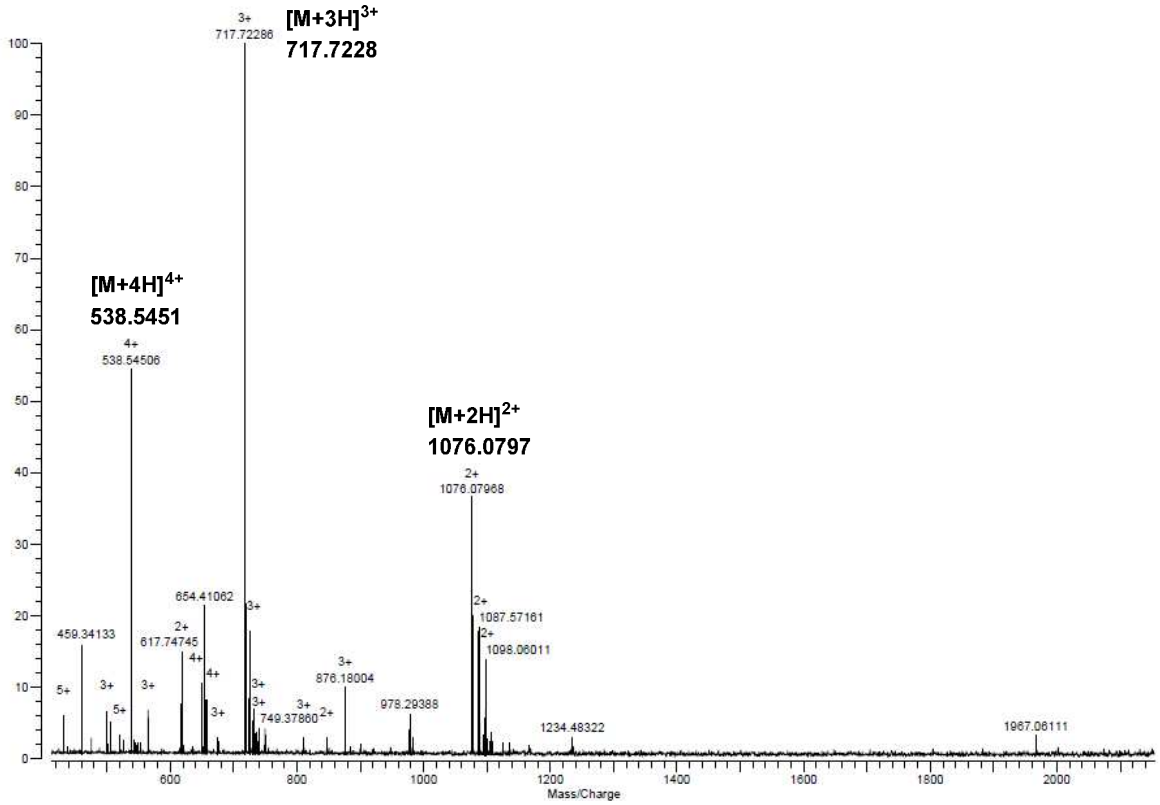

Figure S25. ESI-mass spectrum of **5**

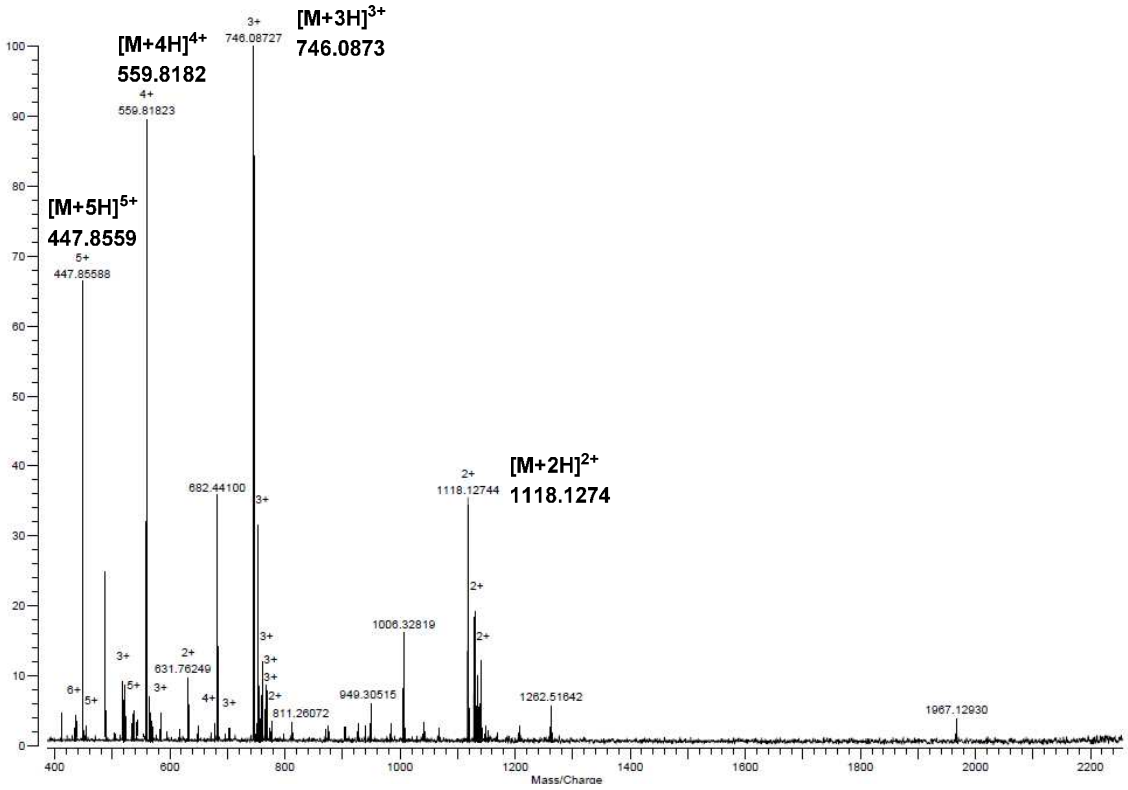

Figure S26. ESI-mass spectrum of **6a**

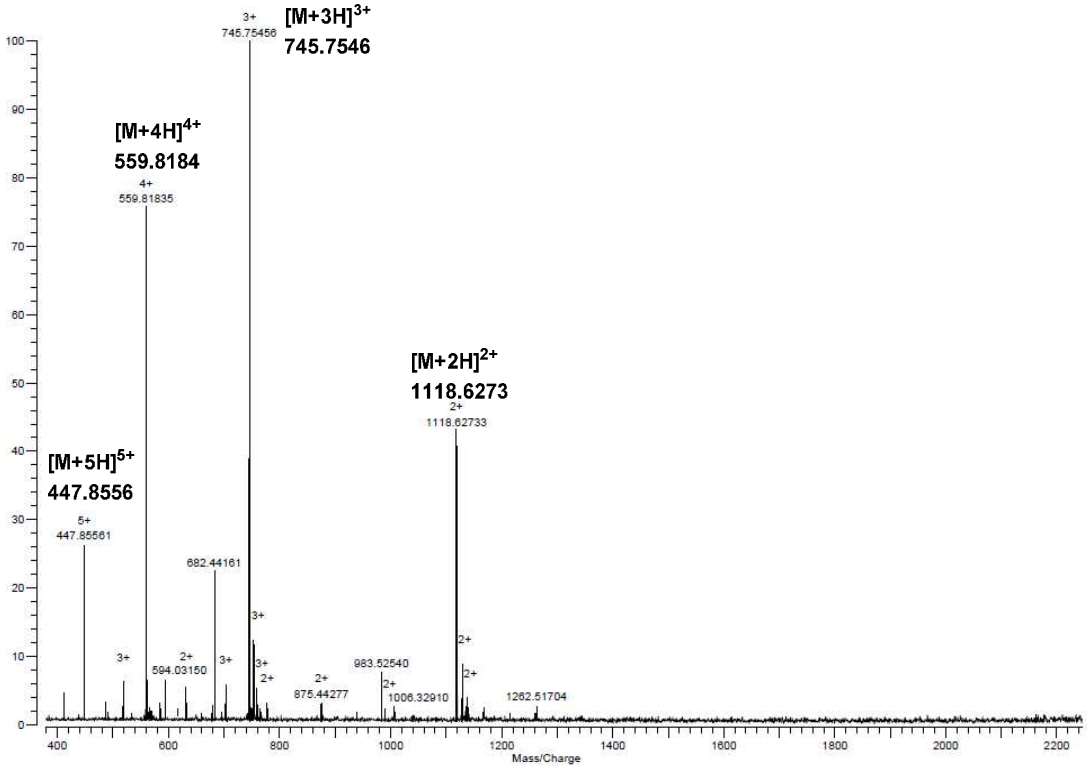

Figure S27. ESI-mass spectrum of **6b**

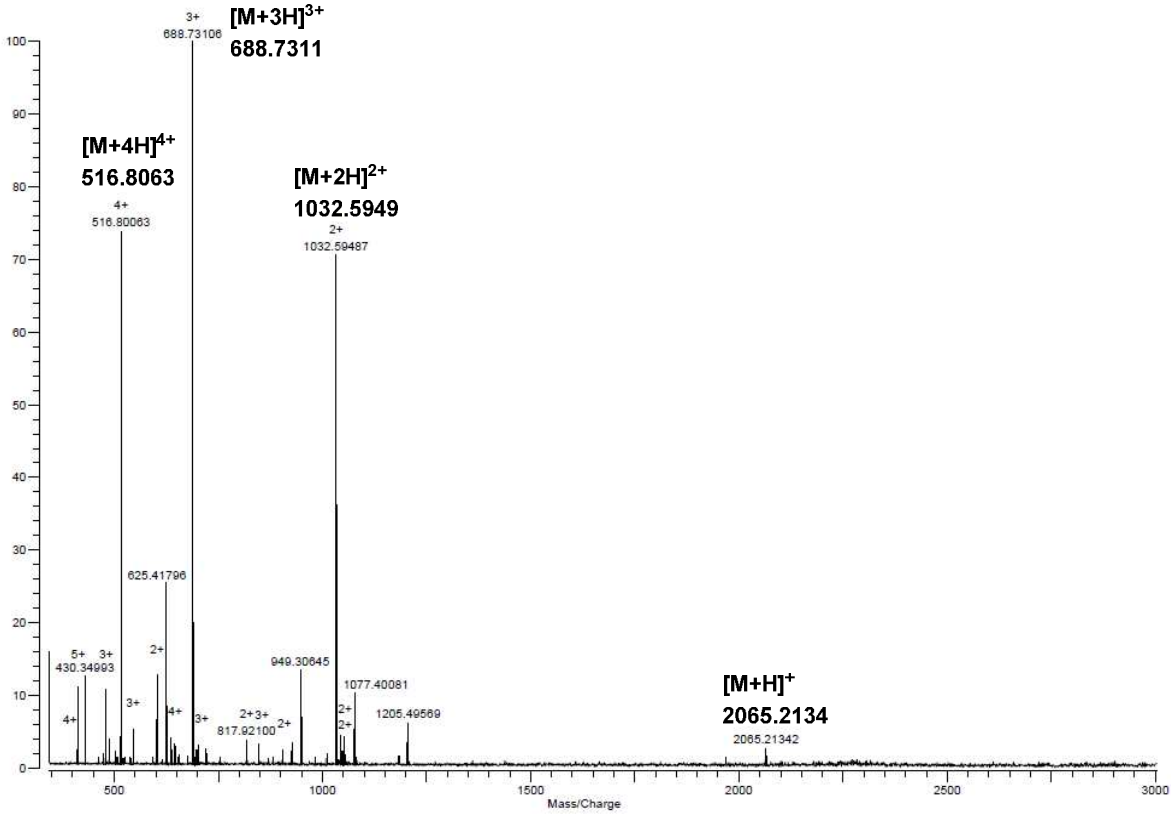

Figure S28. ESI-mass spectrum of **6c**

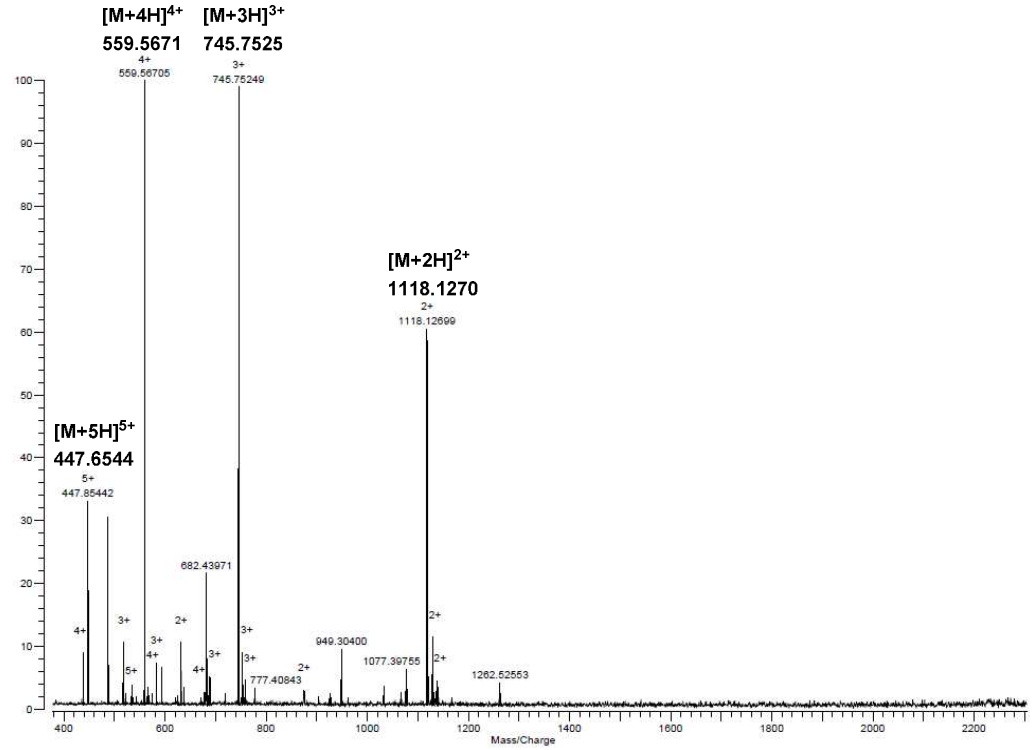

Figure S29. ESI-mass spectrum of **6d**

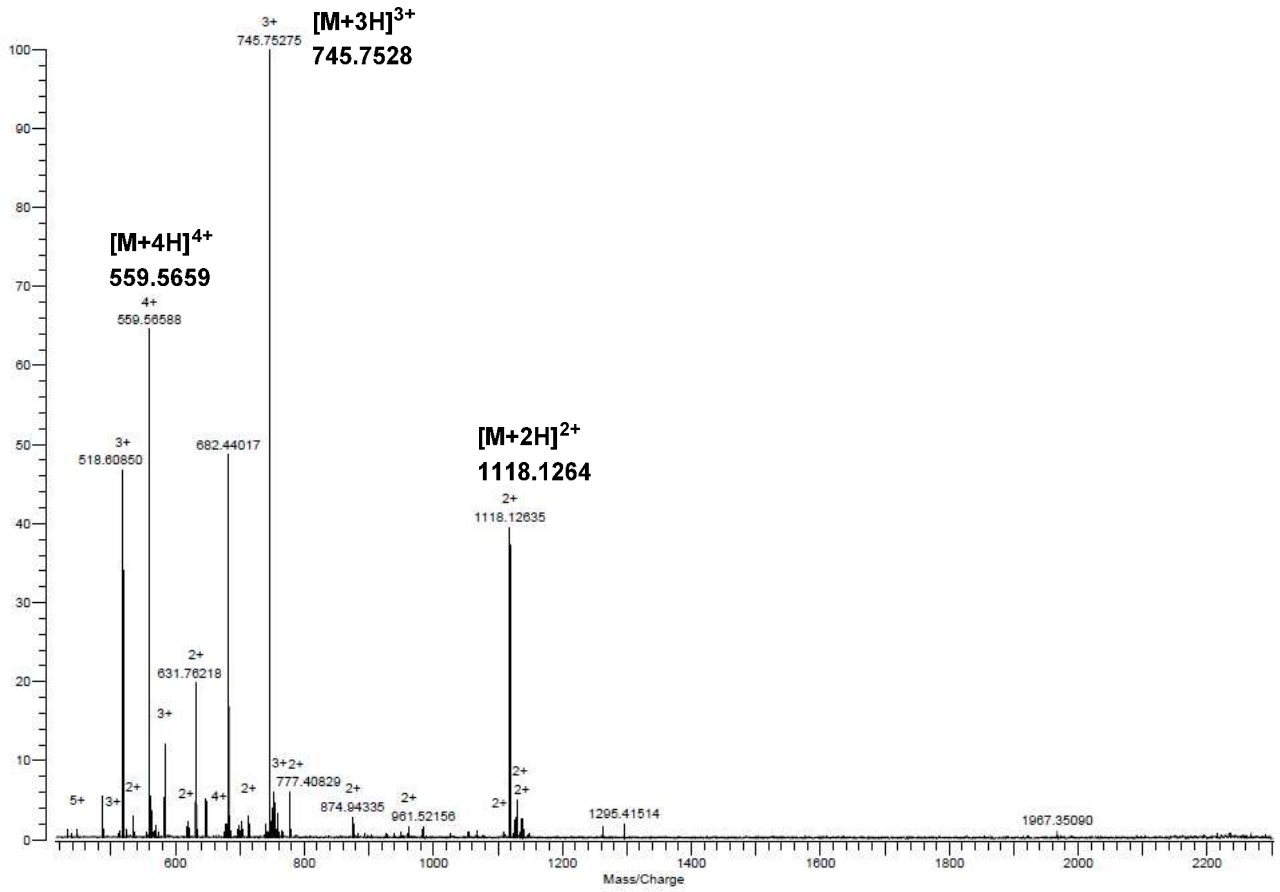

Figure S30. ESI-mass spectrum of **6e**

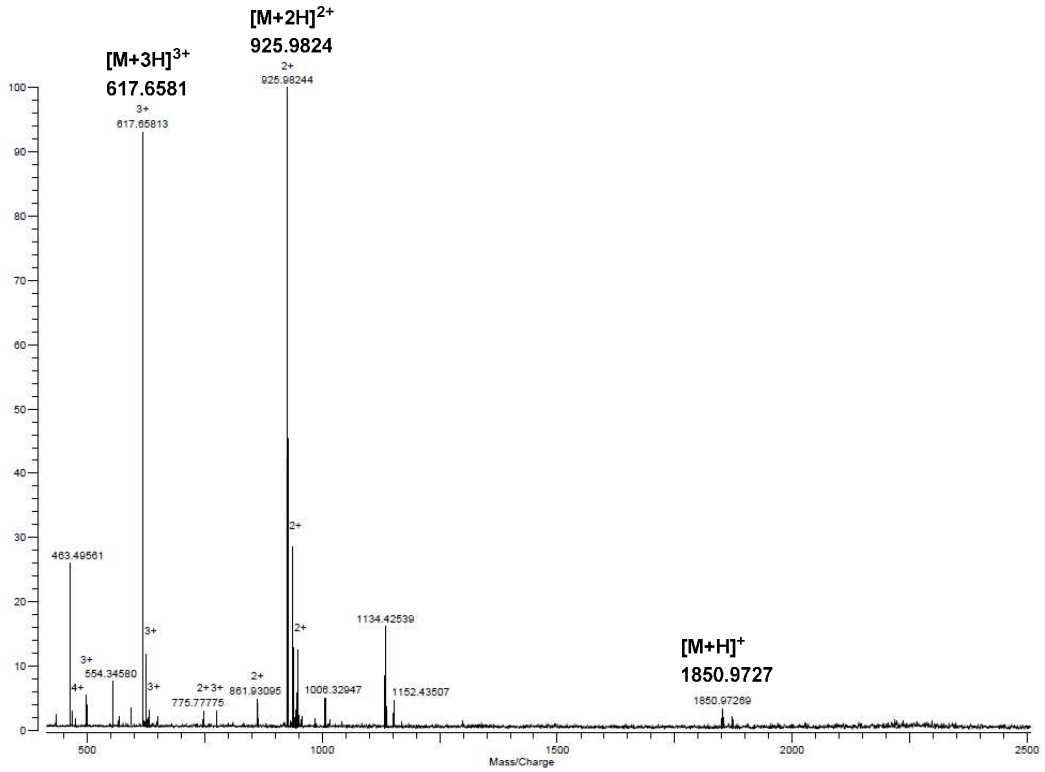

Figure S31. ESI-mass spectrum of **6f**

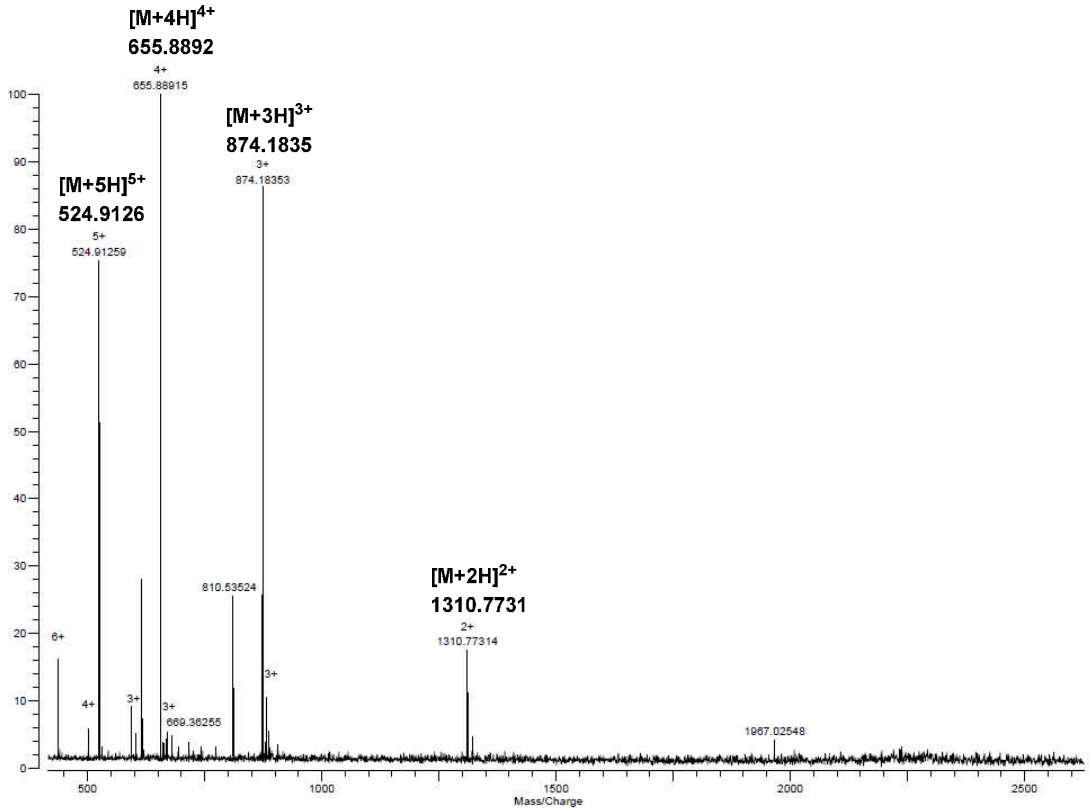

Figure S32. ESI-mass spectrum of **6g**

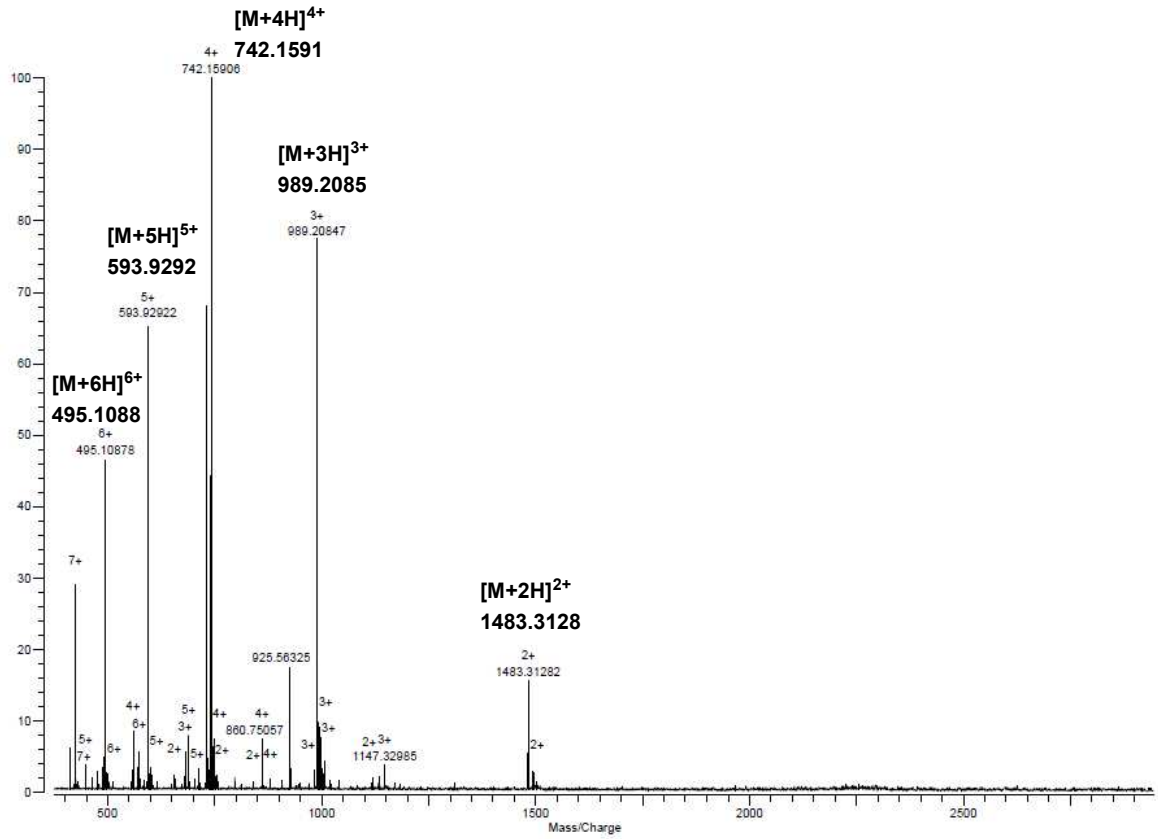

Figure S33. ESI-mass spectrum of **6h**

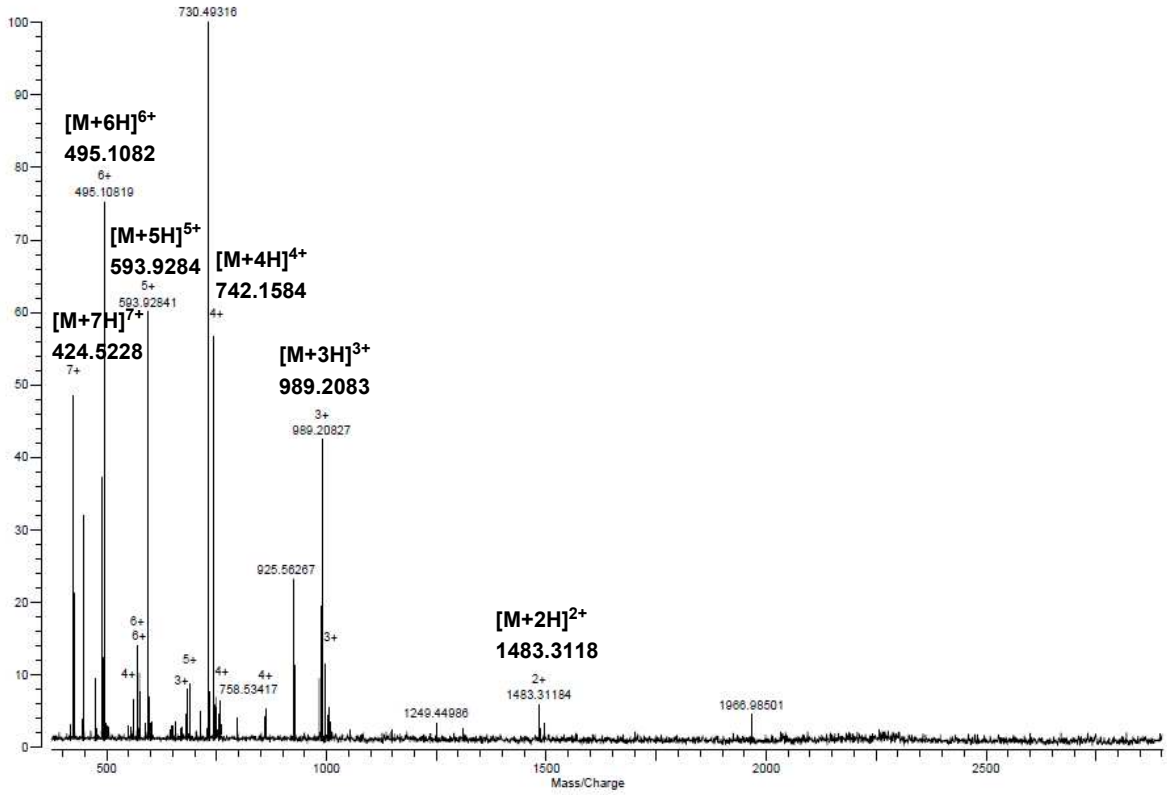

Figure S34. ESI-mass spectrum of **6i**

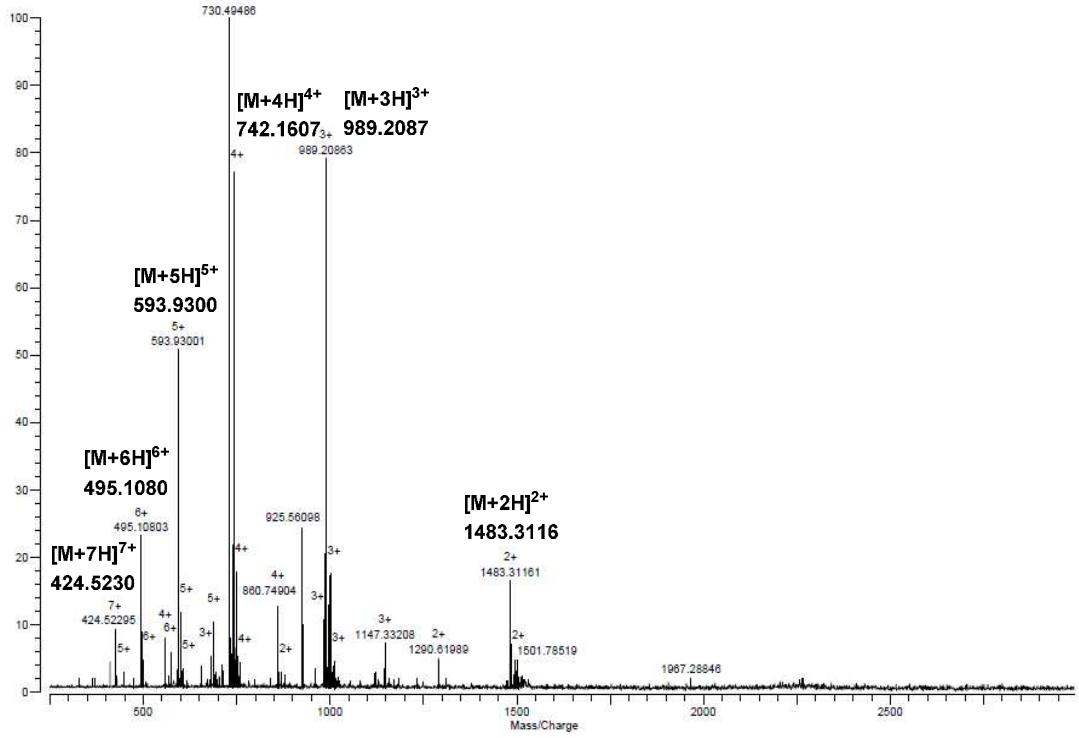

Figure S35. ESI-mass spectrum of **6j**

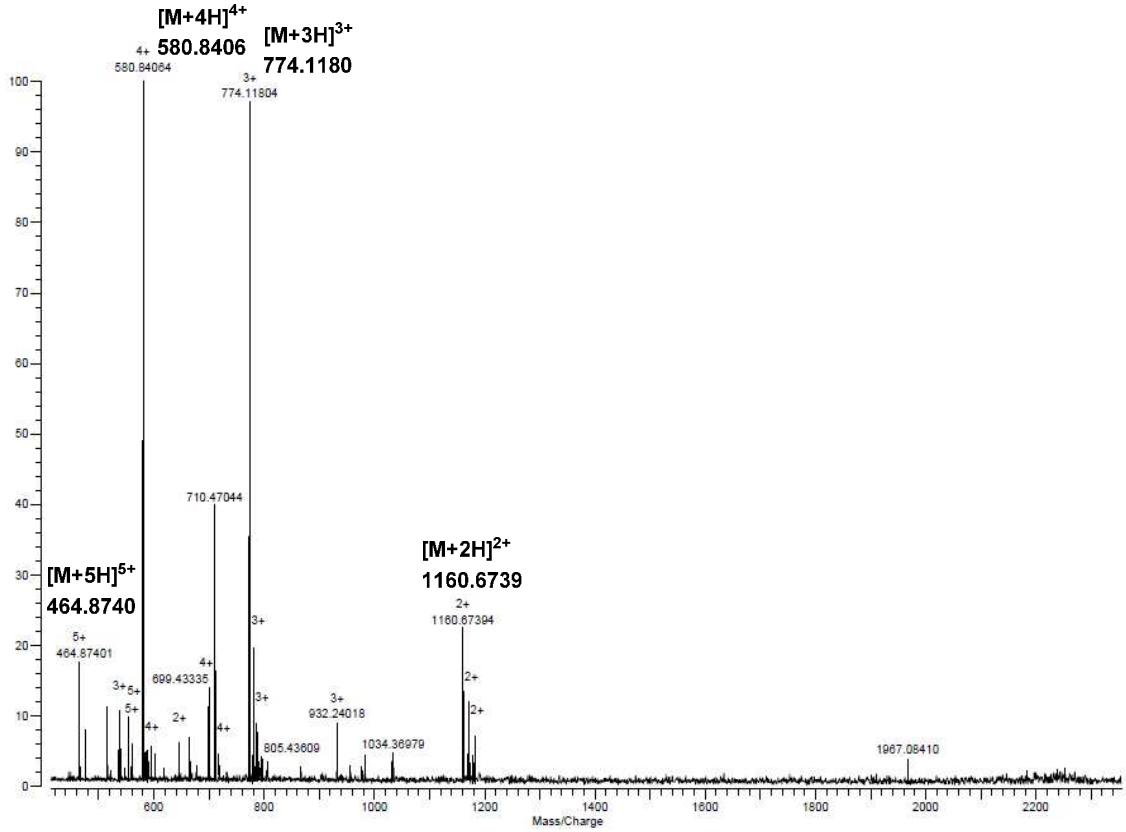

Figure S36. ESI-mass spectrum of **7a**

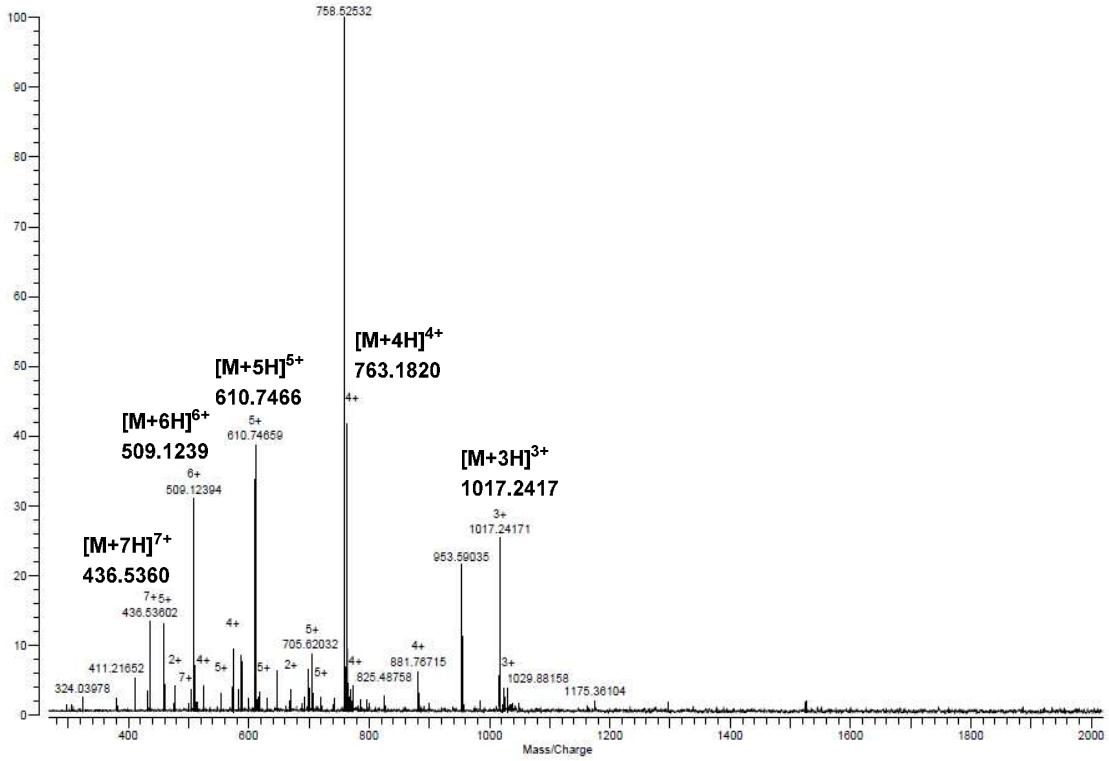

Figure S37. ESI-mass spectrum of **7b**

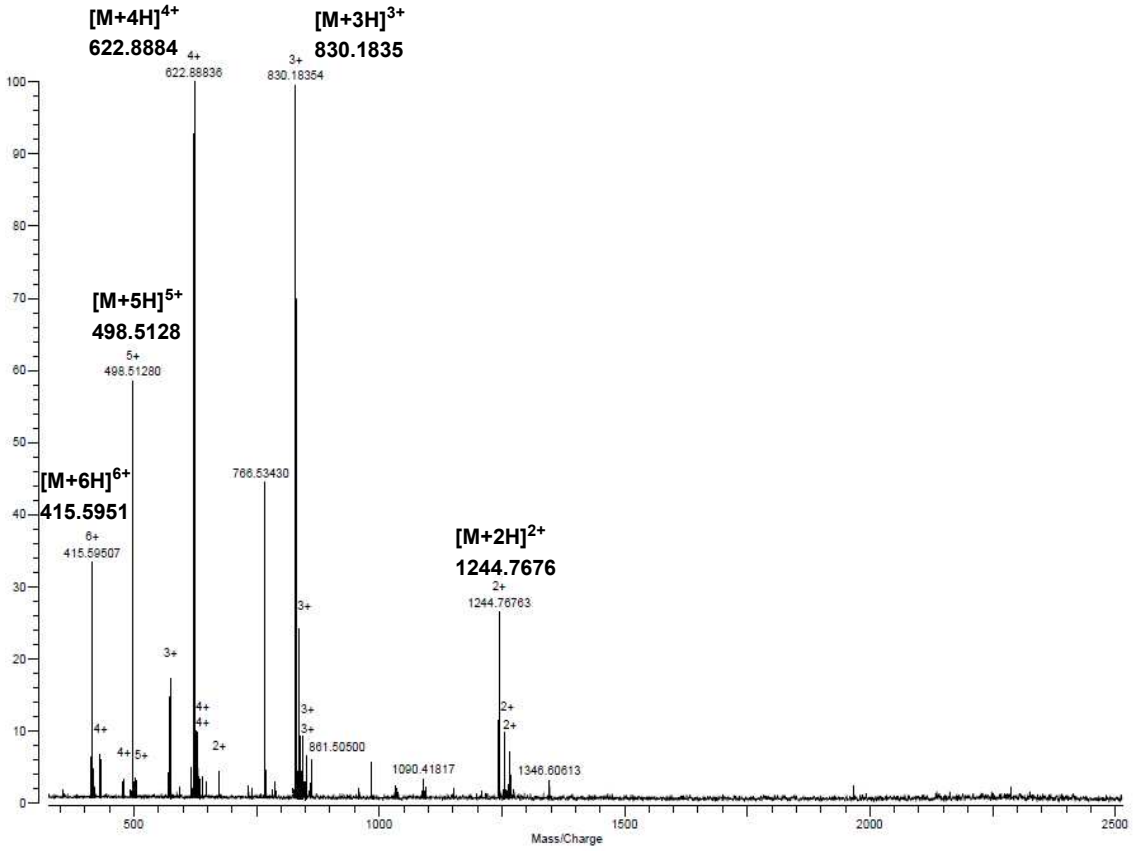

Figure S38. ESI-mass spectrum of **8**

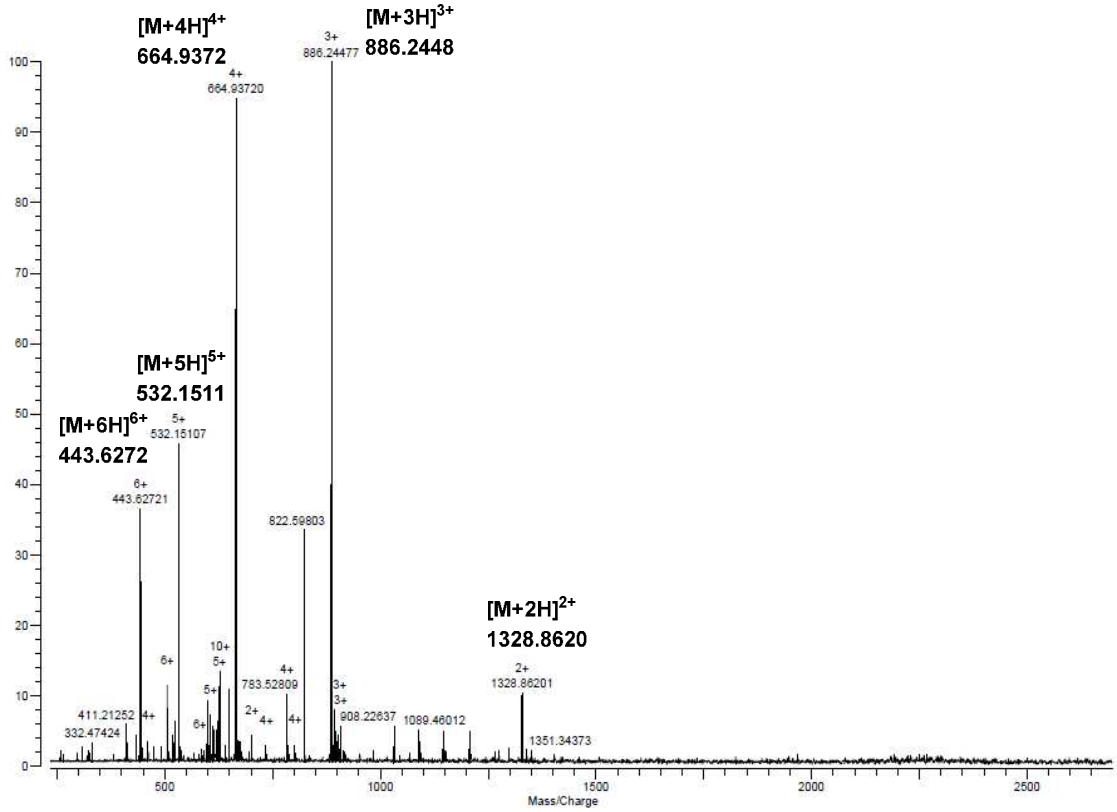

Figure S39. ESI-mass spectrum of **9**

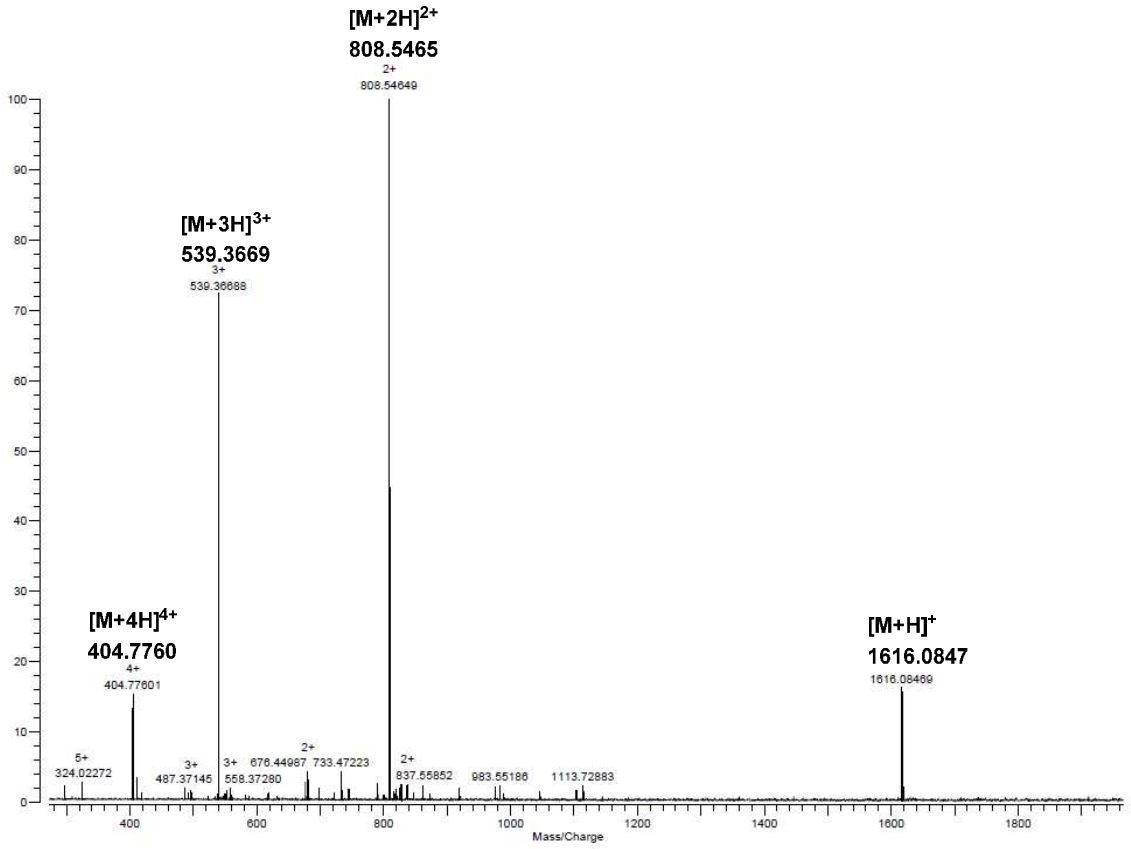

Figure S40. ESI-mass spectrum of **10a**

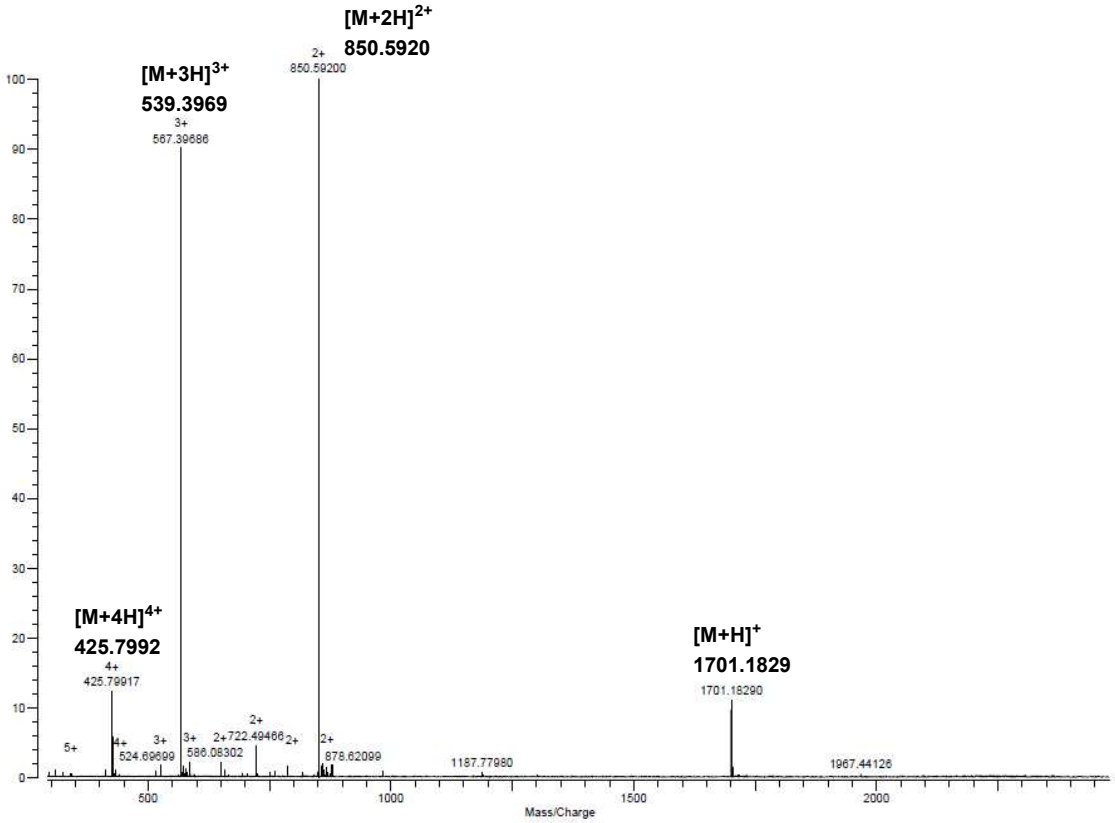

Figure S41. ESI-mass spectrum of **10b**

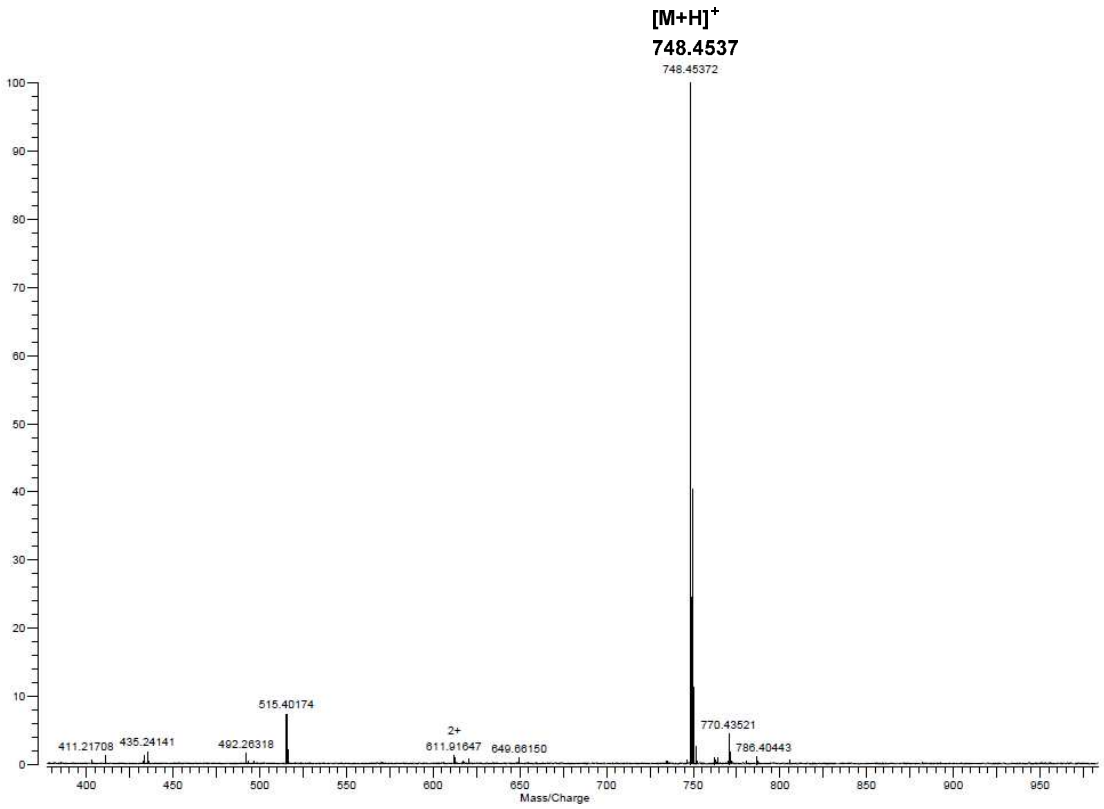

Figure S42. ESI-mass spectrum of **11**

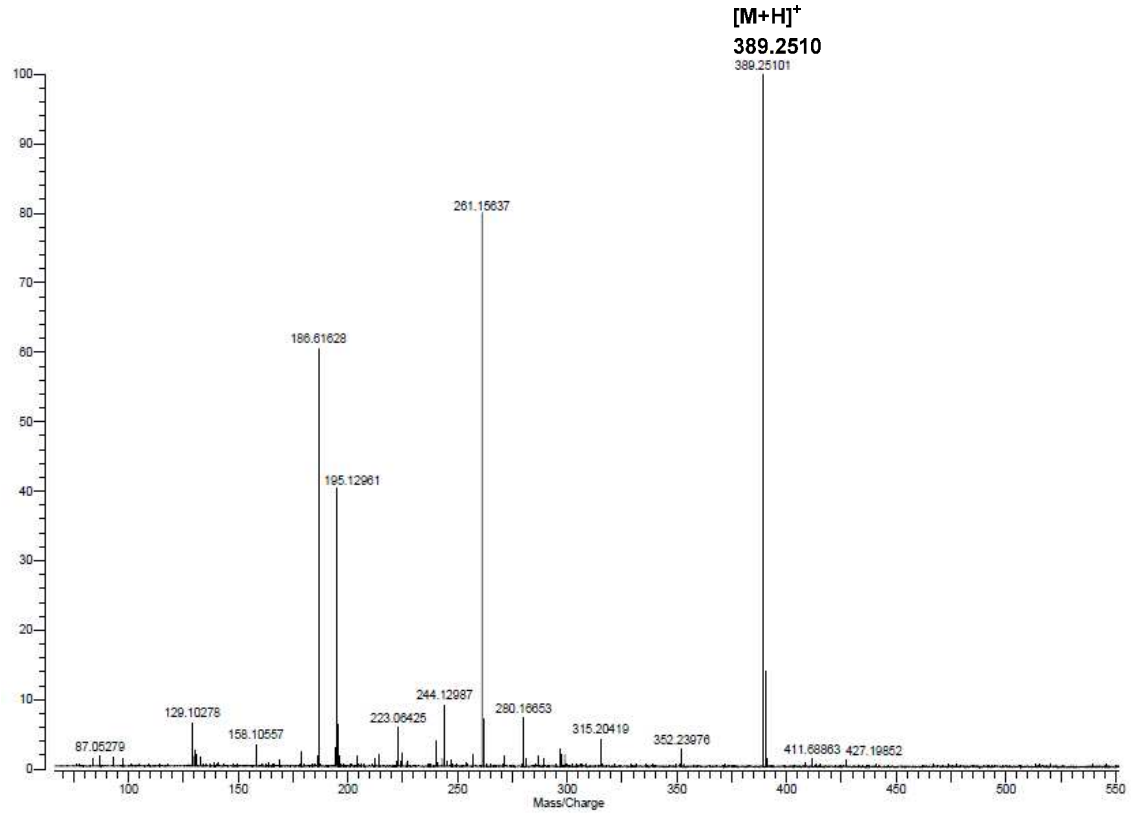

Figure S43. ESI-mass spectrum of **37**

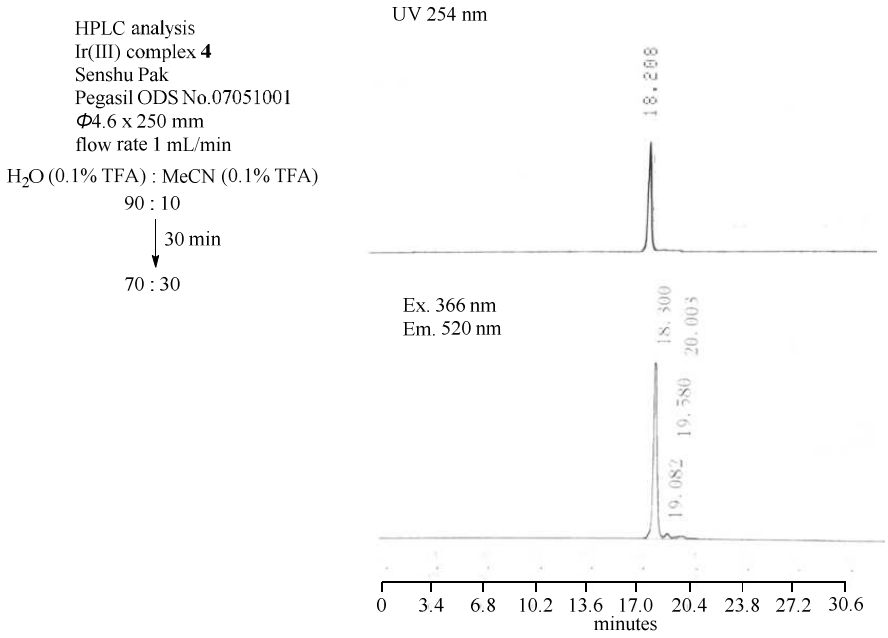

Figure S44. HPLC analysis of **4**

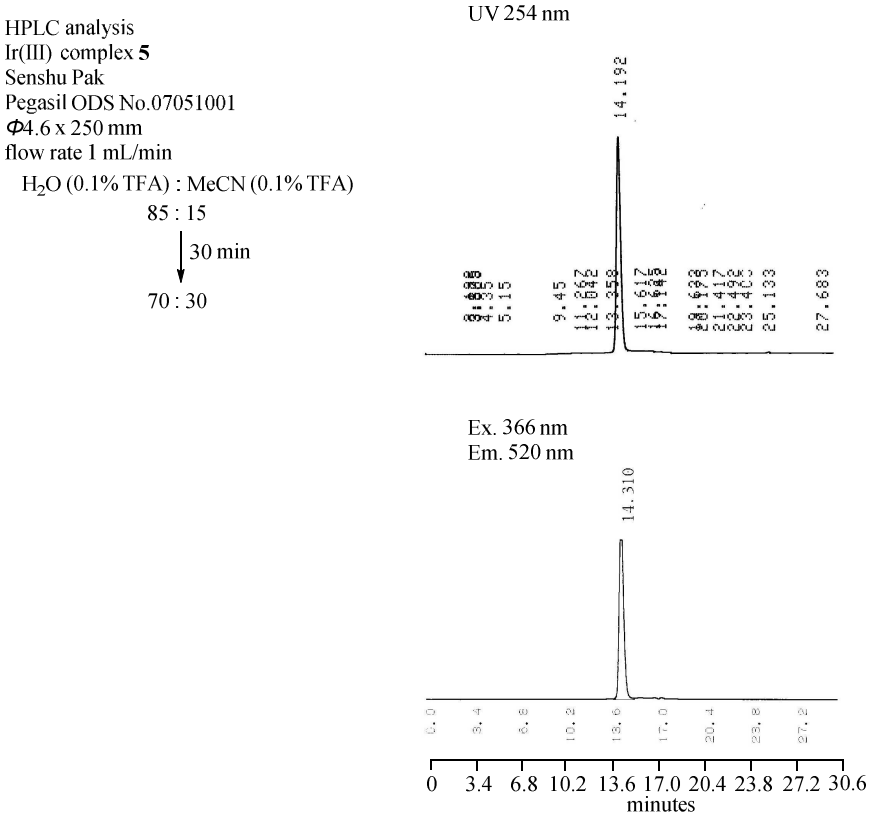

Figure S45. HPLC analysis of **5**

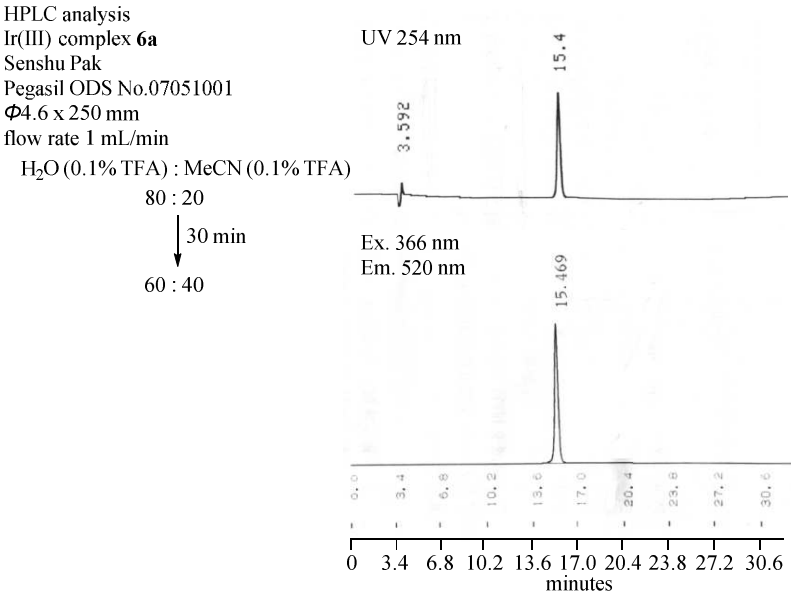

Figure S46. HPLC analysis of **6a**

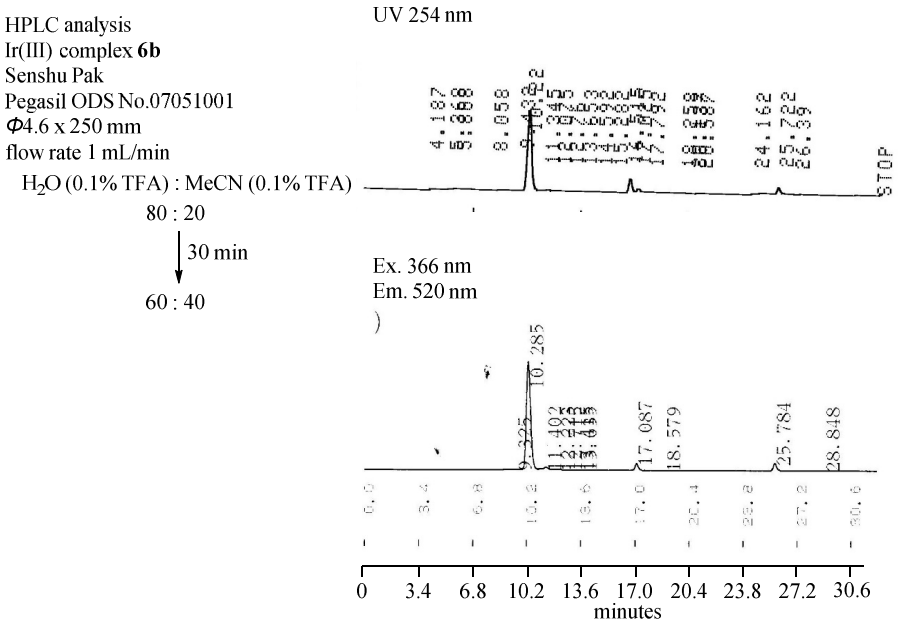

Figure S47. HPLC analysis of **6b**

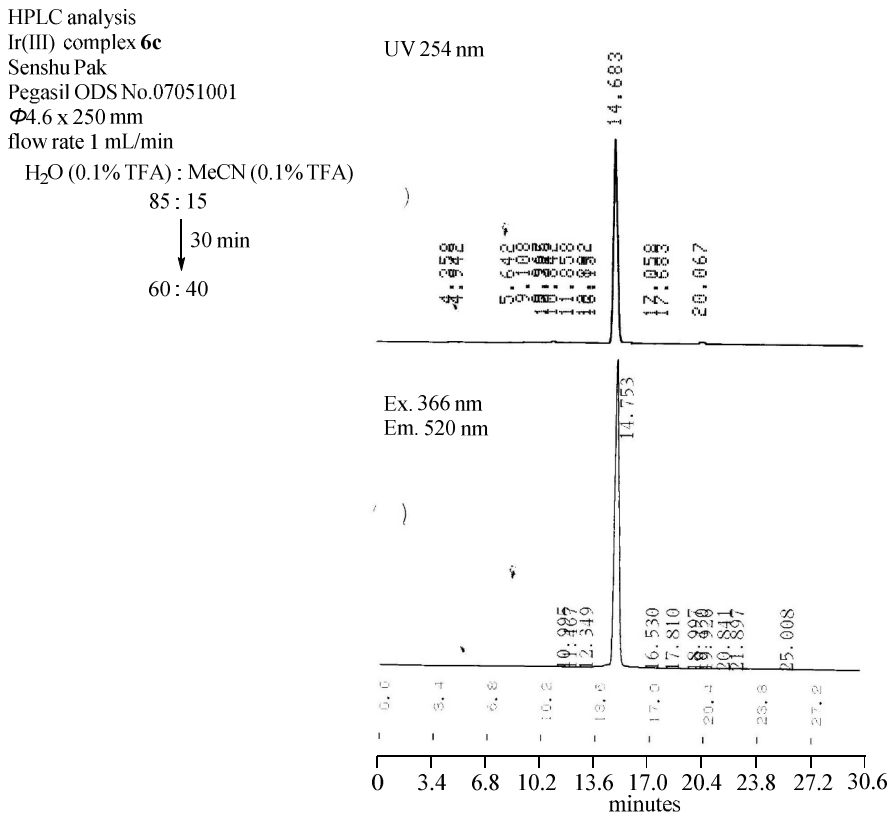

Figure S48. HPLC analysis of **6c**

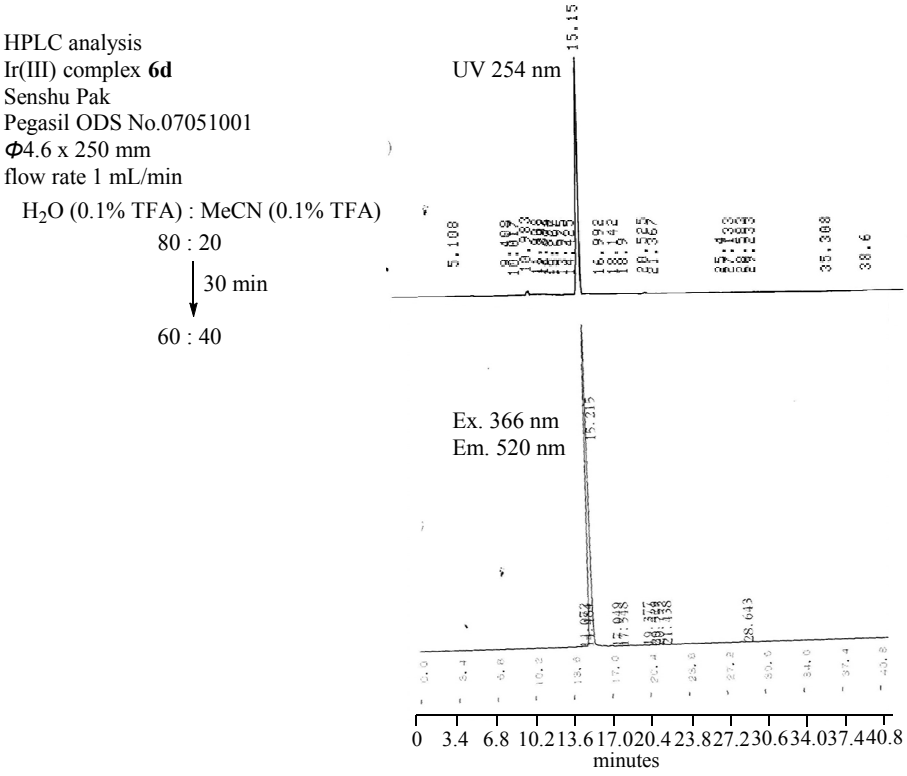

Figure S49. HPLC analysis of **6d**

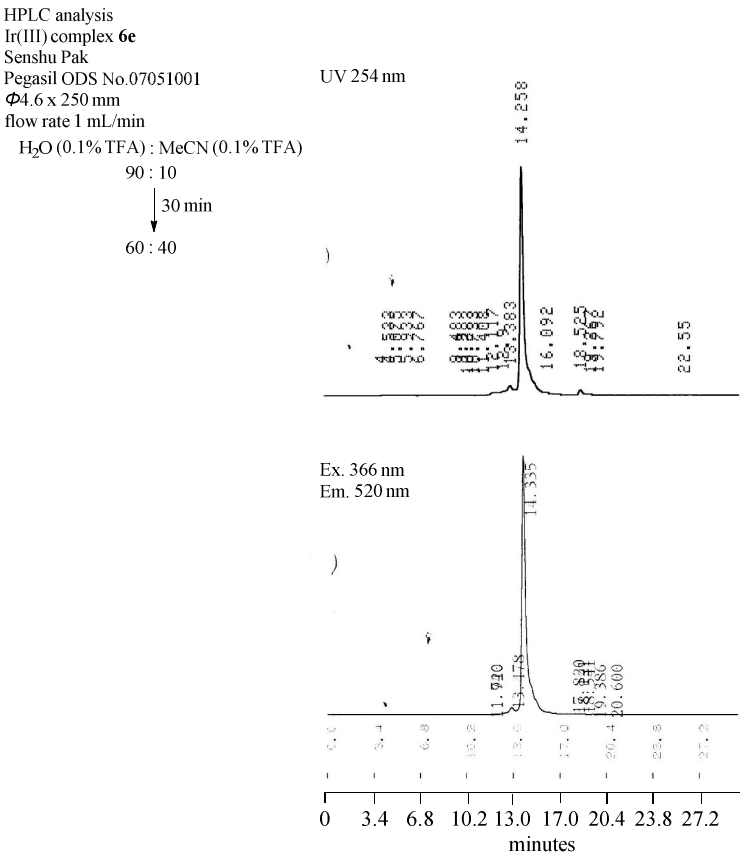

Figure S50. HPLC analysis of **6e**

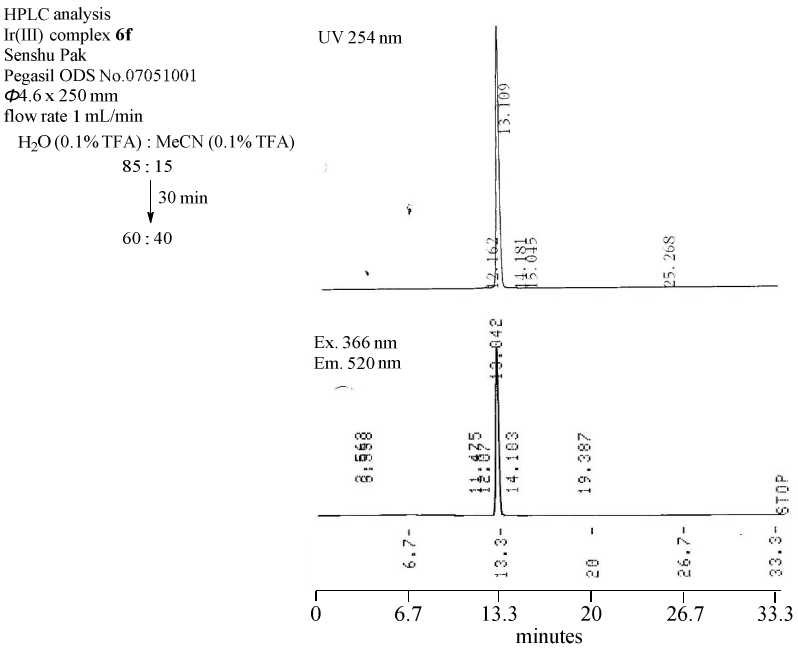

Figure S51. HPLC analysis of **6f**

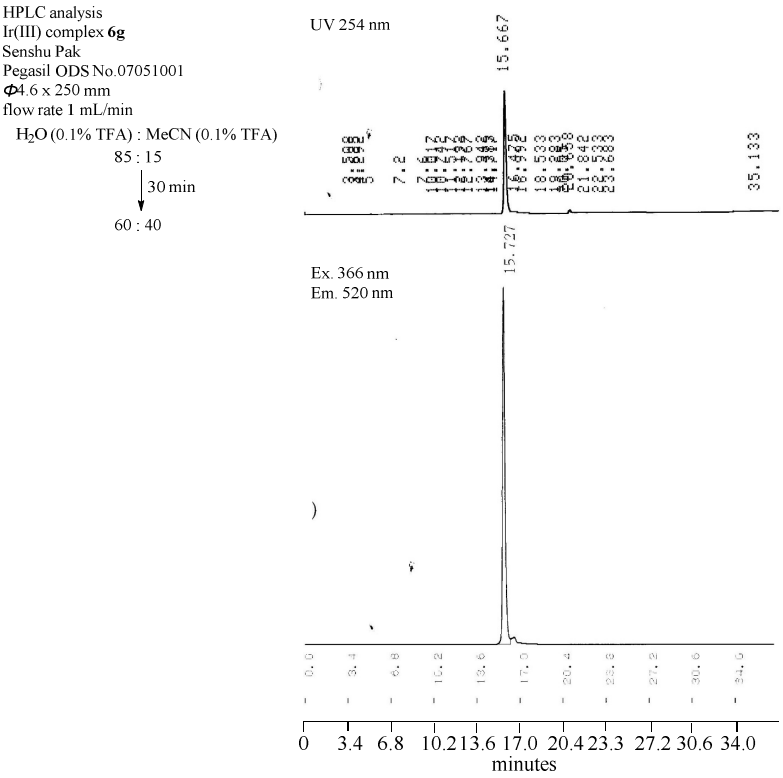

Figure S52. HPLC analysis of **6g**

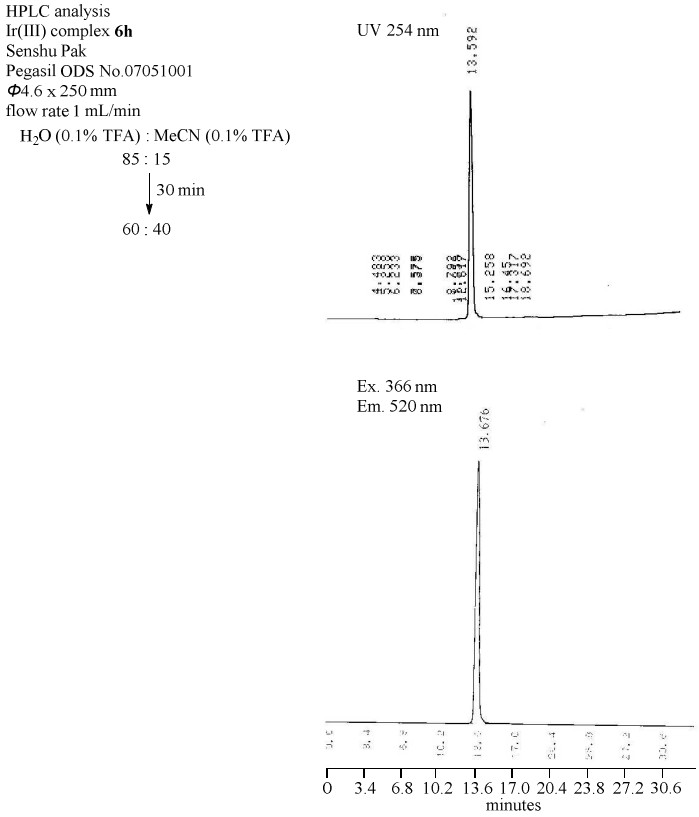

Figure S53. HPLC analysis of **6h**

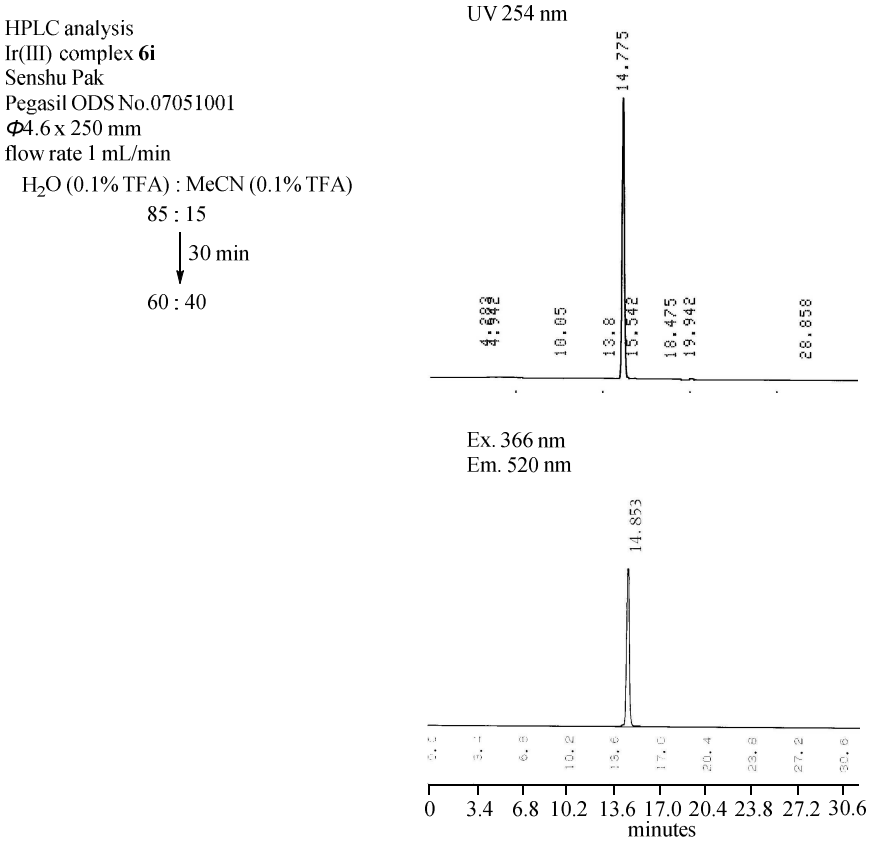

Figure S54. HPLC analysis of **6i**

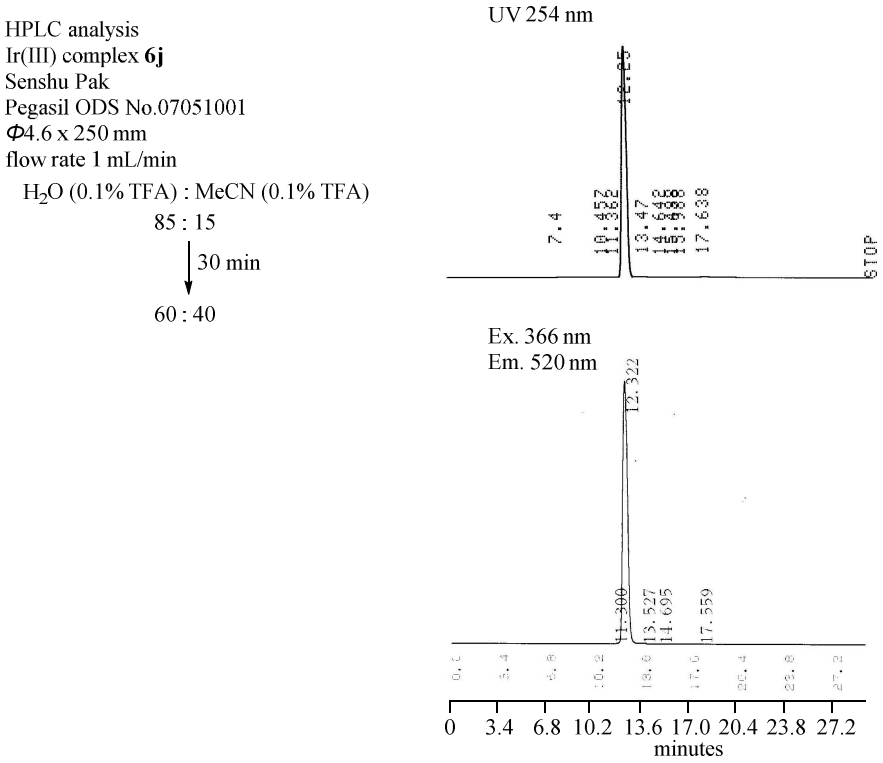

Figure S55. HPLC analysis of **6j**

HPLC analysis
Ir(III) complex **7a**
Senshu Pak
Pegasil ODS No.07051001
Φ4.6 x 250 mm
flow rate 1 mL/min
H_2O (0.1% TFA) : MeCN (0.1% TFA)
80 : 20
30 min
60 : 40

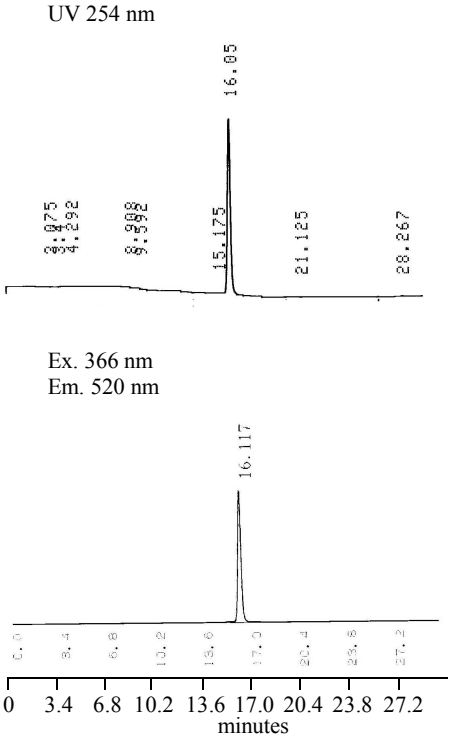

Figure S56. HPLC analysis of **7a**

HPLC analysis
Ir(III) complex **7b**
Senshu Pak
Pegasil ODS No.07051001
Φ4.6 x 250 mm
flow rate 1 mL/min
H_2O (0.1% TFA) : MeCN (0.1% TFA)
85 : 15
30 min
60 : 40

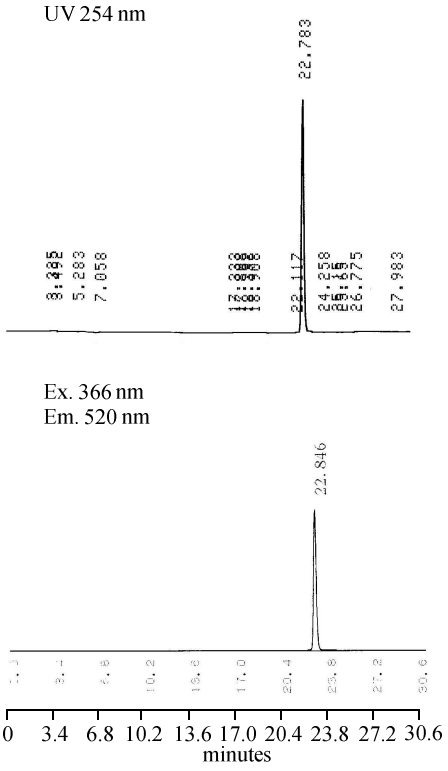

Figure S57. HPLC analysis of **7b**

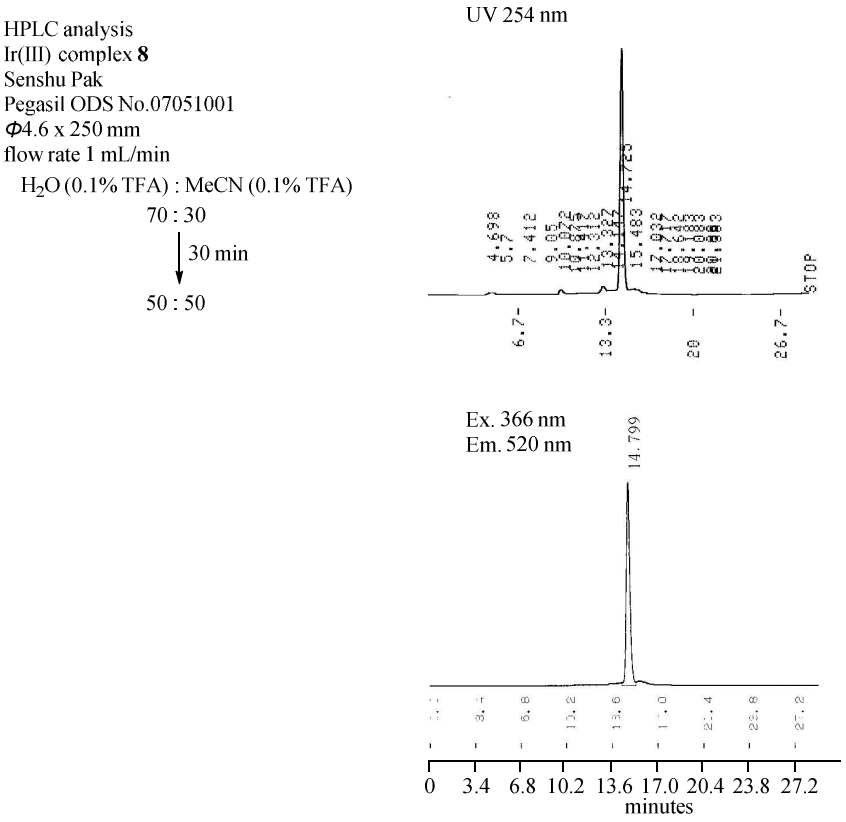

Figure S58. HPLC analysis of **8**

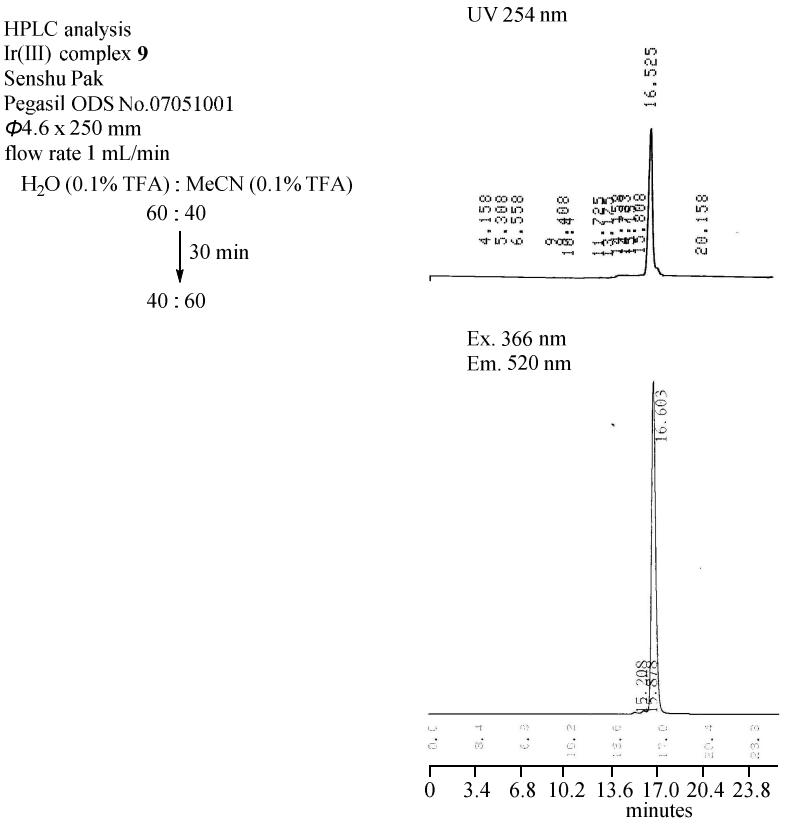

Figure S59. HPLC analysis of **9**

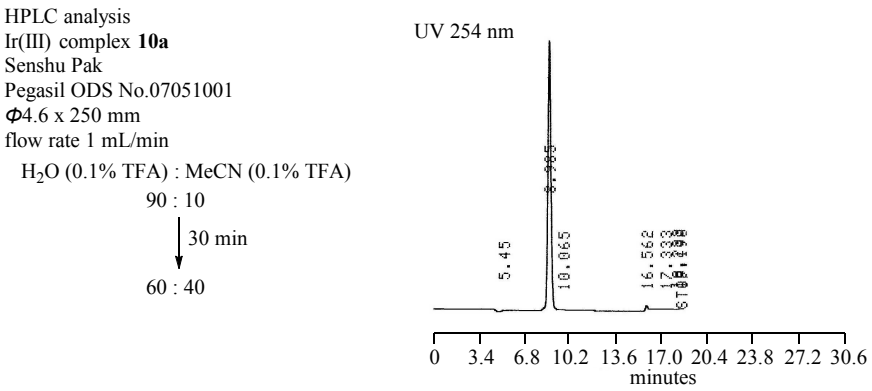

Figure S60. HPLC analysis of **10a**

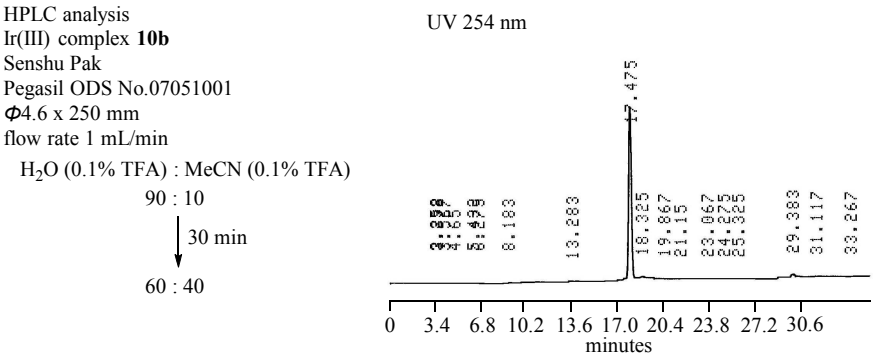

Figure S61. HPLC analysis of **10b**

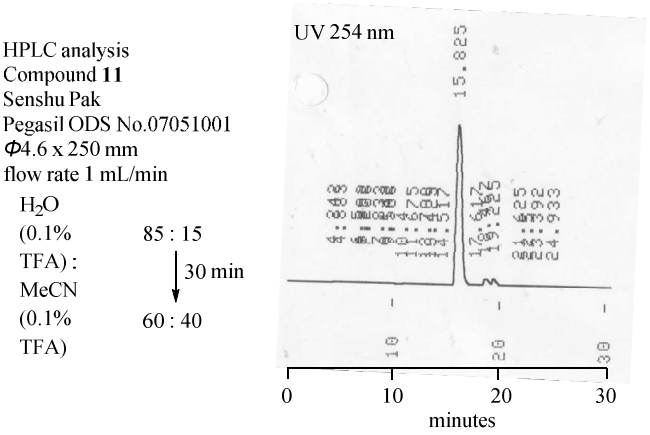

Figure S62. HPLC analysis of **11**

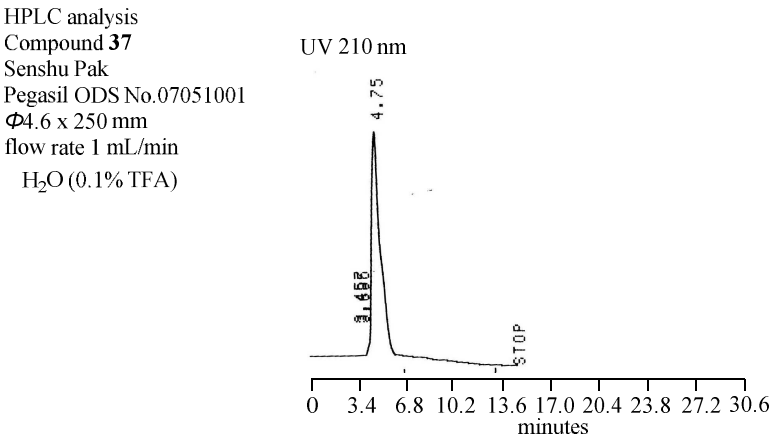

Figure S63. HPLC analysis of **37**

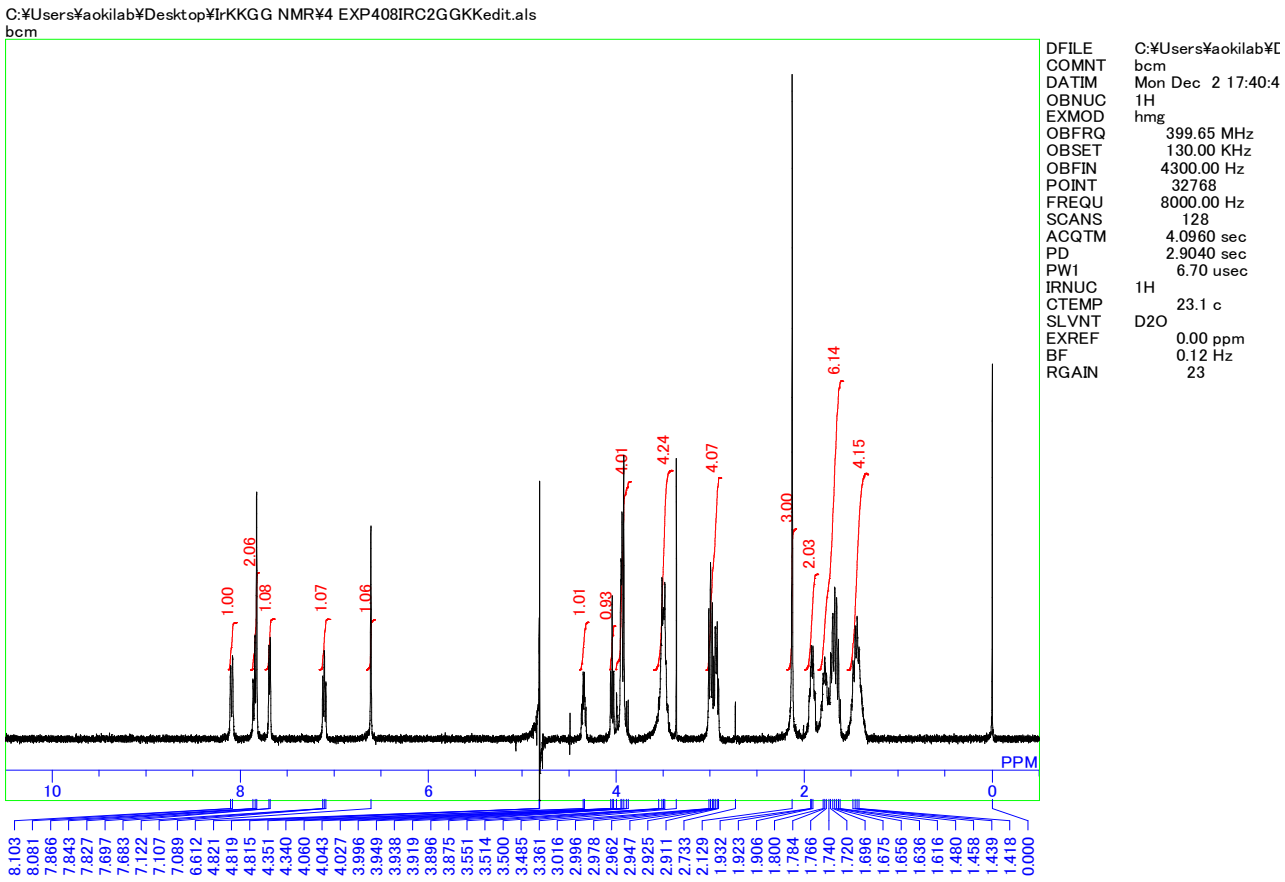

Figure S64. ^{1}H NMR spectrum (D_2O) of **4**

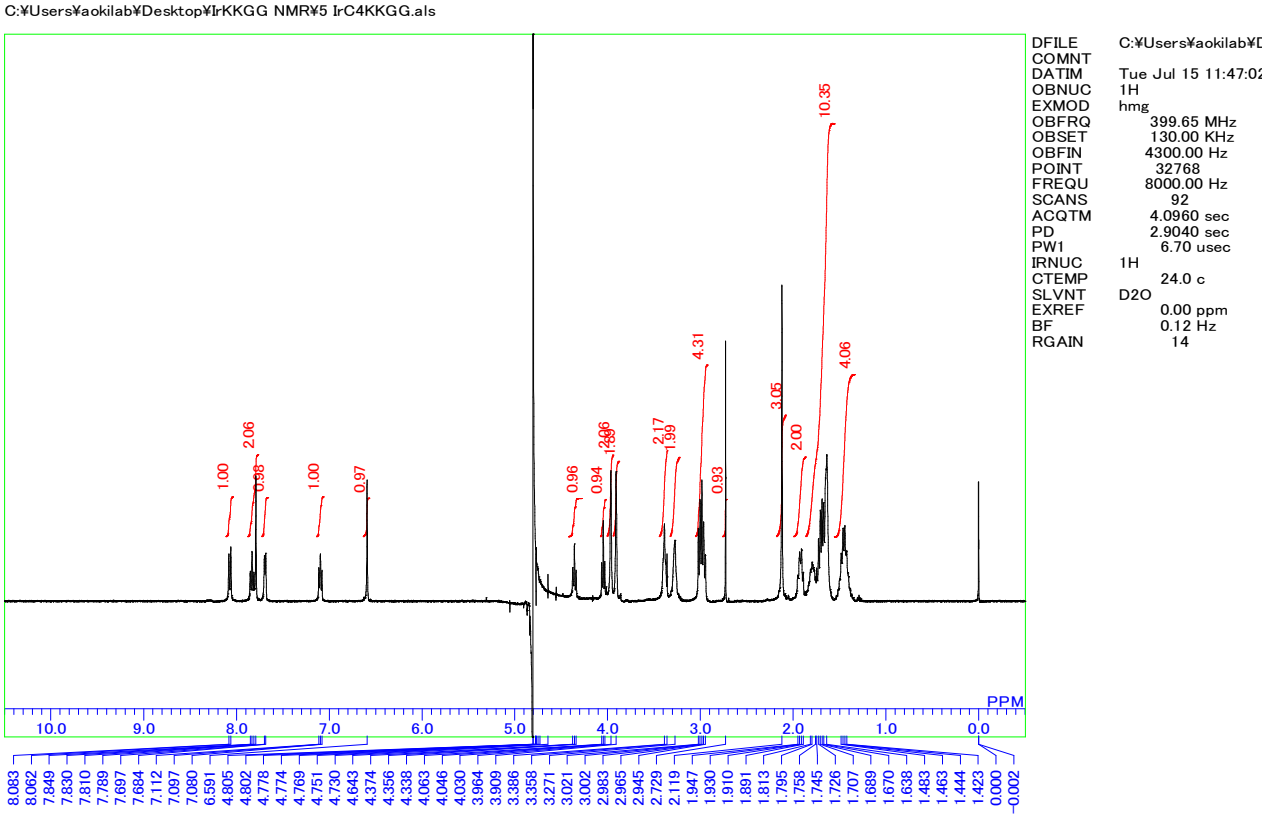

Figure S65. ^{1}H NMR spectrum (D_2O) of **5**

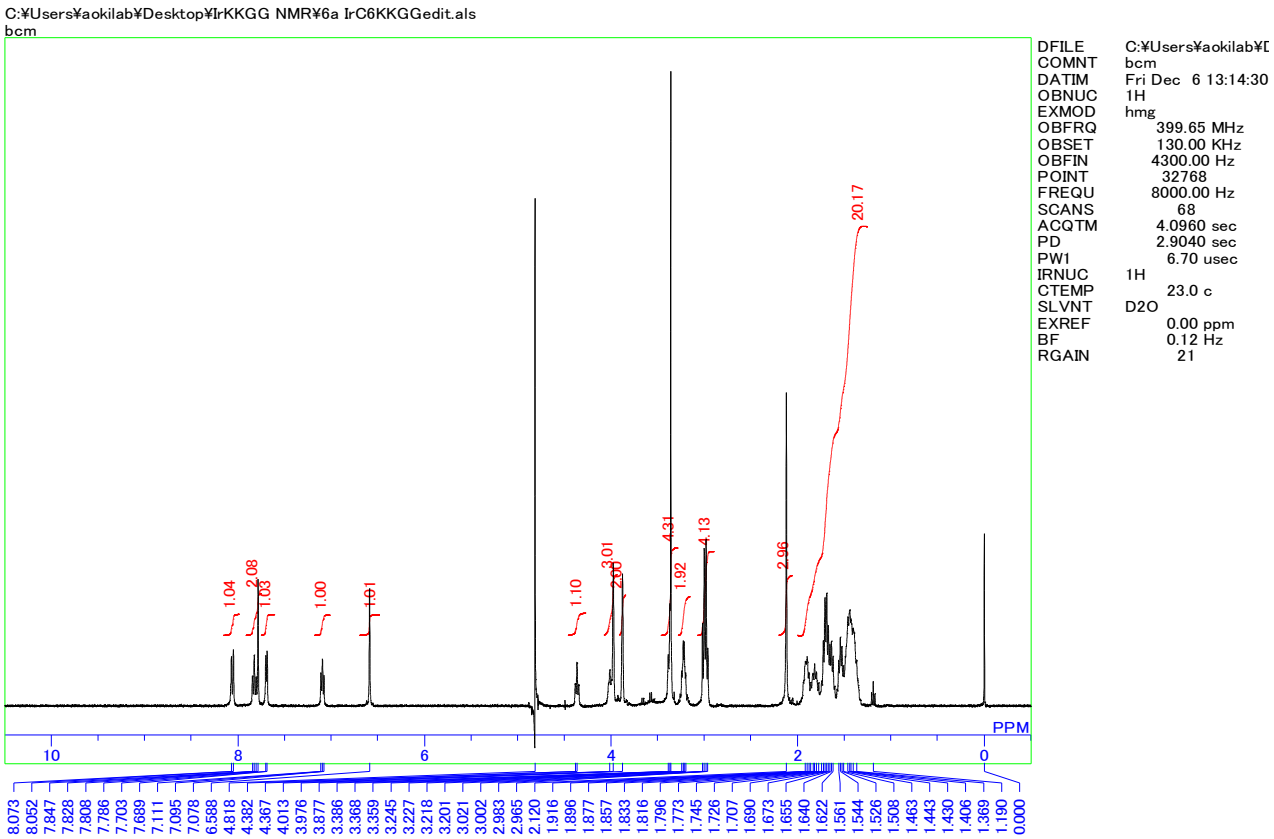

Figure S66. ^{1}H NMR spectrum (D_2O) of **6a**

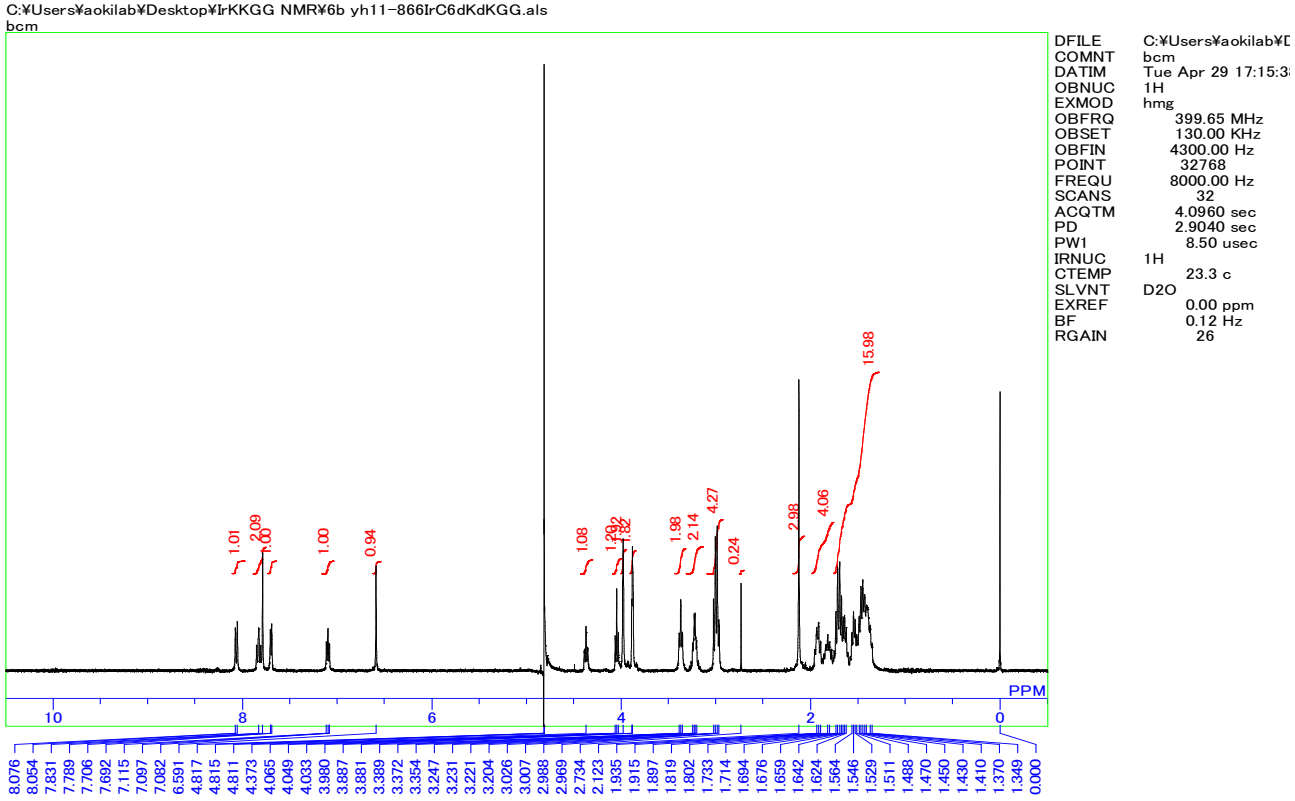

Figure S67. ^{1}H NMR spectrum (D_2O/TSP) of **6b**

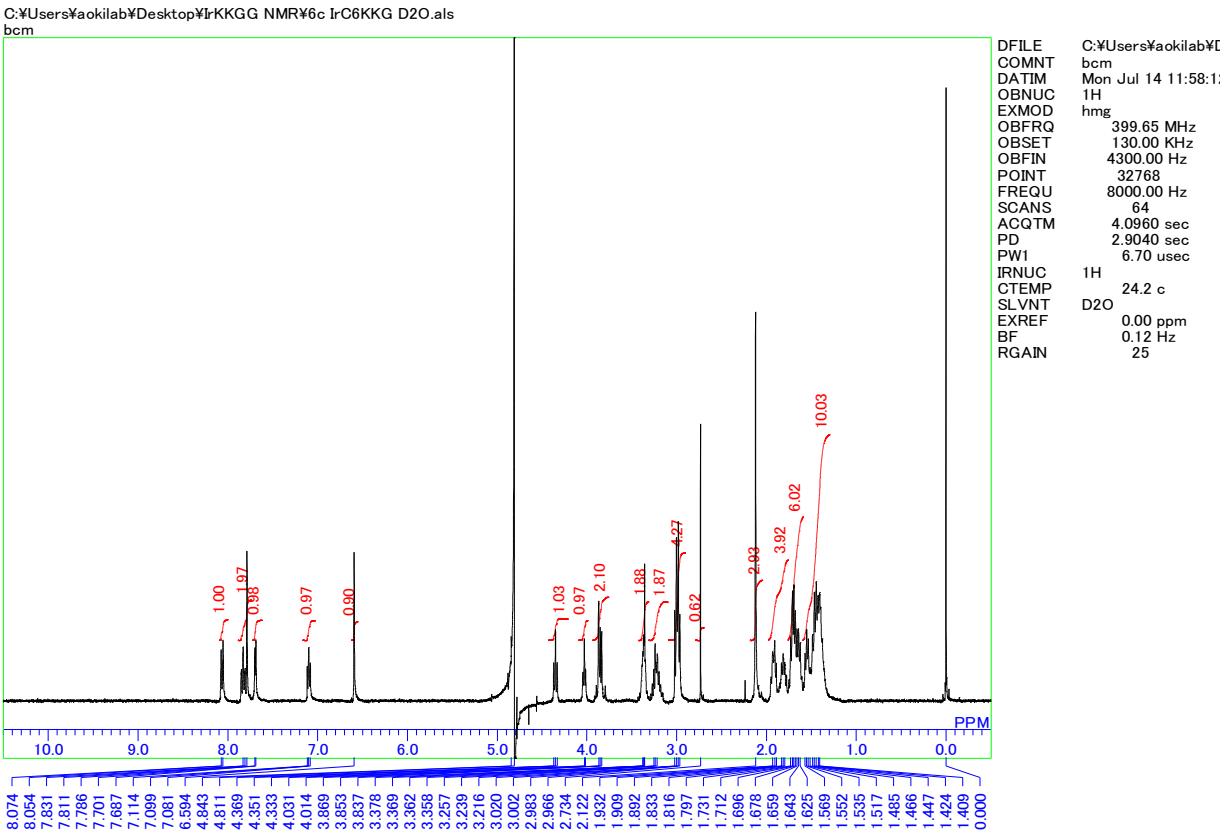

Figure S68. ^{1}H NMR spectrum (D_2O/TSP) of **6c**

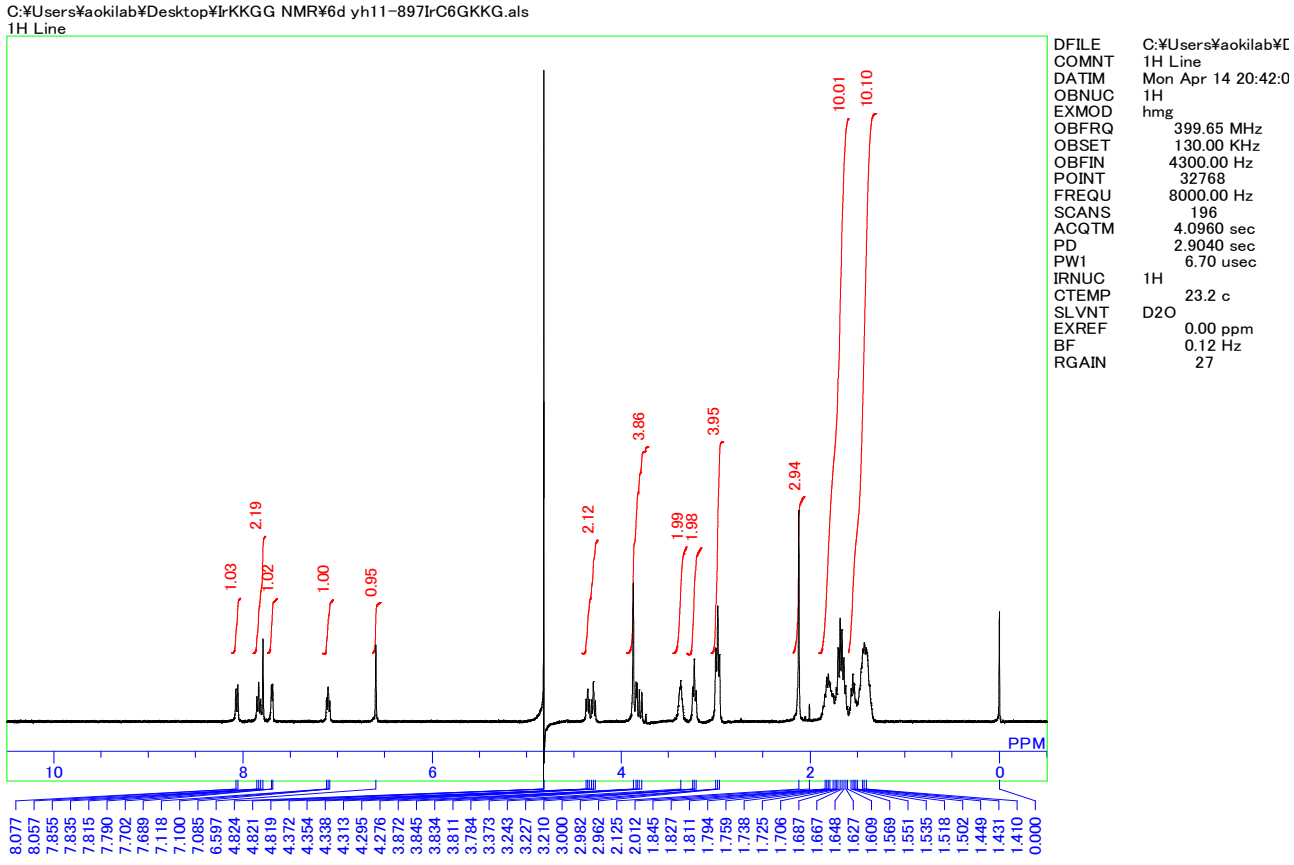

Figure S69. ^{1}H NMR spectrum (D_2O/TSP) of **6d**

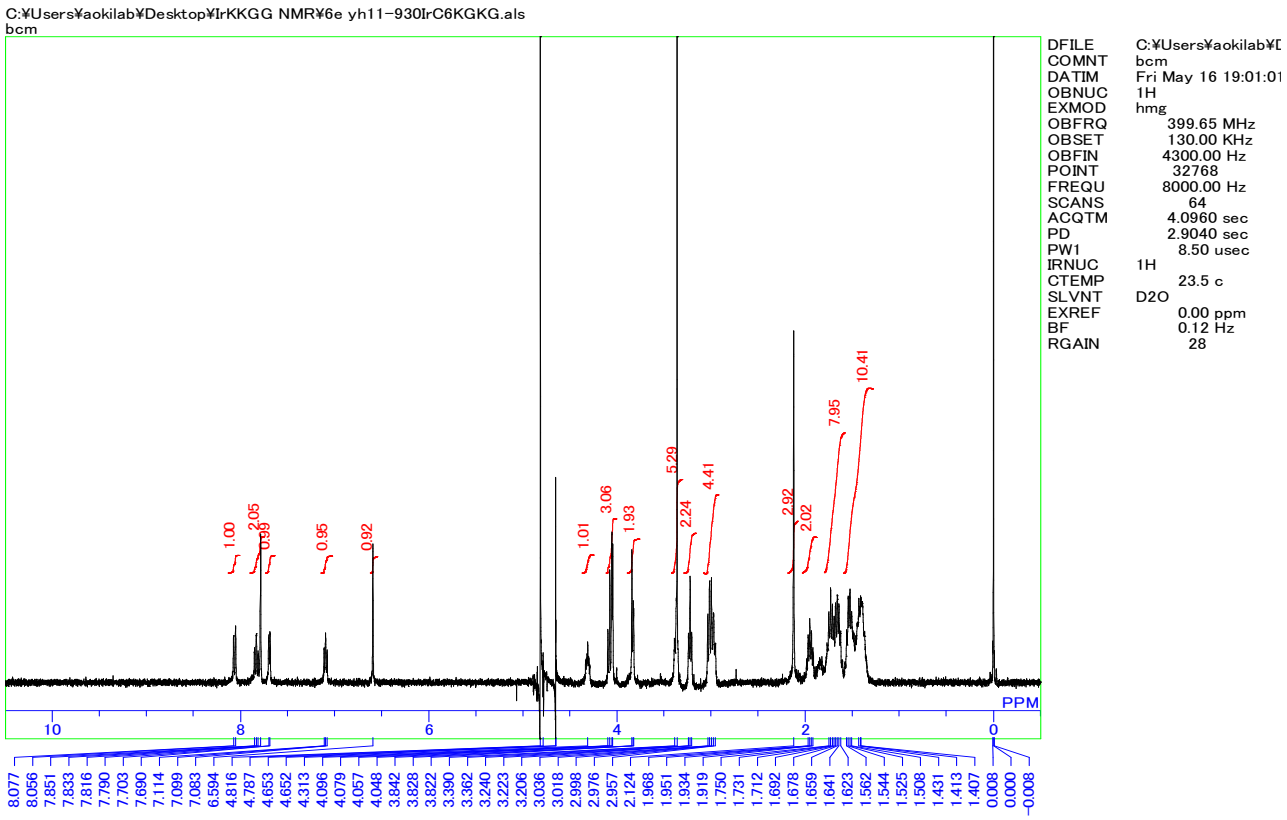

Figure S70. ^{1}H NMR spectrum (D_2O/TSP) of **6e**

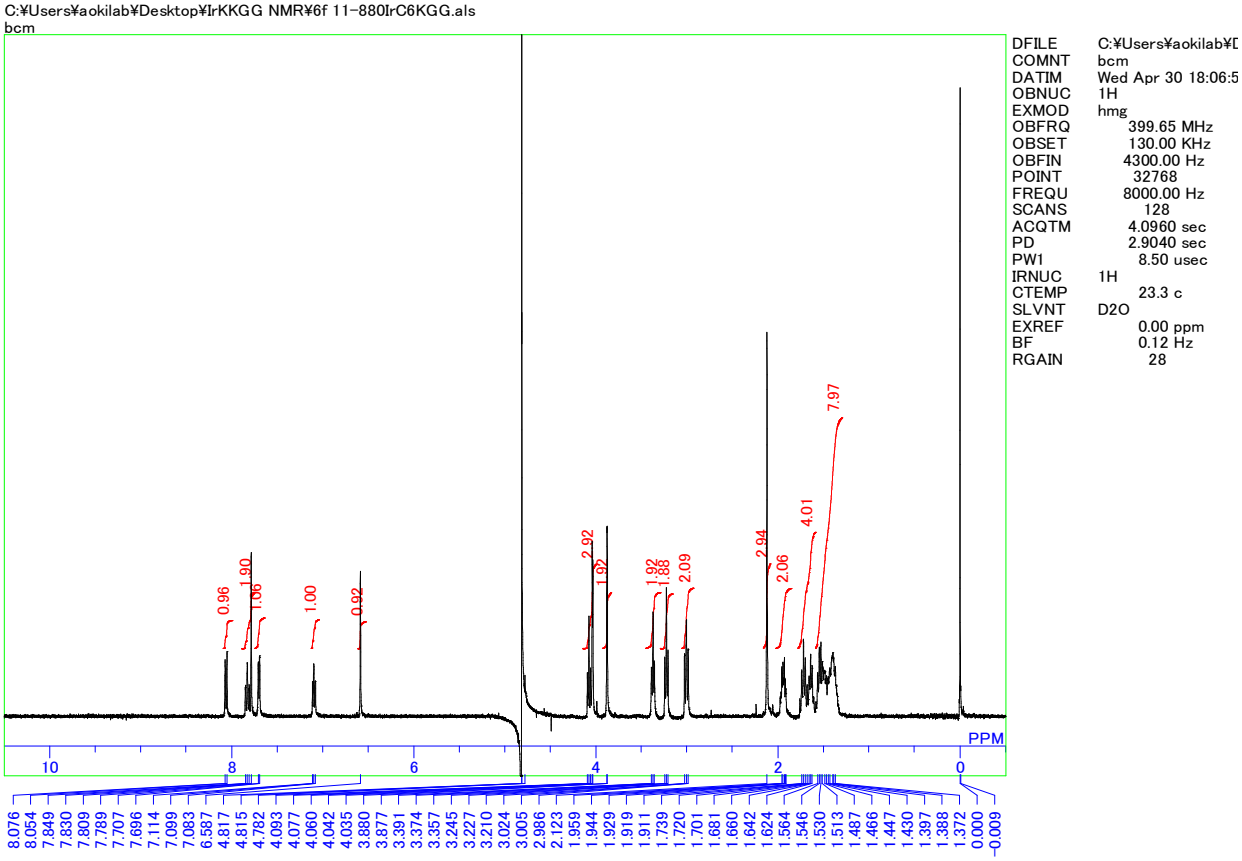

Figure S71. ^{1}H NMR spectrum (D_2O/TSP) of **6f**

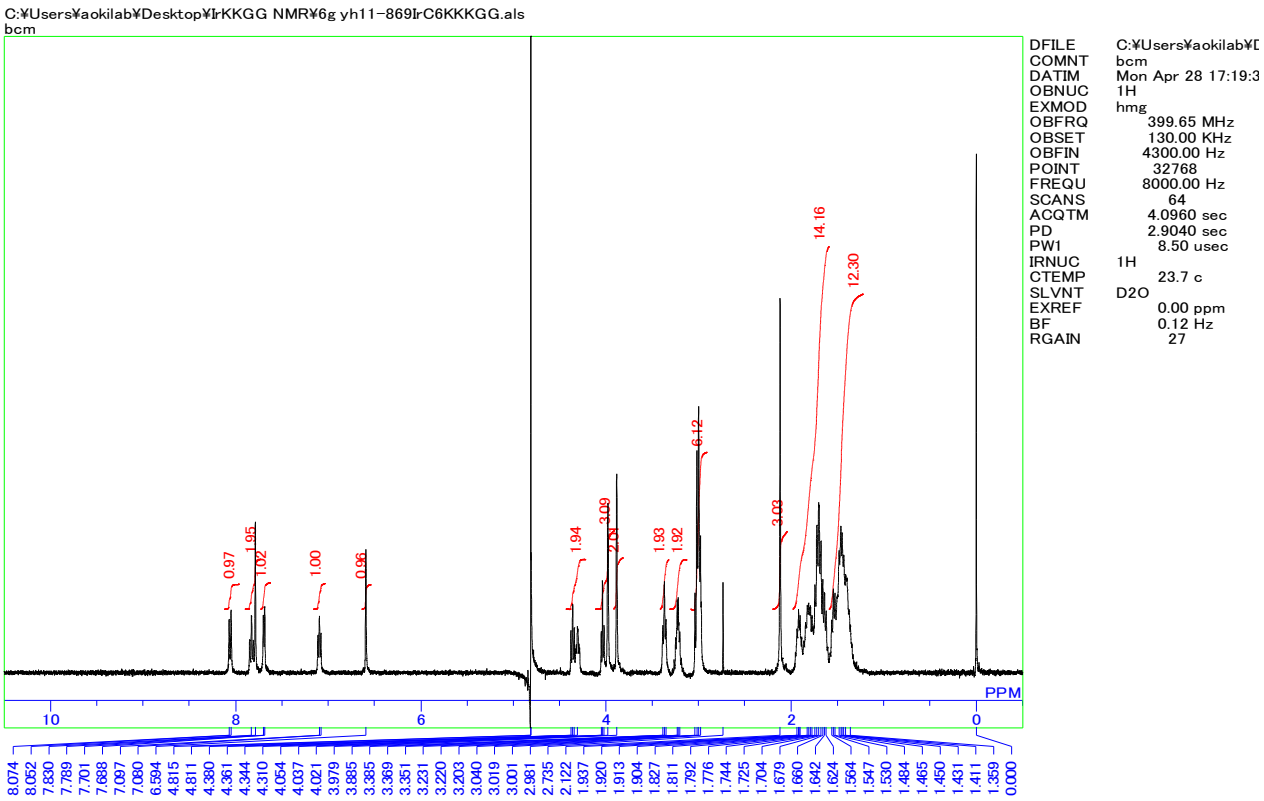

Figure S72. ^{1}H NMR spectrum (D_2O/TSP) of **6g**

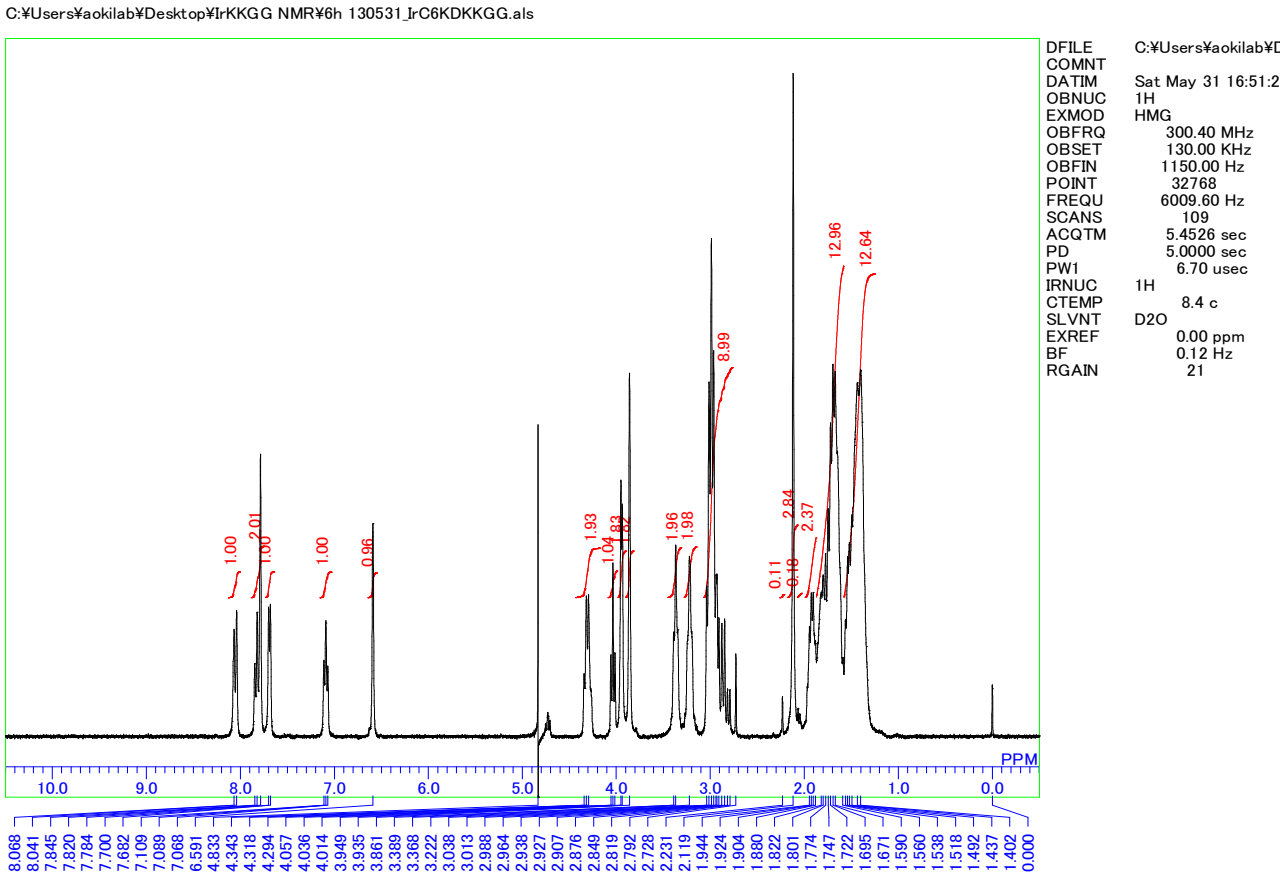

Figure S73. ^{1}H NMR spectrum (D_2O/TSP) of **6h**

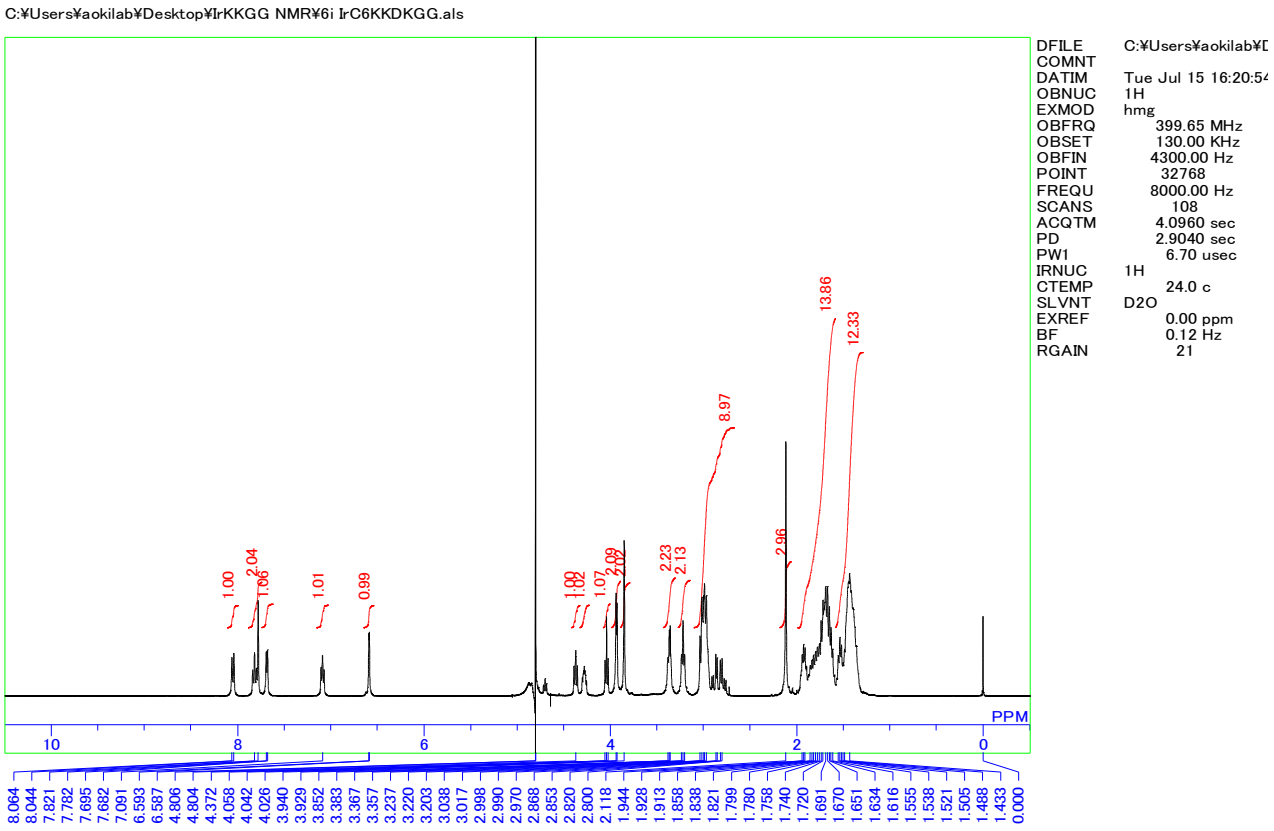

Figure S74. ^{1}H NMR spectrum (D_2O/TSP) of **6i**

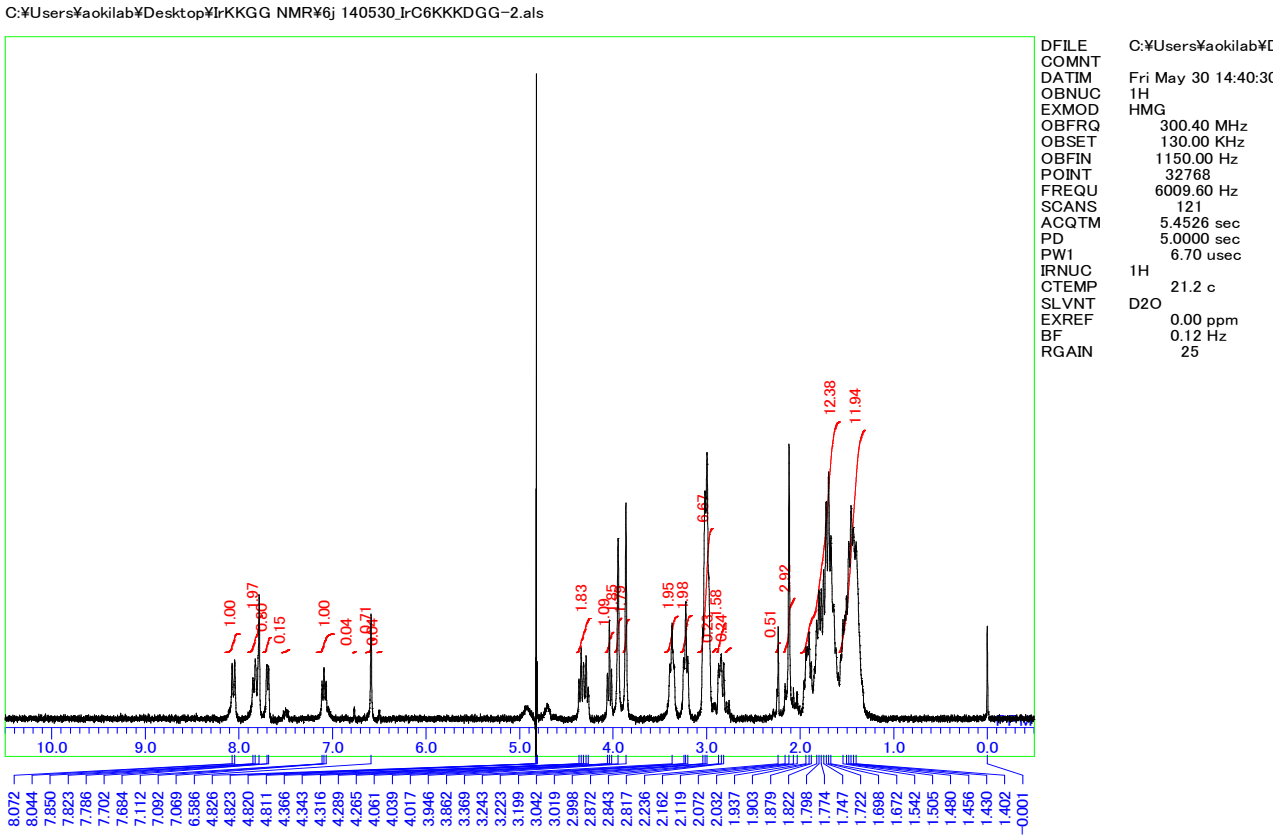

Figure S75. ^{1}H NMR spectrum (D_2O/TSP) of **6j**

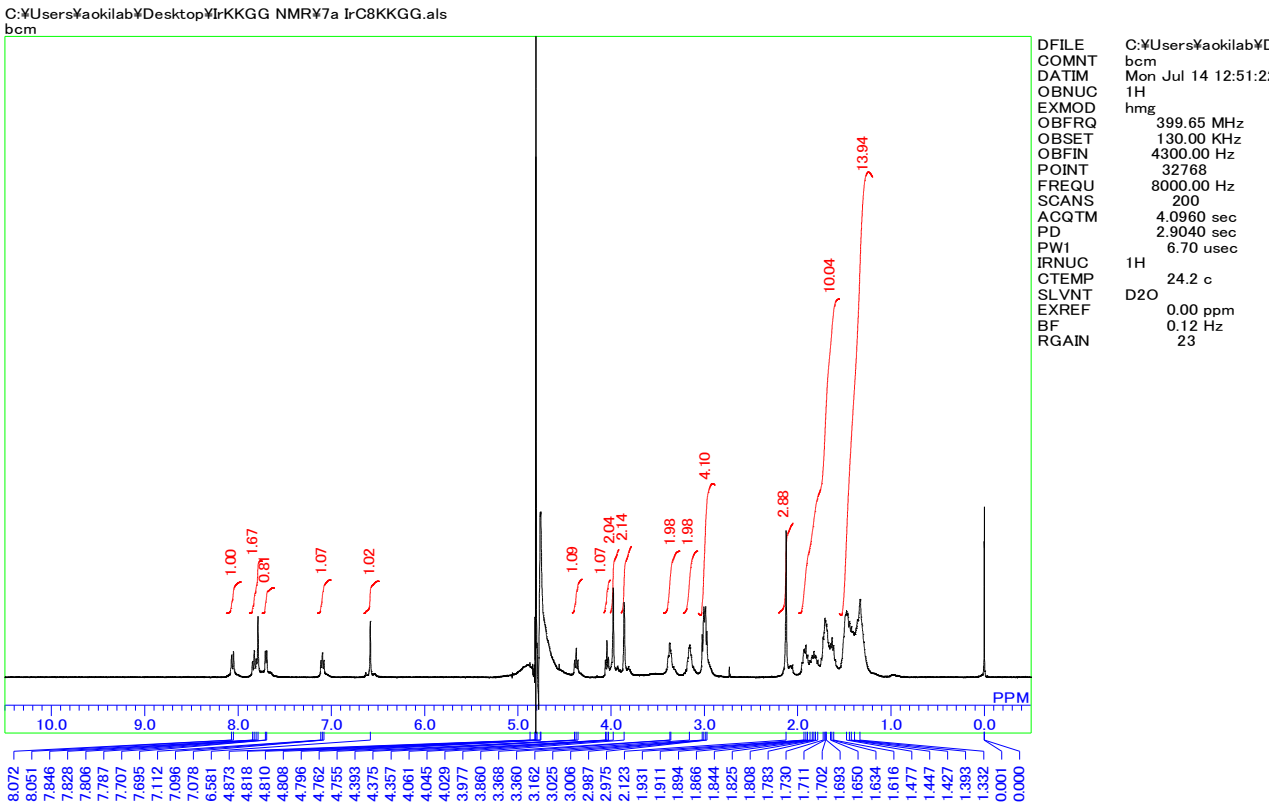

Figure S76. ^{1}H NMR spectrum (D_2O/TSP) of **7a**

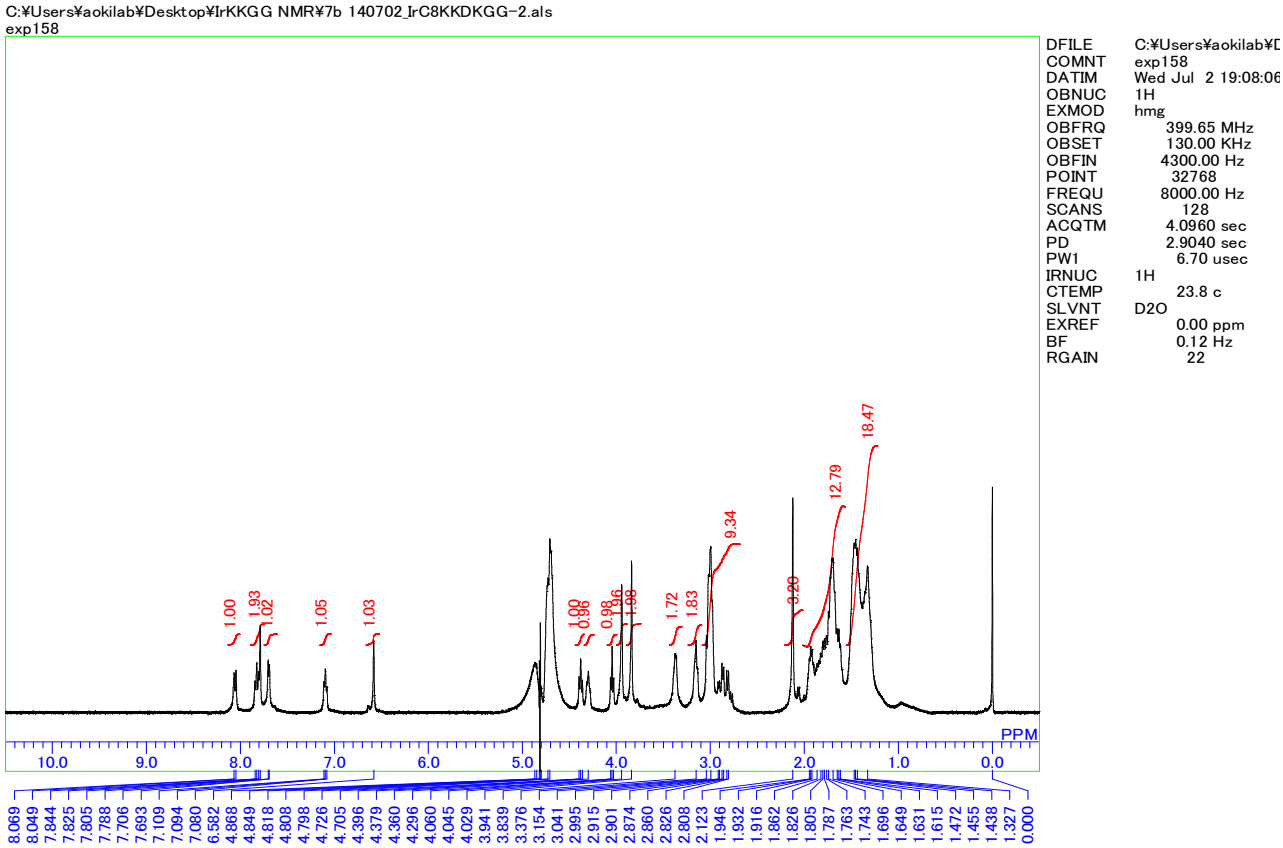

Figure S77. ^{1}H NMR spectrum (D_2O/TSP) of **7b**

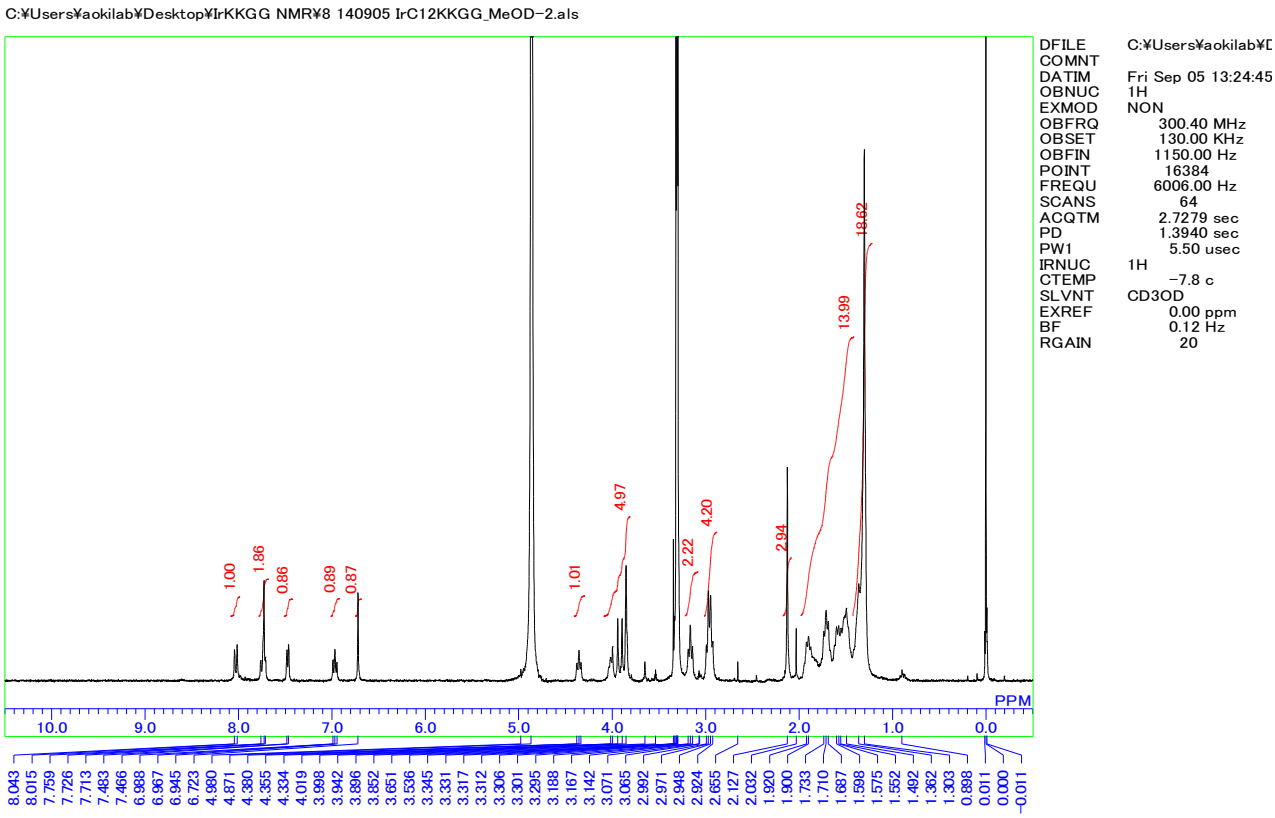

Figure S78. ^{1}H NMR spectrum (CD_3OD/TMS) of **8**

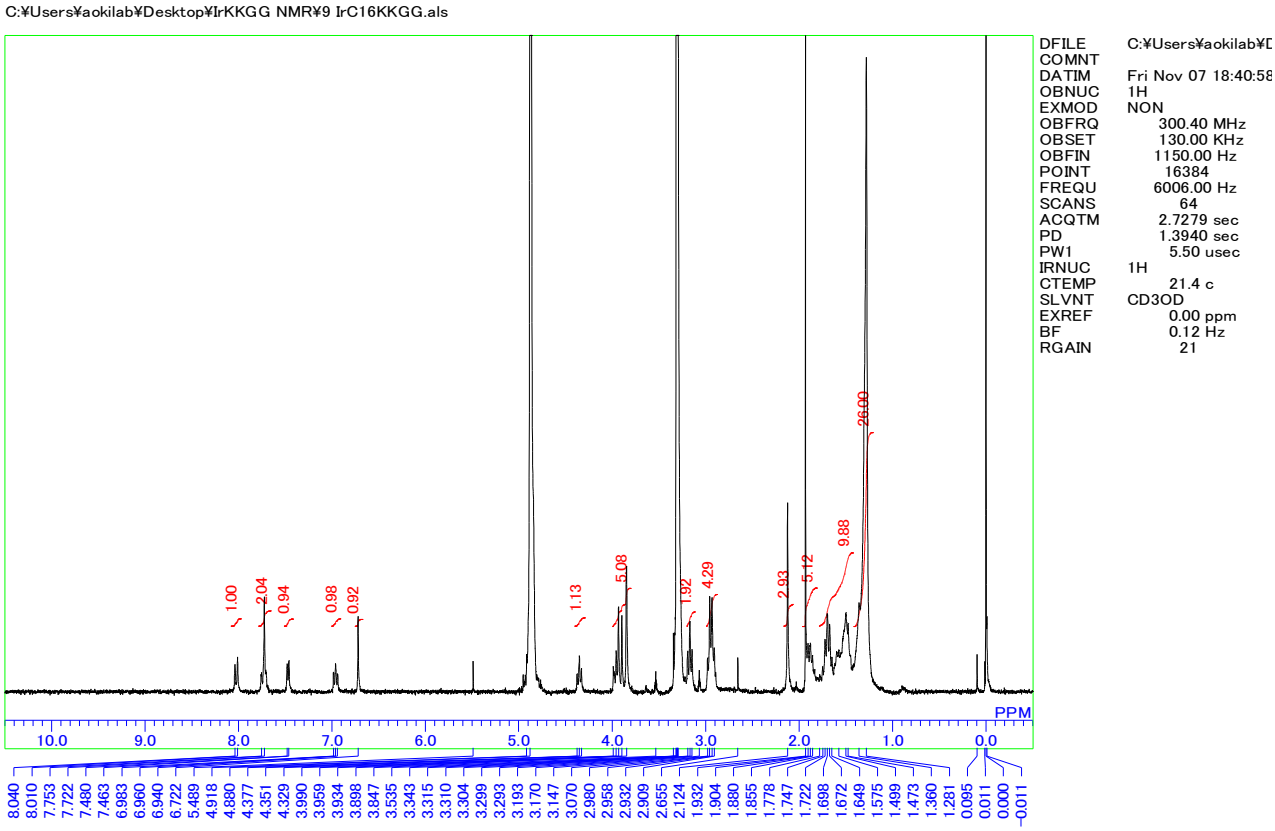

Figure S79. ^{1}H NMR spectrum (CD_3OD/TMS) of **9**

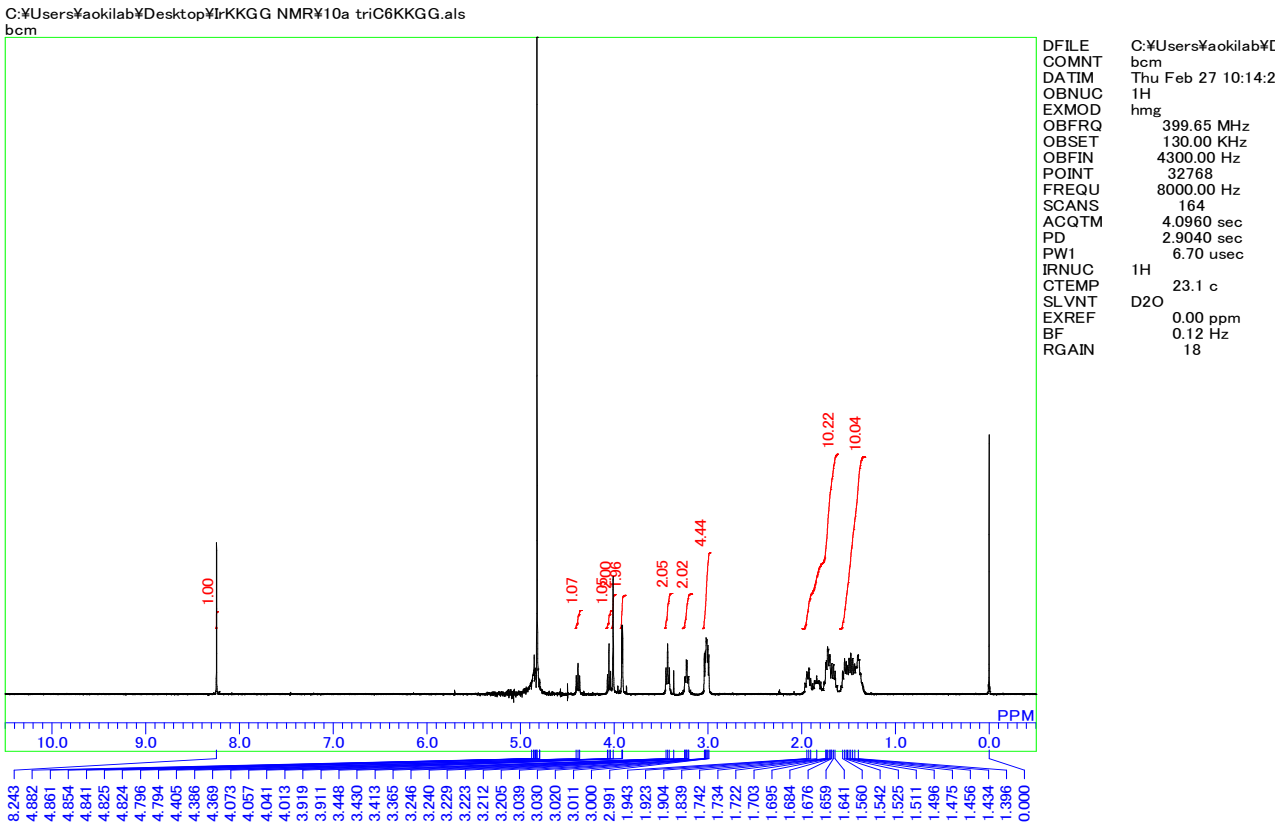

Figure S80. ^{1}H NMR spectrum (D_2O/TSP) of **10a**

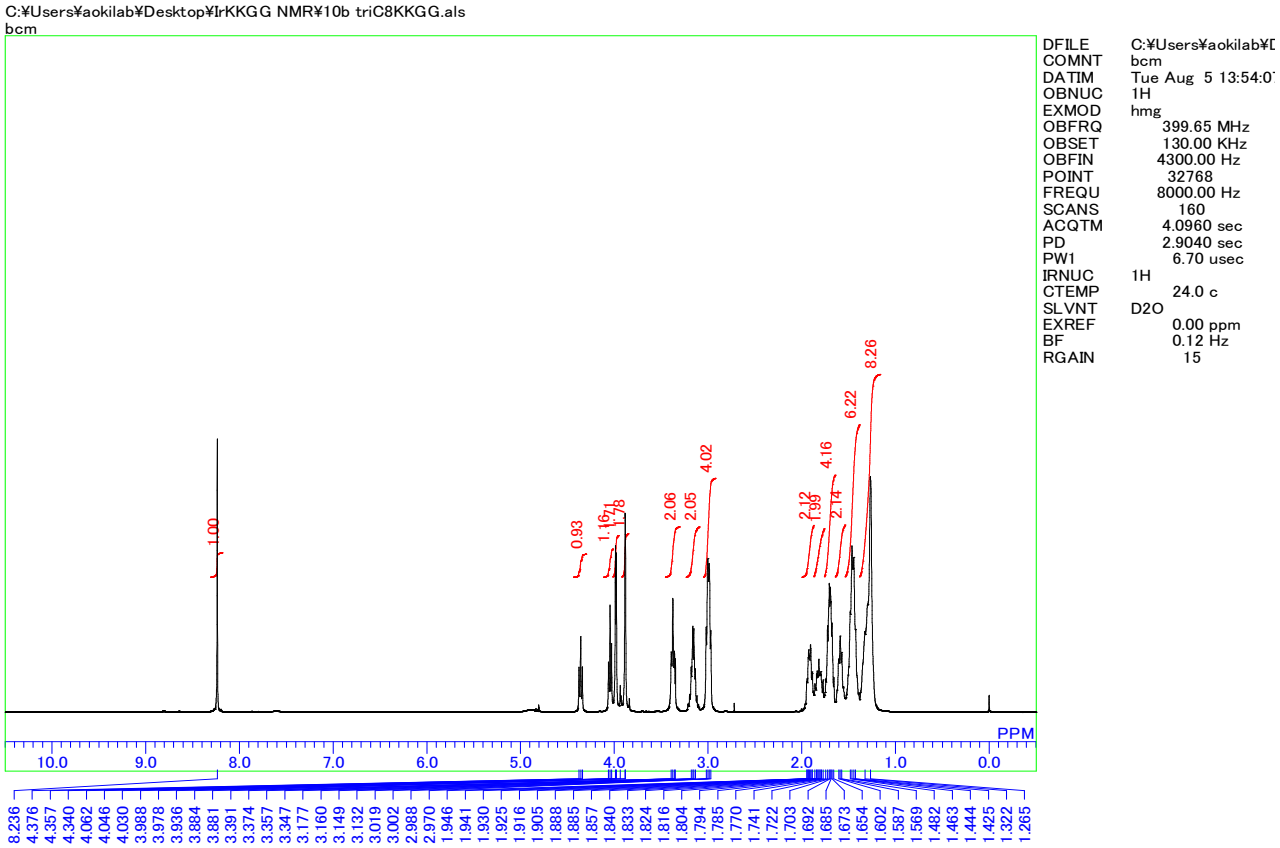

Figure S81. ^{1}H NMR spectrum (D_2O/TSP) of **10b**

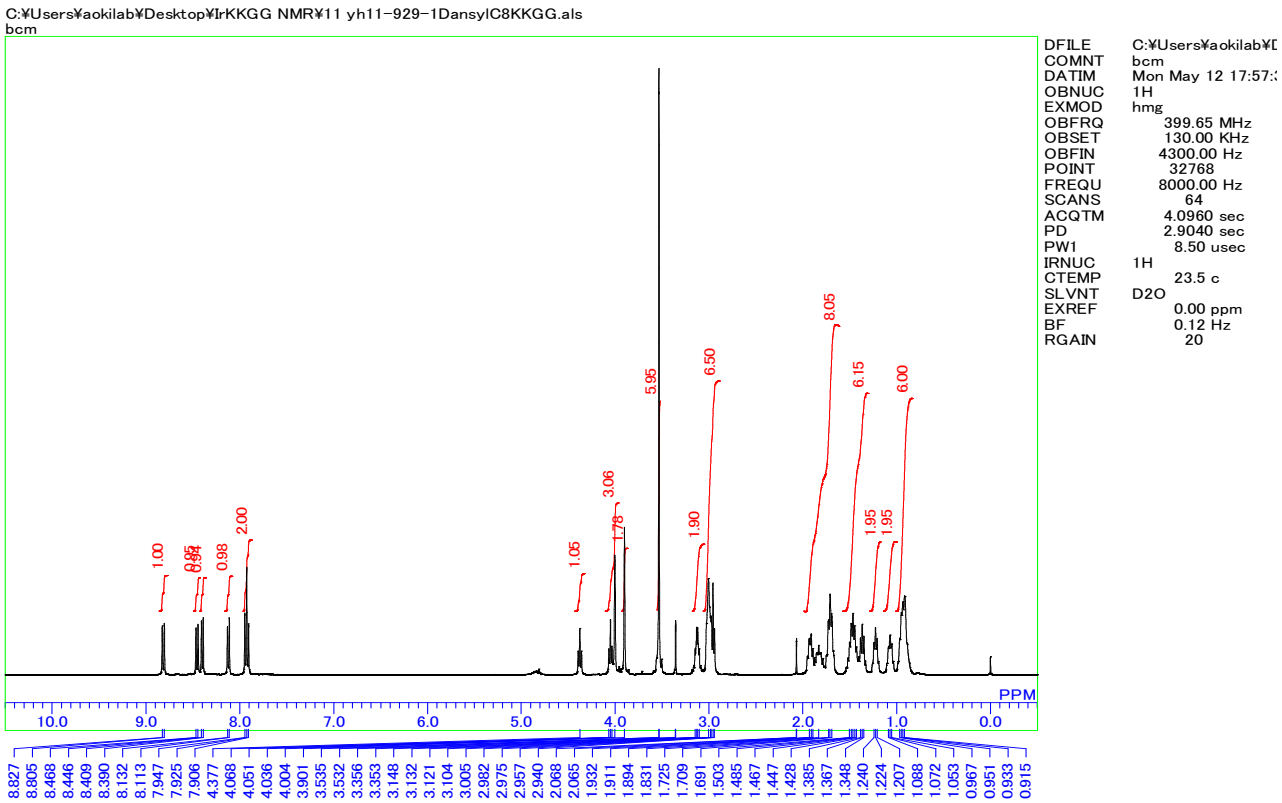

Figure S82. ^{1}H NMR spectrum (D_2O/TSP) of **11**